This is to certify that the

dissertation entitled

STRUCTURAL ANALYSIS OF BRANCHING ENZYME AND ADP-GLUCOSE PYROPHOSPHORYLASE

presented by

KIM BINDERUP

has been accepted towards fulfillment
of the requirements for

Ph.D. degree in Biochemistry

Jack Preiss
Major professor

Date 12/11/00

STRUCTURAL ANALYSIS OF BRANCHING ENZYME AND ADP-GLUCOSE PYROPHOSPHORYLASE

By

Kim Binderup

A DISSERTATION

Submitted to
Michigan State University
In partial fulfillment of the requirements
For the degree of

DOCTOR OF PHILOSOPHY

Department of Biochemistry

2000

ABSTRACT

STRUCTURAL ANALYSIS OF BRANCHING ENZYME AND ADP-GLUCOSE PYROPHOSPHORYLASE

By

Kim Binderup

The biosynthesis of starch and bacterial glycogen involves the enzymes ADP-glucose pyrophosphorylase, starch or glycogen synthase, and branching enzyme.

Branching enzyme catalyzes the cleavage and subsequent transfer of α-1,4-glucan to α-1,6 branch points. Hence, the enzyme plays an important role in the biosynthesis of glycogen and the amylopectin of starch. There is limited structure-function information available for branching enzyme, but its homology with other enzymes that cleave and/or transfer chains of α-glucan has provided some insight. The enzyme is believed to contain a central $(\alpha/\beta)_8$ barrel with extensions at the N- and C-termini. We have investigated the role of three residues at or near the proposed active site and characterized the purified mutant enzymes. We find the activity of all replacements affected the enzyme activity and in some cases, the substrate specificity.

We describe the characterization of the first inhibitor of branching enzyme. The compound BAY e4609 was found to be a slow-binding inhibitor of branching enzyme, similar to its action in α-amylase and related enzymes. We discuss how this may indicate a close functional relationship between α-amylase and branching enzyme, and how we may benefit from BAY e4609 in crystallization experiments.

To investigate the role of the N- and C-terminal of branching enzyme, we subjected the native 84 kDa enzyme from *E. coli* to limited proteolysis. We found a relatively stable 70 kDa fragment, which had an intact C-terminal, but a 111- or 113 residue truncation at the amino terminal. Characterization of this enzyme revealed it had 40-60% residual branching activity. The chain transfer patterns of the native and truncated enzymes were compared by several independent techniques and were found to differ significantly. Furthermore, the truncated branching enzyme was crystallized and diffracted X-rays to about 2.0 Å. As a consequence, this work is leading us to the first three-dimensional structure of a branching enzyme.

The rate of biosynthesis is controlled at the level of ADP-glucose pyrophosphorylase, as the enzyme is modulated by allosteric effectors. The enzyme from plants and cyanobacteria is commonly activated by 3-phosphoglycerate and inhibited by orthophosphate, whereas the enzyme from most bacteria is activated by fructose 1,6-bisphosphate and inhibited by adenosine-monophosphate. Furthermore, although tetrameric in structure, the enzyme's subunit composition differs between sources. ADP-glucose pyrophosphorylase from bacteria and cyanobacteria is a homotetramer, whereas the enzyme from plant is a heterotetrameric structure ($\alpha_2\beta_2$). However, there is no structure of ADP-glucose pyrophosphorylase to explain its complex allosteric behavior or subunit interactions. Here, we describe the crystallization of ADP-glucose pyrophosphorylase from *E. coli* and potato tuber, and discuss how this data is leading us to the first structure of this important enzyme.

ACKNOWLEDGMENTS

This work has been carried out in the laboratory of Dr. Jack Preiss, director of the Starch Bioengineering Group, Department of Biochemistry, Michigan State University.

I would like to thank Jack Preiss for his valuable support. Jack has given me space to develop and pursue my own research ideas, yet provided guidance wherever needed. As a consequence, I have learned more than research techniques- it has enabled me to become an independent researcher.

Several people have been directly involved in the research described in this dissertation. I would like to thank René Mikkelsen, who has been a great colleague and friend. René Mikkelsen performed several of the experiments described in Chapter 2 and 4-6, and assisted in many others. Nathalie Libessart helped me characterize the inhibitor described in Chapter 3. Furthermore, I would like to thank her for correcting my dissertation. The crystallization of the truncated *E. coli* branching enzyme (Chapter 4) was done in collaboration with Dr. James Geiger and his graduate student Marta Abad. Marta Abad grew the crystals of branching enzyme and performed the X-ray data collection and processing. Dr. James Geiger, Dr. Raghuvir Arni, Marta Abad, and Leandra Watanabe all contributed in the project of crystallizing ADP-glucose pyrophosphorylase (Chapter 7).

I would also like to thank my committee members Drs. Raghuvir Arni, James Geiger, Leslie Kuhn, Shelagh Ferguson-Miller, and Honggao Yan for their guidance and valuable comments.

I wish to thank my parents and brother for their support, and for never doubting my abilities. Last but not least, I wish to thank my friend, fiancée, and life-companion Nathalie for her love and unconditional support.

TABLE OF CONTENTS

LIST OF TABLES xi

LIST OF FIGURES xiii

LIST OF ABBREVIATIONS xvii

INTRODUCTION 1
References 4

CHAPTER 1
LITERATURE REVIEW 5
Starch and Bacterial Glycogen 6
The metabolic flow of Carbon into Starch 6
Structure, Organization, and Biosynthesis of Storage Starch 11
Other components of starch 19
Bacterial Glycogen 20
Biosynthesis of Starch and Bacterial Glycogen 22
Starch/ Glycogen Synthase 24
Branching Enzyme 26
Assay of Branching Enzyme Activity 26
Branching Enzyme Isoforms 31
Structure-Function Relationships 32
ADP-Glucose Pyrophosphorylase 37
Allosteric Regulation 37
ADP-Glucose Pyrophosphorylase is a Tetramer 38
Structure of the Pyrophosphorylase Domain 39
Active and Regulatory Sites 49
References 56

CHAPTER 2.
SITE-DIRECTED MUTAGENESIS STUDIES OF TYR-300, GLU-459, AND GLU-527 IN *ESCHERICIA COLI* BRANCHING ENZYME 66
Abstract 67
Introduction 68
Materials and methods 70
E. coli BE expression vector 70
Constructions of mutants 70
Expression of wild-type and mutant *E. coli* BE 70
Purification of *E. coli* BE wild-type and mutants 71
Assay of BE activity 71
Analysis of the chain length distribution by high performance anion exchange chromatography 71
Results 73
Identification of targets for mutagenesis 73

Expression and purification of mutant enzymes 73
Replacement of Glu-459 75
Replacement of Glu-527 80
Replacement of Tyr-300 83
Discussion 88
References 90

CHAPTER 3.
SLOW-BINDING INHIBITION OF BRANCHING ENZYME BY THE PSEUDOOLIGOSACCHARIDE BAY-E4609 93
Abstract 94
Introduction 95
Materials and methods 97
Expression and purification of *E. coli* BE 97
Assay of BE activity 98
Gel filtration 98
Results 100
Fractionation of BAY-e4609 107
Discussion 110
References 112

CHAPTER 4.
LIMITED PROTEOLYSIS OF *ESCHERICIA COLI* BRANCHING ENZYME 115
Abstract 116
Introduction 117
Materials and methods 119
E. coli BE expression vector 119
Limited proteolysis of branching enzyme 119
Purification of proteinase K treated branching enzyme 119
Construction of Nd_{1-112} truncated BE 119
Expression of WT and truncated *E. coli* BE 120
Expression of seleno-methionine substituted Nd_{1-112} 120
Purification of BE WT and N_{d-112} 121
SDS-PAGE and western blotting 121
Protein sequencing 122
Assay of BE activity 122
Protein assay 123
Mass spectrometry 123
Protein crystallization 123
X-ray diffraction analysis 123
Results 126
Purification of *E. coli* BE WT 126
Proteolysis of *E. coli* branching enzyme 126
Analysis of the 70 kDa fragment 129
Activity of PK-BE and Nd_{1-112} 132
Crystallization of *E. coli* branching enzyme 132

Production of selenium-methionine Nd_{1-112} 135
Discussion 138
References 142

CHAPTER 5.
TRUNCATION OF THE AMINO TERMINAL DOMAIN RESULTS IN ALTERED CHAIN TRANSFER PATTERN OF BRANCHING ENZYME 144
Abstract 145
Introduction 146
Materials and methods 148
Plasmids 148
Expression of wild-type and truncated BE in *E. coli* strain AC71 ($glgB^-$) 148
Purification of branching enzyme 148
Branching enzyme activity 148
Glycogen synthase assay 149
Protein assay 149
Analysis of branched chain length 150
HPAEC analysis 150
Analysis of chain length by gel filtration 150
Glucan-iodine complex 150
Average α-glucan chain length determination 151
Results 152
Chain transfer by PK-BE, Nd_{1-112} and BE-WT 152
Discussion 167
References 170

CHAPTER 6.
AN *IN VITRO* RECONSTITUTION SYSTEM FOR GLYCOGEN BIOSYNTHESIS 172
Abstract 173
Introduction 174
Materials and methods 177
Purification of enzyme material 177
Branching enzyme activity 177
Glycogen synthase activity 177
Phosphorylase activity 177
Protein assay 178
SDS-PAGE analysis 178
Synthesis of α-D-glucan by branching enzyme and glycogen synthase 178
Synthesis of α-D-glucan by branching enzyme and phosphorylase a 178
Analysis of branched chain length 179
HPAEC analysis 179
Results 180

Enzymatic activities 180
Synthesis of α-D-glucan 182
Structures of α-D-glucans 184
Discussion 196
References 198

CHAPTER 7.
CRYSTALLIZATION OF ADP-GLUCOSE PYROPHOSPHORYLASE 200
Abstract 201
Introduction 202
Materials and methods 204
Reagents 204
Plasmids and bacteriophages 204
Expression of *E. coli* ADP-Glc PPase 204
Purification of *E. c*oli ADP-Glc PPases 205
Expression and purification of potato tuber α4 and $\alpha_2\beta_2$ 206
ADP-Glc PPase assay 207
Protein assay 208
Protein crystallization 208
X-ray diffraction analysis 208
Results 210
Expression and purification of ADP-Glc PPases 210
Crystallization of *E. coli* ADP-Glc PPase WT 212
Crystallization of potato tuber ADP-Glc PPase 219
Crystallization of *E. coli* ADP-Glc PPase mutant G336D 222
Discussion 224
References 226

CHAPTER 8.
CONCLUDING REMARKS AND RESEARCH PERSPECTIVES 228
References 234

LIST OF TABLES

CHAPTER 1.

1. Properties of potato tuber small subunit and the native enzyme 38

2. Matrix of amino acid sequence identity/ similarity of ADP-glucose pyrophosphorylases 40

CHAPTER 2.

1. Specific activities of E459 mutants measured using assay A, B and C 76

2. Kinetic parameters of WT *E. coli* and mutant E459D BEs 78

3. Specific activities of E527 mutans measured using assay A, B and C 82

4. Specific activities of Y300 mutants measured using assay A, B and C 84

CHAPTER 4.

1. Purification table of BE-WT 125

2. Purification table of Nd_{1-112} 131

3. Specific activities of *E. coli* BE WT, PK-BE and Nd_{1-112} 133

4. Kinetic parameters of *E. coli* BE WT, PK-BE and Nd_{1-112} 133

5. Statistics for the branching enzyme X-ray diffraction data collection 134

6. Branching enzyme crystal properties 135

7. Mass spectrometry of truncated branching enzyme 137

CHAPTER 5.

1. Expression of BE WT and truncated branching enzyme in *E. coli* AC71 (*glgB*$^-$) and properties of the synthesized α-glucans 162

CHAPTER 7.

1. Pyrophosphorolysis assay of ADP-Glc PPase 208

2. Summary of single enzyme purifications 212

3. Mass spectrometry analysis of *E. coli* ADP-Glc PPase 212

4. Data collection and processing statistics for potato tuber small subunit crystal forms α_4#1 and α_4#2 221

LIST OF FIGURES

CHAPTER 1.

1. Simplified model of plant starch synthesis in photosynthetic cells and storage cells 7

2. The flow of carbon into starch by the hypothetical SS-ADP-Glc pathway, as proposed by Pozueta-Romoeo *et al.* 10

3. Structure of amylose and amylopectin 12

4. Overview of the starch granule organization, adapted from Ball *et al.* 15

5. Discontinuous synthesis model for amylopectin biosynthesis, adapted from Ball *et al* 17

6. Model of the organization of amylose and amylopectin in the starch granule as proposed by Lineback 18

7. Biosynthetic pathway of starch and bacterial glycogen 23

8. The iodine stain assay 27

9. The phosphorylase A stimulation assay 28

10. The branching linkage assay 29

11. Schematic representation of some branching enzymes from plants and bacteria 34

12. Amino acid alignment of several ADP-glucose pyrophosphorylases 41

13. Amino acid alignment of ADP-glucose pyrophosphorylases and N-acetylglucoseamine 1-phosphate uridylyltransferase 43

14. Structure of the pyrophosphorylase domain of N-acetylglucoseamine 1-phosphate uridylyltransferase 46

15. G-1-P binding site of ADP-Glc PPase 50

16. Proposed ATP binding site of ADP-Glc PPase 51

17. Activator sites of cyanobacterial and plant ADP-Glc PPases 52

18. *E. coli* ADP-Glc PPase Nd_{1-11} 53

19. Proposed *Anabaena* phosphate binding site 54

20. Position of G336 of *E. coli* ADP-Glc PPase, indicated in bold 55

CHAPTER 2.

1. Partial sequence alignment of several branching enzymes from various organisms 74

2. HPAEC analysis of the debranched α-glucan formed by the action of *E. coli* BE WT on reduced amylose and of E459D 79

3. pH profile of *E. coli* BE WT and E459A mutant 81

4. Heat stability curve of BE WT and Y300F 86

5. Relative activity of BE WT and Y300F at elevated temperatures 87

CHAPTER 3.

1. Structures of the pseudo-oligosaccharides acarbose and BAY e4609 96

2. Inhibition of *E. coli* BE by BAY e4609 101

3. Lineweaver-Burk plot of *E. coli* BE in presence of BAY e4609 103

4. Rate of loss of branching enzyme activity 105

5. Preincubation of *E. coli* BE with BAY e4609 106

6. Progress curve of *E. coli* BE with BAY e4609 108

7. Gel filtration of BAY e4609 109

CHAPTER 4.

1. SDS-PAGE and branching activity of *E. coli* BE treated with 1:1000 molar ratio of proteinase K to BE at various incubation times 127

2. SDS-PAGE of BE-WT treated with various proteases as described in materials and methods 128

3. SDS-PAGE and western blot analysis of wild-type and truncated branching enzymes 130

4. Crystal of the truncated *E. coli* branching enzyme 136

5. Schematic diagram of several branching enzymes 140

CHAPTER 5.

1. Analysis of transferred chain length by gel filtration after 2 hrs and 4 hrs of branching using reduced amylose AS-320 as substrate 153

2. Relative distribution of transferred oligosaccharide chain sizes after 2 hrs and 4 hrs branching based on the data from gel filtration 155

3. High Performance Anion Exchange Chromatography of debranched α-glucans formed by the action of BE-WT and $Nd_{1\text{-}112}$ on reduced amylose AS-320 after 2 hrs and 16 hrs of branching 157

4. Difference in chain distribution between $Nd_{1\text{-}112}$ and BE-WT resulting from branching amylose AS-320 for 16 hrs 159

5. Staining of cell colonies with iodine vapor 160

6. High Performance Anion Exchange Chromatography of debranched α-glucans purified from *E. coli* B+pET23d, AC71+pGBE, AC71+pTRC, and AC71+pET23d 163

7. Difference in chain distribution between α-glucans purified from *E. coli* B, AC71+pGBE and AC71+pTRC 166

CHAPTER 6.

1. Reaction scheme of *de novo* glucan synthesis 176

2. SDS-PAGE of purified enzymes for glycogen reconstitution system 181

3. Effects of different ratios of enzymatic activities on α-glucan yields 183

4. Effect of reaction time on glucan yields 185

5. Analysis of transferred chain lengths after 1 hr, 3 hrs and 16 hrs of branching, using 10 units of BE activity and 1 unit of GS/PA activity..... 186

6. Difference plot showing the effect of BE-WT vs. Nd_{1-112} on the glucan structure 189

7. Difference plot showing the effect of reaction time on the synthesized glucan structures 190

8. Difference plot showing the effect of phosphorylase A vs. glycogen synthase 191

9. Analysis of transferred chains using BE:GS and BE:PA ratios of 3:1, 6:1, and 20:1 193

10. Difference plot showing the effect of enzyme ratio on the synthesized glucan structures 195

CHAPTER 7.

1. SDS-PAGE of purified enzymes for protein crystallization 211

2. Crystallization conditions for *E. coli* ADP-Glc PPase WT 214

3. X-ray data set of *E. coli* ADP-Glc PPase crystal form ECWT#1 215

4. X-ray data set of *E. coli* ADP-Glc PPase crystal form ECWT#2 217

5. X-ray data set of *E. coli* ADP-Glc PPase crystal form ECWT#3 218

6. Crystallization conditions for potato tuber α_4 ADP-Glc PPase 220

7. Crystallization conditions for *E. coli* ADP-Glc PPase G336D 223

CHAPTER 8.

1. Proposed catalytic mechanism for branching enzyme 230

LIST OF ABBREVIATIONS

3-PGA: 3-phosphoglycerate
ADP-Glc PPase: ADP-Glucose pyrophosphorylase.
Am: Amylose
AMP: Adenosine monophosphate.
Ap: Amylopectin.
BE: Branching enzyme.
BE-WT: *E. coli* wild-type branching enzyme.
c.l.: Chain length.
CGTase: Cyclodextrin glucanotransferase.
d.p.: Degree of polymerization.
DBE: Debranching enzyme
DTNB: 5,5' dithiobis-2-nitrobenoiz acid.
DTT: Dithiothreitol.
EDTA: Ethylenediaminetetracetic acid.
FBP: Fructose 1,6-bisphosphate.
G-1-P: Glucose 1-phosphate.
G-6-P: Glucose 6-phosphate.
GBSS: Granule bound starch synthase.
GlmU: N-acetylglucoseamine 1-phosphate uridylyltransferase
GS: Glycogen synthase.
HPAEC: High performance anion exchange chromatography.
IPTG: Isopropyl-D-thiogalactoside.
MAD: Multiple anomalous dispersion.
mBE: Maize endosperm branching enzyme.
mBEI: Maize branching enzyme isoform I.
mBEII: Maize branching enzyme isoform II.
MW: Molecular weight.
Nd_{1-112}: *E. coli* branching enzyme with 112 amino acids deleted at N-terminal.
PA: Phosphorylase A.
PAD: Pulsed amperometric detector.
Pi: Orthophosphate.
PK-BE: Proteinase K cleaved *E. coli* branching enzyme.
PLP: Pyridoxal phosphate.
PPA: Porcine pancreatic α-amylase.
Se-met: Selenium-methionine.
SS: Starch synthase.
SSS: Soluble starch synthase.
TAA: Taka α-amylase.
TP: Triosephosphates.
WT: Wild-type.

INTRODUCTION.

Starch is not only the primary intake of calories in a normal human diet but also the raw material for conversion to many useful commercial products by chemical and biochemical reactions (1). In the food-industry for example, the starch is converted into maltodextrins, cyclodextrins and glucose-syrup, and in the nonfood-industry it has found use in biodegradable packaging material, paper-manufacturing, cosmetics, pharmaceutics, and much more. Although it is evident that starch is important, its metabolism in plants is not fully understood as the exact roles of the biosynthetic enzymes remain unknown (2, 3).

The biosynthesis of plant starch and bacterial glycogen involves at least three enzymes: ADP-glucose pyrophosphorylase (ADP-Glc PPase), starch synthase (SS) or glycogen synthase (GS), and branching enzyme (BE). ADP-Glc PPase synthesizes ADP-glucose from glucose-1-phosphate (G-1-P) and ATP, and is believed to be the major regulatory enzyme in the biosynthetic pathway (2, 4, 5). SS or GS form the α-1,4-linkages of glucan by transfer of the glycosyl unit of ADP-glucose to the non-reducing terminal of an α-1,4-glucan primer. Finally, BE forms the α-1,6-linkages of starch and glycogen by cleavage and subsequent transfer of α-1,4 glucan to α-1,6 branch points. Starch synthase and branching enzymes are believed to be major determinants of the starch structure in plants, although other enzymes are almost certainly involved (6-8).

In chapter 1, a brief summary of our current understanding of the structure and biosynthesis of plant starch and bacterial glycogen is provided. A detailed description of protein structure-function relationships of branching enzyme and ADP-glucose

pyrophosphorylase is presented. For completion, glycogen synthase and starch synthase are briefly described, but for detailed information of these enzymes please refer to a number of recent reviews (4, 5, 7-9).

Our laboratory focuses on elucidating the structure-function relationship of the starch and glycogen biosynthetic enzymes, using conventional biochemical and molecular biological approaches. Much of the work described here has aimed at increasing the understanding of branching enzyme structure-function relationships. Not only do we lack a structure of branching enzyme, but also the regions responsible for the properties of the enzyme, including transferred chain length and substrate specificity, are largely unknown. Chapter 2 describes site-directed mutagenesis studies of the *E. coli* branching enzyme, which includes substitution of three residues near or at the proposed active site. In chapter 3, the identification and characterization of the first inhibitor of branching enzyme is described. This work indicates a close relationship of branching enzyme to α-amylase, as the compound investigated has the same mechanism of inhibition in both enzymes. The limited proteolysis of *E. coli* branching enzyme is presented in chapter 4. We find that cleavage of 112 amino acids at the amino terminal produces a branching enzyme with a 40-60% reduction in activity. In contrast to the full-length *E. coli* BE, crystallization experiments of the truncated enzyme was successful in producing single crystals suitable for X-ray diffraction analysis. We present a native data set complete to 2.3 Å and the production of selenium-methionine protein necessary for solving the first structure of branching enzyme. In chapter 5, the truncated branching enzyme is analyzed in detail with respect to its chain transfer pattern. We find the truncated enzyme transfers longer α-glucan chains than the native *E. coli* enzyme, and conclude the amino terminal domain is

involved in determining the chain transfer pattern of branching enzymes. A glycogen biosynthetic reconstitution system is described in chapter 6. Here, we use purified branching enzymes, glycogen synthase, and phosphorylase to synthesize α-glucan structures *in vitro*. The α-glucans are then analyzed by high performance anion exchange chromatography (HPAEC) and the chromatograms compared, allowing us to draw conclusions about multiple parameters affecting on the final α-glucan product.

Despite being intensely studied for decades, there is not currently any three-dimensional structure of ADP-Glc PPase available. Crystals of the enzyme from *E. coli* has been reported (10), but the crystals were subjected to rapid decay in the X-ray beam and furthermore diffracted poorly (> 5Å). Chapter 7 concentrates on the challenge of obtaining a three-dimensional structure of ADP-Glc PPase. We have expressed recombinant ADP-Glc PPases from *E. coli* and potato tuber, and purified the proteins to near-homogeneity. Crystallization trials have produced single protein crystals of the enzyme from *E. coli* and the potato ADP-Glc PPase small unit. We discuss the various crystal forms obtained and their potential in solving a structure of this enzyme. Furthermore, selenium-methionine *E. coli* ADP-Glc PPase has been produced and multiple anomalous dispertion (MAD) data sets collected of two separate crystal forms.

Finally in Chapter 8, I discuss the perspectives for future studies of Branching Enzyme and ADP-glucose pyrophosphorylase with emphasis of obtaining the three-dimensional structures of these enzymes. In addition, I propose a catalytic mechanism for branching enzyme.

Kim Binderup - East Lansing, December 2000.

References

1. Hizukuri S. (1995) *in* Carbohydrates in Food (Elliasson, A.C, Ed.). Acad. Press, NY. pp. 347-428.
2. Preiss, J. and Sivak, M.N. (1998) *in* Comprehensive Natural Products Chemistry (Pinto, B.M, Ed.) Pergamon Press, Oxford, Vol. 3, pp. 441-495.
3. Sivak, M.N. and Preiss, J. (1998) Advances in Food and Nutrition Research, Academic Press, San Diego, CA., Vol 41.
4. Preiss, J. (1996). Regulation of Glycogen Synthesis. *in Escherichia coli* and *Salmonella typhimurium*: Cellular and Molecular Biology, second edition, Amer. Soc. Microbiol., Washington, DC. Vol. 1, pp. 1015-1024.
5. Preiss, J. (1984). *Annu Rev. Microbiol.* **38**, pp. 419-458.
6. Ball, S., Guan, H.P, James, M., Myers, A., Keeling, P., Mouille, G., Buleon, A., Colonna, P., and Preiss, J. (1996). *Cell.* **86**, 349-352.
7. Smith, A.M., Denyer, K., and Martin, C. (1997). *Annu. Rev. Plant Physiol. Plant. Mol. Biol.* **48**, 67-87.
8. Myers, A.M., Morell, M.K., James, M.G., and Ball, S.G. (2000). *Plant Physiol.* **122**, 989-997.
9. Preiss, J. (1991) *Oxf. Surv. Plant. Mol. Cell Biol.* **7**, 59-114.
10. Mulichak, A.M., Skrzypzak-Jankun, E., Rydel, TJ., Tulinsky, T., Preiss, J. (1988). *J. Biol. Chem.* **263**, 17237-17238.

CHAPTER 1

LITERATURE REVIEW

1. Starch and Bacterial Glycogen.

1.1 The Metabolic Flow of Carbon into Starch.

Starch is a major reserve polysaccharide in green plants and probably the second most abundant carbohydrate in nature after cellulose (1).

Starch is an end-product of carbon fixation in photosynthesis and is found in almost all green plants (1-4). It is present in virtually every type of plant tissue and organ including leaves, roots, fruits, pollen, tubers, grains, and stems. A distinction is made between transient starch, mainly synthesized in leaves, and storage starch synthesized in the storage organs of the plant (5). Transient starch is synthesized in the chloroplast of photosynthetically active tissue, where triose-phosphate (TP) from the Calvin cycle *via* gluconeogenesis is converted into hexose monophosphate, which then enters the starch biosynthetic pathway (reviewed in ref. 6; Figure 1). Transient starch is deposited in granules in the chloroplasts during active photosynthesis throughout the day and degraded by respiration during the night, thus ensuring a constant availability of photosynthates to the whole plant (2, 7). In the plant, fixed carbon destined for export is transported from the chloroplast to the cytosol as triose-phosphate *via* the TP/Pi translocator (8, 9; Figure 1). The triose-phophate is then converted to sucrose, which is transported from the photosynthetic tissue and delivered through the phloem to the rest of the plant. The rapid turnover of transient starch in a day-night cycle makes it an important energy-buffer in growing plants. In *Arabidopsis thaliana*, for example, mutants unable to synthesize starch can grow at continuous light, but show a dramatic decrease in growth-rate when grown in a day-night cycle (7).

Figure 1. Simplified model of plant starch synthesis in photosynthetic cells (transient starch, top half of figure) and storage cells (storage starch, lower half of figure). In photosynthetic tissue, the fixed CO_2 can be stored as starch in the chloroplast through the use of pathway I. For export of fixed carbon from photosynthetic cells, triosephosphates (TP) are transported from the chloroplast to the cytosol *via* the TP/Pi translocator, and converted to sucrose by pathway II. The sucrose is then transported from the photosynthetic tissue, often over long distances in the phloem, where it can be unloaded into storage cells. Subsequently, sucrose is converted to hexosephosphate (pathway III) and transported into the amyloplasts by a hexosephosphate translocator. The amyloplast is able to store large amounts of carbon by conversion of the hexosephosphate into starch by pathway IV.

Some proteins involved in pathways I-IV are indicated as numbered:

1) Phosphoglucoisomerase

2) Phosphoglucomutase

3) ADP-glucose pyrophosphorylase

4) Starch synthases and branching enzymes

5) Triosephosphate/Pi translocator

6) UDP-glucose pyrophosphorylase

7) Sucrose phosphate synthase

8) Sucrose phosphatase

9) Sucrose synthase

10) Fructokinase

11) Hexosephosphate translocator

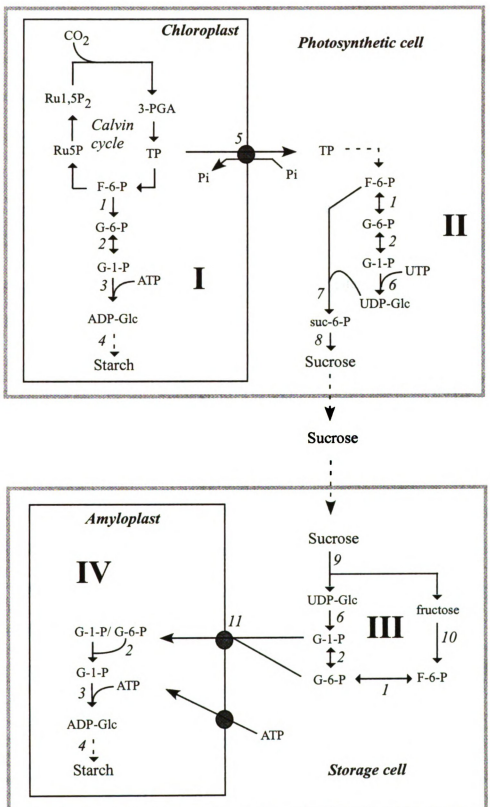
Chloroplast
Photosynthetic cell
CO2
Ru1,5P2
3-PGA
Calvin cycle
Ru5P
TP
F-6-P
1
G-6-P
2
G-1-P
3
ATP
I
ADP-Glc
4
Starch
5
Pi
Pi
TP
F-6-P
1
G-6-P
2
G-1-P
UTP
6
7
UDP-Glc
suc-6-P
8
Sucrose
II
Sucrose
Amyloplast
IV
G-1-P/ G-6-P
2
G-1-P
3
ATP
ADP-Glc
4
Starch
11
ATP
Sucrose
9
UDP-Glc
6
G-1-P
2
G-6-P
1
F-6-P
fructose
10
III
Storage cell

The major site of starch accumulation is in the storage organs (as storage starch) including seeds, tubers and storage roots. In contrast to transient starch, the metabolic turnover of storage starch is very slow and accumulates over long periods, sometimes several months of the growing season. Once synthesized, it normally remains unchanged until the next growing season, when it is rapidly mobilized to support new growth. Storage starch is synthesized in specialized plastids of non-photosynthetic tissue named amyloplasts, which are committed primarily to starch production. These develop directly from proplastids and have little internal lamella structure (10). The flow of carbon into the amyloplast is in the form of the hexose monophosphates glucose-1-phosphate (G-1-P) or glucose-6-phosphate (G-6-P; 11-13; Figure 1). In the cytosol of the non-photosynthetic tissue, sucrose is first converted into Glc-1-P or Glc-6-P before transport into the amyloplast by specific translocators (14, 15). Some studies have suggested that in addition to hexose phosphates, C_3 intermediates is also transported into amyloplasts for starch synthesis (16, 17), perhaps *via* a modified TP/Pi transporter. Detailed carbon labeling studies have since concluded the direct route of hexose phosphate, rather than C_3 intermediates, is the far-most likely candidate for entry into the amyloplasts (13, 18).

A proposed alternative pathway of starch synthesis deserves mention here. Akazawa and coworkers have shown the presence of an ADP/ATP translocater in chloroplasts and amyloplasts of spinach that also appeared capable of transporting ADP-glucose (19). A mechanism was subsequently proposed where ADP-glucose is synthesized in the cytosol directly from sucrose by sucrose synthase and then transported in the amyloplasts where it is utilized directly by starch synthase (Figure 2). This alternative pathway, called the SS-ADP-Glc pathway (Sucrose Synthase-ADP-glucose

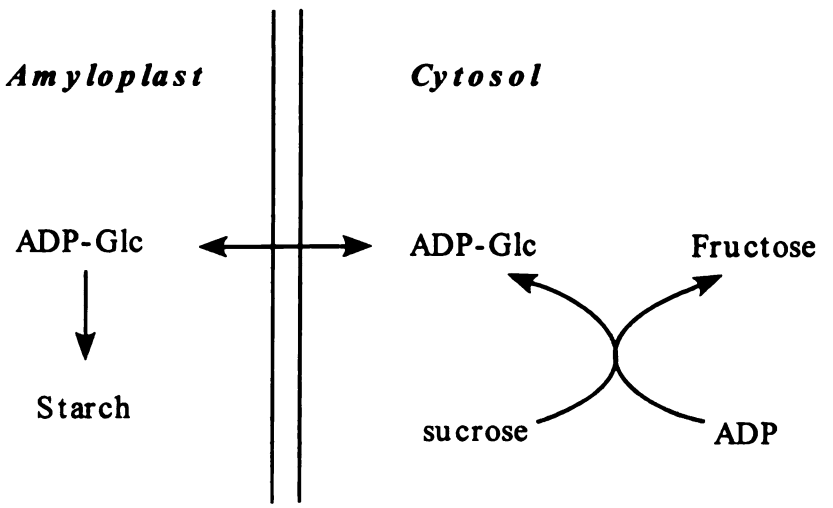

Figure 2. The flow of carbon into starch by the hypothetical SS-ADP-Glc pathway, as proposed by Pozueta-Romeo *et al* (19). The pathway uses a cytosolic sucrose synthase for formation of ADP-glucose, which is translocated to the amyloplast. The ADP-glucose is used for glucan synthesis by starch synthase, and therefore the pathway predicts ADP-glucose pyrophosphorylase to have a minor role in starch synthesis.

pathway), depends on sucrose synthase for formation of ADP-glucose and hence predicts ADP-Glc PPase to have a minor role in starch synthesis. These predictions do not satisfy results obtained from mutants deficient in ADP-Glc PPase (7, 20) or antisense studies targeting the ADP-Glc PPase genes (21). In Arabidopsis, for example, there were undetectable levels of starch in a mutant plant lacking one of the two subunits of ADP-Glc PPase (7). Also, the expression of a bacterial ADP-Glc PPase, desensitized to allosteric regulation, in tobacco, tomato, and potato dramatically increased the starch content in these plants (22). In light of these results we can conclude that the ADP-glucose used in starch synthesis is formed *via* the ADP-Glc PPase, and that the SS-ADP-Glc pathway plays little, if any, role in this process.

1.2 Structure, Organization, and Biosynthesis of Storage Starch.

Starch accumulates as a complex granular structure made of α-glucans (α-1,4-linked and α-1,6-branched) both in leaf cell chloroplasts (transient starch) and in the amyloplasts of the plant storage tissue cell (storage starch; 5). Starch at first appears to be a simple compound because it is comprised only of glucose, however, its structure is far from being fully understood. The storage polysaccharide is usually defined as a mixture of two distinct fractions: amylose and amylopectin (2, 23, 24). Amylose is mainly found as linear chains of 840 to 22,000 α-1,4 linked D-glucopyranosyl units with a molecular weight of 10^5-10^6 (Figure 3). Although first defined as a linear polymer, some molecules found in the amylose fraction are branched (α-1,6-D-glucopyranose; one per 170 to 500 units.). Amylopectin is the major polymer fraction of starch, usually making up ~70 % of the starch, although this number varies highly depending on the plant

Figure 3. Structure of amylose and amylopectin. (A) Simple representation of the mostly linear amylose and the highly branched amylopectin. Amylose is composed of α-1,4-linked glucose, whereas amylopectin is α-1,4-linked and α-1,6-branched. (B) Detail of the α-1,4-glucosidic linkage present in both amylose and amylopectin, and the α-1,6-glucosidic linkage of amylopectin. (C) Diagrammatic representation of an amylopectin molecule, adapted from ref. 73. α-1,4 lined glucans are attached by α-1,6 linkages to from a highly branched structure. The outer short glucan chains (A chains) are unbranched and linked to the multiple branched B chains. Only the single C-chain has a reducing terminal in each amylopectin molecule.

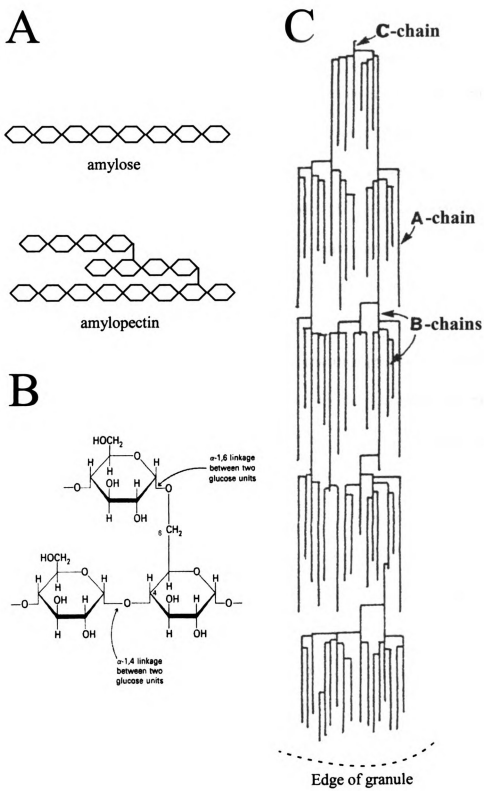
A
amylose
amylopectin
B
HOCH2
α-1,6 linkage between two glucose units
CH2
α-1,4 linkage between two glucose units
C
C-chain
A-chain
B-chains
Edge of granule

species, variety, and storage organ (25). It is a highly branched polymer with 4 to 5 % α-1,6 glucosidic linkages and a molecular weight of 10^7 to 10^9. The amylopectin forms a highly regular and organized structure with three types of α-glucan chains (Figure 3). The A chains are the "outer" chains of the amylopectin molecule that are not substituted on the 6-OH position. The A chains are α-1,6-linked to the inner branches termed B chains, which may be branched at one or several points. Only a single chain (the C chain) has a free reducing end per amylopectin molecule. The α-glucan chains of amylopectin are not randomly arranged, but form a repeating motif of crystalline and amorph lamella of approximately 9 nm (Figure 4; 26). Interestingly, this motif is seen throughout the plant kingdom, and suggests the existence of a highly ordered and well-conserved biosynthetic pathway (27). Many different proposed structures have attempted to explain the semi-crystalline nature of amylopectin (1, 28-31), but only the most satisfactory in fitting experimental data, and widely accepted model, is discussed here. The crystalline lamella consists of linear and parallel α-glucans that intertwine to form double helicies, as determined by X-ray diffraction analysis (32, 33). These parallel α-glucans are the A- and B chains of amylopectin. Starch from various plant sources is known to have ranging degrees of crystallinity. This is probably a function of their different average branch lengths (i.e. size of B and A chains), and indeed the length of the crystalline lamella has been reported to range 4-6 nm, which is equivalent of 12-18 glucose residues arranged in a helix (34, 35).

Most of the α-1-6-branch points are believed as clustered in the amorphous lamella approximately 3 nm in length. How such an asymmetric distribution of the α-1,6-linkages is achieved in the plant cell has been object of much speculation. Only

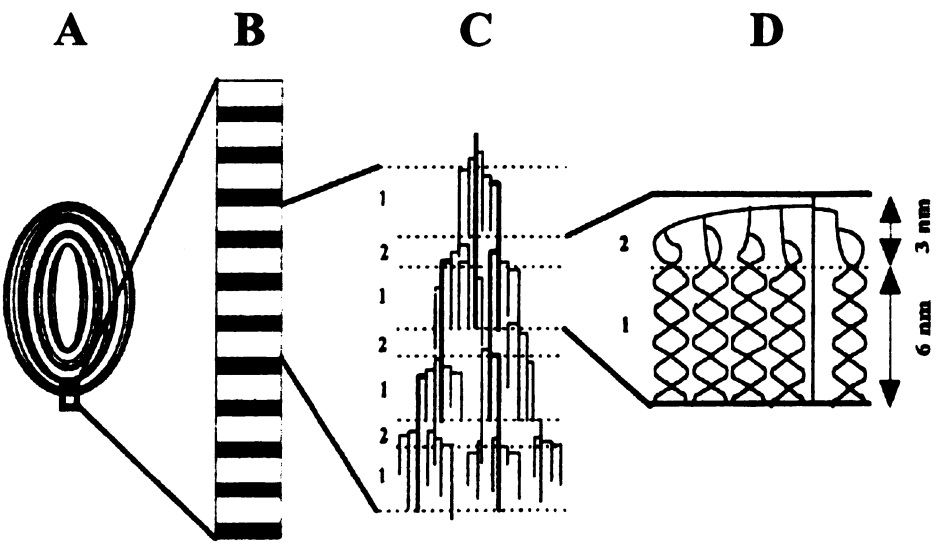

Figure 4. Overview of the starch granule organization, adapted from Ball *et al.* (36).

(A) The starch granule (1.5 μm thick) with the amorphous (dark regions) and semi-crystalline growth rings (clear regions). Each semi-crystalline growth ring consist of a repeating motif of amorphous and crystalline lamella.

(B) An enlargement of a segment of the semi-crystalline growth rings, where each amorphous and crystalline lamella is represented as a shaded or clear region, respectively.

(C) The relation between the lamella and the amylopectin structure. The dotted lines define the limits between the crystalline (1) and amorphous (2) lamella.

(D) The panel shows the helical organization of the glucan chains in the crystalline lamella (1) and the clustering of the α-1,6-branch points in the amorphous lamella.

recently have researchers gained insight into this mechanism. Work by Ball and coworkers has demonstrated a discontinuous synthesis model for amylopectin biosynthesis (36). The model is based on the *sugary* (*su1*) mutants of maize, long known to be defective in some aspect of starch biosynthesis (37). These mutants do not produce starch, but rather a glucan structure reminiscent of glycogen and was hence named phytoglycogen (38, 39). Later, the enzyme responsible for the *sugary* phenotype was demonstrated to be a defect in debranching enzyme (40-43). The model by Ball *et al* involves the action of debranching enzymes in amylopectin biosynthesis (in addition to ADP-Glc PPase, SS and BE) to perform glucan trimming of the growing carbohydrate polymer. The glucan trimming is required to generate order in the amorphous lamella for subsequent synthesis of the crystalline lattice (Figure 5). This action at the surface of the growth rings presumably prevents the formation of phytoglycogen, and allows for a continuous elongation of the highly ordered amylopectin molecule.

Although there has been much progress in understanding the structures of amylopectin and amylose, their assembly into the final starch structure is still largely unknown. A model by Lineback (31) proposes that several amylopectin molecules, each consisting of 20-40 repeating motifs of crystalline and amorph lamella, align much like the spokes of a wheel (Figure 6). The reducing ends of the C-chains are believed to face the hilum (center) of the starch granule, whereas the branches extend in a radial orientation toward the edge of the granule. In Lineback's model, the amylose is packed alongside the amylopectin, but this fails to explain how amylose is protected from branching enzyme and is not consistent with current views of its synthesis (44, 45). The amylose is now believed to pack in the amorphous regions, where it is protected from the

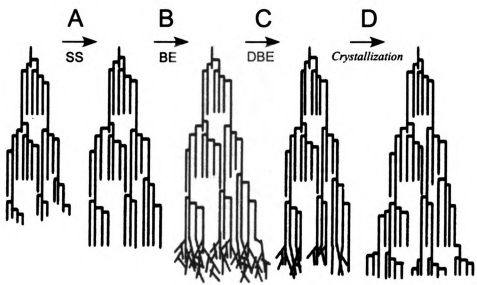

Figure 5. Discontinuous synthesis model for amylopectin biosynthesis, adapted from Ball *et al.* (36). (A) The chains of amylopectin in the water-soluble, amorphous lamella are elongated by starch synthases (SS). (B) When the chains are sufficiently long to serve as substrate, branching enzymes (BE) perform extensive random branching of the polymer. (C) Debranching enzymes (DBE) work simultaneously to trim the loosely branched glucans. (D) The trimming by DBE will enable crystallization of elongated chains and the remaining branches will form the next amorphous lamella.

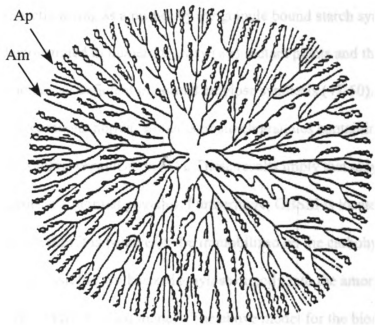

Figure 6. Model of the organization of amylose (Am) and amylopectin (Ap) in the starch granule as proposed by Lineback (31). The reducing termini of the C-chains face the hilum (center) of the starch granule, and the amylopectin polymers align radially towards the edge of the starch granule. In this particular model, the amylose is proposed to pack parallel to and between the amylopectin molecules.

starch branching enzymes, that have been found located in the stroma near the edge of the starch granule by electron microscopy (46). Furthermore, the packing of amylose in the amorphous lamella is consistent with its proposed biosynthesis. Amylose is synthesized from amylopectin acting as a primer by the granule bound starch synthase I (GBSSI), as has been demonstrated in numerous *waxy* (*wx*) mutant plants and the *sta2* mutant of Chlamydomonas, all deficient in normal amylose synthesis (47-50). The *waxy* ($GBSSI^-$) mutants all accumulate normal amounts of starch granules containing amylopectin with wild-type crystalline organization (34). These results imply that amylose is not required for the biogenesis of normal granules. Furthermore, GBSSI is located throughout the starch granule where it is believed to be immobilized on the carbohydrate matrix, thus being able to deposit the synthesized amylose directly into the amorphous lamella (see Figure 9 in ref. 44 for detailed model). The above model for the biogenesis of storage starch (here greatly simplified) is currently the most favored by researchers, but is by no means a complete description, as many questions remain unanswered. The exact roles of the many different enzyme isoforms in starch biosynthesis remains to be determined, and it is very likely that additional enzymes and isoforms, yet undiscovered, are involved in the making of starch.

1.3. Other components of starch.

In addition to carbohydrate, the starch granule contains small amounts (0.2-0.5 %) of protein (including the enzymes of starch biosynthesis) and 0.5-1.0 % of lipids. Also, some amylopectins, notably amylopectin from potato tubers, are known to be phosphorylated, with up to 1 phosphate per 300 glucose residues (51).

1.4 Bacterial Glycogen.

In this report, we will only consider glycogen from bacteria, as its metabolism in mammals differs completely. However, the biosynthetic pathway of bacterial glycogen shares many features of plant starch biosynthesis, as described below. Many bacteria will store glycogen as a carbohydrate reserve when cell growth is slow and carbon is in abundance. The rate of glycogen accumulation is often highest in the stationary phase, when growth ceases due to depletion of a nutrient such as nitrogen, sulfur, or phosphate (see review in ref. 52). *E. coli* B in particular, has been shown to accumulate large amounts of glycogen in nitrogen-limited media with glucose as the carbon source (53). However, the inability of bacteria to synthesize glycogen is not lethal, and bacteria deficient in the glycogen biosynthetic enzymes grow as well as their normal parent strains. The glycogen is generally considered an energy-storage polymer, which becomes rapidly degraded upon carbon starvation. One example is glycogen-containing *E. coli* cells that have prolonged viability in media with no exogenous carbon source compared to their glycogen-less counterparts (54). Also, for some spore-forming bacteria, the glycogen may have a role as endogenous source of carbon and energy for spore formation as seen in *Bacillus cereus* (52, 55).

Glycogen is similar to amylopectin by being α-1,4 linked and α-1,6 branched. Glycogen is more branched than amylopectin with approximately 10 % α-1,6 glucosidic linkages and a degree of polymerization (d.p.) of about 10^4 units. Perhaps the most significant difference between the structure of glycogen and amylopectin is that amylopectin is a highly organized semi-crystalline molecule. In contrast, glycogen has a random arrangement of regular branching lengths, making the smaller glycogen granule

highly water-soluble. It is possible to calculate the maximum size attainable by the glycogen granule before steric hindrance impairs further growth. Those calculations are in good agreement with the size (~25 nm in diameter) measured for these particles (56). Thus, the highly water-soluble glycogen and the semi-crystalline starch differ mainly by the decreased branching observed in the plant polysaccharide and its asymmetric distribution of the α-1,6-linkages.

It is widely accepted that the glycosyl donor in biosynthesis of bacterial glycogen is ADP-glucose and that the pathway consists of three enzymes: ADP-Glucose pyrophosphorylase, glycogen synthase and branching enzyme (52, 57, 58). These enzymes are believed to be necessary and sufficient for glycogen biosynthesis, although the presence of a bacterial glycogenin-like protein was hypothesized in the 1970s (59), but later proofed incorrect (60). However, some bacteria can form α-glucans from sucrose or maltose by amylosucrase and amylomaltase, respectively (52, 61, 62). These enzymes are not believed to be significant in α-glucan formation under normal conditions, as they are scarce in bacteria and their enzymatic activities repressed in presence of glucose (52). The ADP-Glc PPase, glycogen synthase and branching enzyme is each encoded by a single gene in bacteria (63, 64). This contrasts the equivalent enzymes in plants, where multiple isoforms are always found (2). Probably this difference can be attributed to the higher degree of control and regulation needed in plant starch biosynthesis and the increased complexity of the storage polymer. Furthermore, the allosteric regulation of the key enzyme ADP-Glucose PPase differs between bacteria and plants, as will be discussed in detail below.

Several plant enzymes involved in starch biosynthesis have been expressed in *E. coli*, including ADP-Glc PPase (65, 66), Starch Synthase (67), and Branching enzyme (68, 69). Of particular interest was the complementation by recombinant maize starch BE isoforms of the *E. coli* mutant AC71 (*glgb*$^-$) lacking the endogenous branching enzyme (70). These experiments failed to reproduce the typical asymmetric pattern of amylopectin *in E. coli*, but resulted instead in glycogen-like products. These experiments clearly demonstrate the biosynthesis of starch is more complex and probably involves more enzymes, than the glycogen biosynthesis of bacteria.

2. Biosynthesis of Starch and Bacterial Glycogen

Glycogen synthesis in bacteria and starch synthesis in plants follow similar pathways and have at least three enzymes in common: ADP-Glc pyrophosphorylase, glycogen synthase or starch synthase, and branching enzyme (Figure 7). First, ADP-glucose pyrophosphorylase activates a glucose molecule by forming the sugar-nucleotide ADP-glucose. Glycogen/starch synthase elongates the growing α-glucan chain by forming an α-(1,4) glucosidic linkage between the activated sugar and a primer. Finally, branching enzyme catalyses the formation of branch points by cleavage and transfer of the α-1,4 glucan chain to α-1,6 branch points.

As will be discussed in detail, ADP-glucose pyrophosphorylase is an allosteric regulated enzyme and is considered a major regulatory step in the rate of glycogen and starch synthesis in bacteria and plants, respectively (2). It is thought that the specificities of glycogen/ starch synthases and branching enzymes are mainly responsible for the

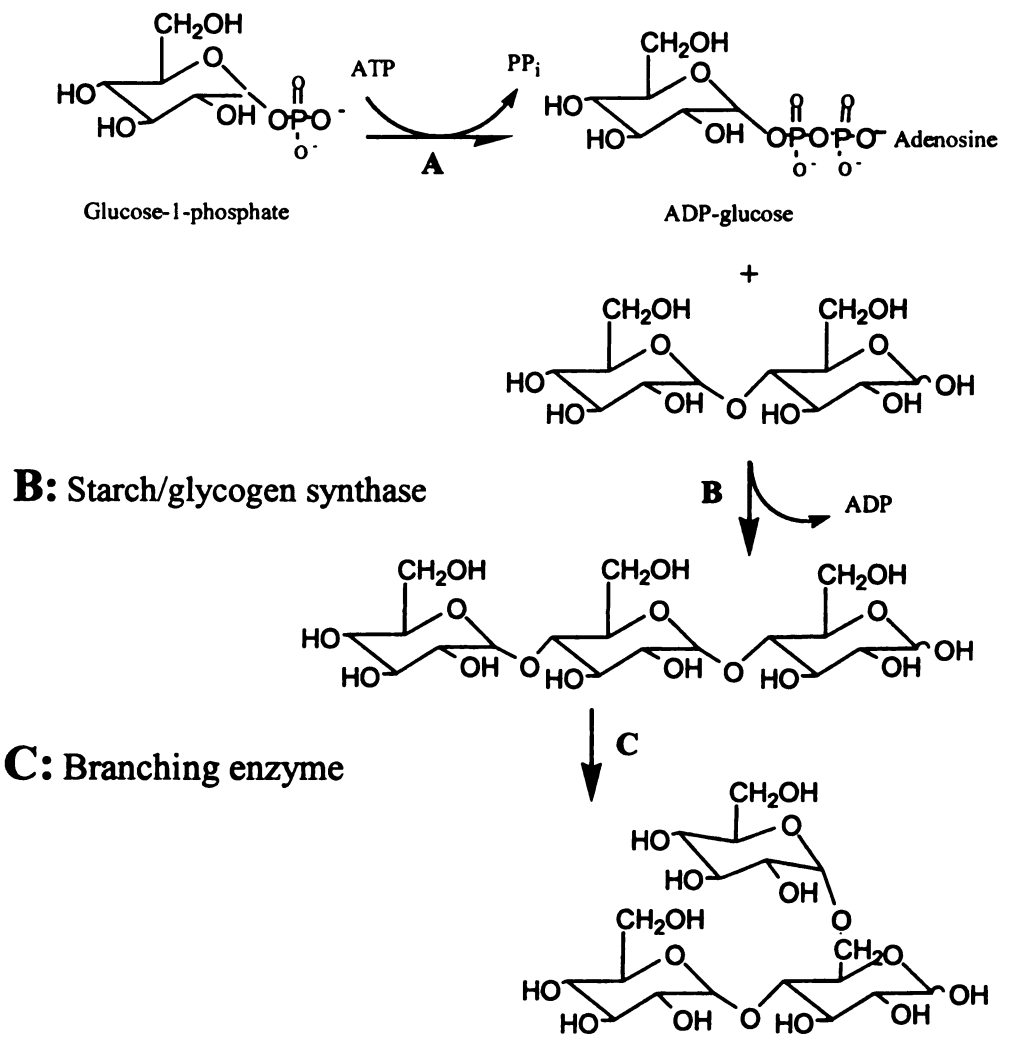

Figure 7. Biosynthetic pathway of starch and bacerial glycogen. ADP-glucose pyrophophorylase catalyzes the formation of ADP-glucose (A), which is added on to a primer by starch/ glycogen synthase (B). Branching enzyme then forms the branch points of amylopectin and glycogen.

different structures of glycogen and starch. A brief summary of our current level of understanding of these enzymes is provided next.

3. Starch/ Glycogen Synthase.

In bacterial systems (e.g. *E. coli*) only one glycogen synthase isoform has been found (71), whereas in plants there are at least four different starch synthase genes and therefore four different enzymes (67, 72). Some starch synthases are bound to the starch granule (granule bound starch synthases, GBSS), while others are found in the soluble portion of the cell extracts (soluble starch synthases, SSS). It is not clear whether some of the soluble and granule bound starch synthases are indeed the same proteins. The roles of each of these starch synthases in the synthesis of the starch granule components, amylose and amylopectin, is not well understood. However, plants defective in one or more starch synthase genes suggest the various soluble and granule bound starch synthases have different roles in amylose and amylopectin biosynthesis. Probably the most studied, and best understood starch synthase is GBSSI which now is well established as being involved in amylose biosynthesis (see section 1.2). The role of the various soluble starch synthases remains confusing, especially as the different SSS isoforms appear to dominate in various plant systems (73). For example, *in vitro* measurements of SSS activity from maize indicate SSSI as the dominant activity, whereas similar experiments in pea and potato tuber found SSSII and SSSIII, respectively, as having the greatest enzyme activity (74). It is clear that more work is needed, but as the native α-glucan primers are yet uncharacterized and the specificities of SSS isoforms partly overlap, this remains a challenging research subject.

Until recently, the only 1,4 α-D-glucan synthase reported to be cloned and over-expressed was the *E. coli* and *S. typhimurium* enzymes (71, 75). The *E. coli* enzyme can be purified to homogeneity with good yield, which has facilitated biochemical analysis including studies using chemical modification, kinetic measurements, and site-directed mutagenesis (76-78). Crystallization of the recombinant *E. coli* glycogen synthase (GS) has also been attempted, but with limited success (Binderup and Preiss, unpublished results). Glycogen synthase is associated with the glycogen in *E. coli* and released by α-amylase treatment during its purification (76). The resulting maltooligosaccharides in the purified enzyme preparation are speculated to inhibit formation of protein crystals due to microheterogeneity. The expression of GS in the glycogen-less *E. coli* mutant strain G6MD3 (deficient in ADP-Glc PPase) should therefore be performed.

The bacterial enzyme shows several regions of similarity with plant starch synthases. Chemical modification studies and site-directed mutagenesis of the *E. coli* enzyme has demonstrated the ADP-Glc binding site to be located at the amino terminal of the protein, specifically at a conserved Lys-X-Gly-Gly motif (76-78). Furthermore, Holmes and Preiss (79) have described chemical modification of GS with the sulfhydryl specific reagents iodoacetate and 5,5' dithiobis-2-nitrobenoiz acid (DTNB). ADP or ADP-glucose protected the enzyme against iodoacetate, whereas glycogen protected the enzyme against DTNB. The results indicated two distinct Cys residues may be located at or near the binding site for ADP-glucose and glycogen. Besides these observations structure-function information of this enzyme remains very limited.

4. Branching Enzyme.

4.1 Assay of Branching Enzyme Activity.

There are several assays available for measuring branching activity. The iodine stain assay (Figure 8) is based on the decrease in absorbance of a glucan-iodine complex with increased branching (80). Although the assay is quite insensitive it allows for testing of different substrate (i.e. maltodextrins, amyloses, and amylopectins). The phosphorylase stimulation assay (Figure 9) is based on incorporation of ^{14}C labeled glucose into α-glucan as branching enzyme increases the number of non-reducing ends (81). Although an indirect measure of branching activity, the phosphorylase stimulation assay is very sensitive and the assay that best imitates the function of branching enzyme *in vivo*. The branching linkage assay is the most quantitative assay (82), as its determines the number of branching events on an amylose substrate, making the assay suitable for kinetic studies (Figure 10). After branching of the substrate, the chains transferred by BE are cleaved at the α-1,6-branch points by isoamylase and the reducing ends detected by a modified Park-Johnson method (83). Alternatively, the cleaved chains can be analyzed by gel-filtration or high performance anion exchange chromatography (HPAEC) to determined by transferred chain pattern by branching enzyme (Figure 10). For a complete characterization of branching enzyme it is best to employ all three assays. However, it is important to work with enzyme preparations free from α-glucan degradative enzymes, as these interfere with all three branching enzyme assays.

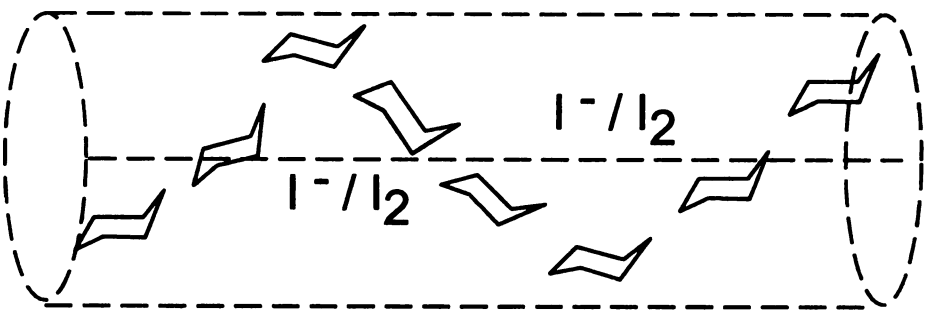

Helical Iodine / α-D-glucan complex

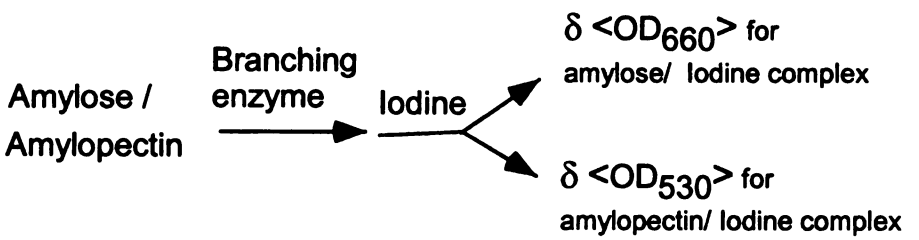

Fig. 8. The iodine stain assay (assay C). The substrate, amylose or amylopectin, is branched by branching enzyme. This gives rise to a lower absorbance of the helical iodine/α-D-glucan complex. The wavelengths used are 530 nm and 660 nm for amylopectin and amylose, respectively.

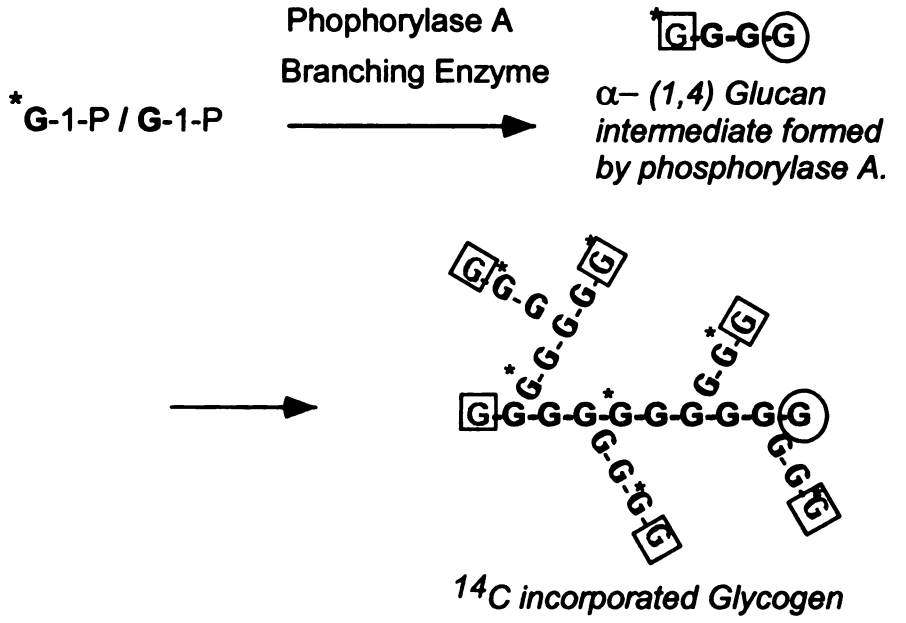

Fig. 9. The phosphorylase A stimulation assay (assay A). Phosphorylase A elongates a primer from the non-reducing end [G] . Branching enzyme produces for each branch point an additional non-reducing terminal, which then phosphorylase A elongates further. The synthesized polymer has incorporated ^{14}C-labeled glucose (*G). The reducing end is indicated (G)

Figure 10. The branching linkage assay (assay B) and high performance anion exchange chromatography (HPAEC). The α-(1,6) linkages are introduced into the amylose substrate by branching enzyme. After heat inactivation of the reaction mixture, the polymer is debranched by isoamylase, producing one reducing terminal, illustrated as an encircled G, per chain. In assay B, the reducing termini are quantified by a modified Park-Johnson method. In HPAEC and gel filtration analysis, the distribution of the transferred chains is monitored.

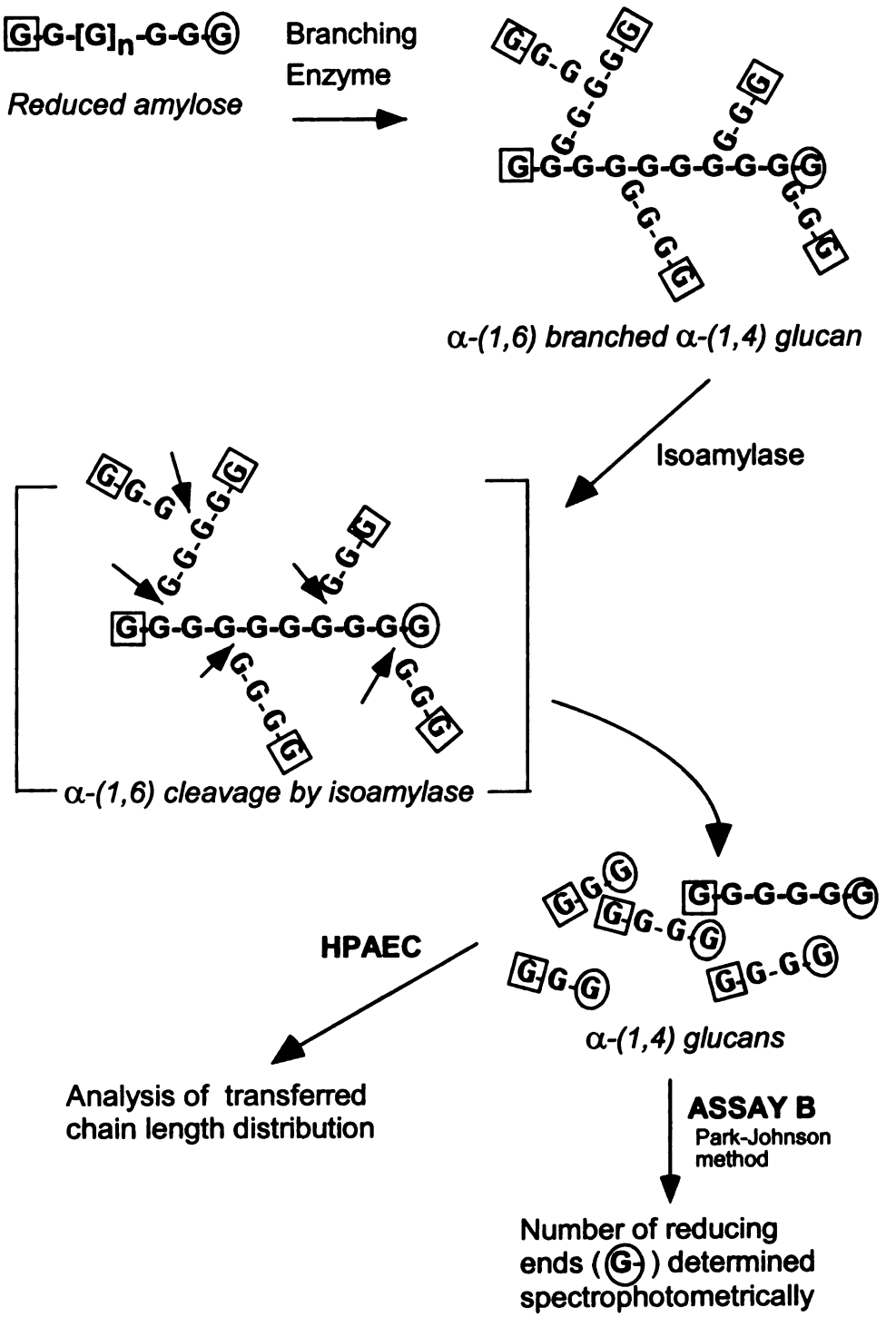
G-G-[G]n-G-G-G
Reduced amylose
Branching Enzyme
α-(1,6) branched α-(1,4) glucan
Isoamylase
α-(1,6) cleavage by isoamylase
HPAEC
Analysis of transferred chain length distribution
α-(1,4) glucans
ASSAY B
Park-Johnson method
Number of reducing ends (G-) determined spectrophotometrically

4.2 Branching Enzyme Isoforms

Branching enzymes from a variety of sources have been identified and described, including *E. coli* (84, 85), maize (86, 87), and rice endosperm (88, 89). In contrast to bacteria, multiple isoforms of the branching enzyme, encoded by distinct genes, have been reported for many plants, including maize, rice, and Arabidopsis (81, 85, 89, 90). These isoforms appear to fall into two classes of branching enzymes that can distinguished by their biochemical properties (91). Class I branching enzymes transfer long α-glucan chains and have a relative high activity with amylose as substrate. Members of class I branching enzymes include maize isoform I, pea isoform B, rice isoform I, and potato isoform II. Class II branching enzymes transfer short α-glucan chains and preferentially use amylopectin as substrate. Members of class II branching enzymes include maize isoform II, pea isoform A, rice isoform III, and potato isoform I.

The division of branching enzymes into classes according to their biochemical properties, and their proposed distinct roles in starch synthesis, evolved from studies of the maize branching enzyme isoforms. The investigation of the mode of chain transfer and substrate specificity in the maize endosperm branching enzyme I (mBEI) and branching enzyme II (mBEII; 91) led to the hypothesis that these enzymes have different roles in the synthesis of amylopectin *in vivo*. The mBEI can transfer long branches (d.p. 40 to 100) whereas mBEII transfers shorter chains (d.p. 6 to 14). Furthermore, the preferred substrate for mBEI is amylose, whereas mBEII prefers amylopectin. The differences between mBEI and mBEII isoforms suggest that mBEI first branches the growing α-glucan polymer transferring long chains and mBEII, in turn, uses this product for further branching to amylopectin. There are also mutant plants deficient in class II

branching enzymes that support this theory. Both the *rugosus* (*r*) mutant of pea, originally used in genetic crossing experiments by Mendel (92-94), and the *amylose extender* (*ae*) mutants of maize and rice (95, 96) are deficient in class II BE activity. Total starch content in these plants are reduced by 20 % in maize and 50 % in pea, and the amylopectin content is lowered from ~70 % to ~30 %. The amylopectin in these mutants has longer branches than the wild-type plants, and the degree of polymerization is reduced. The effect of the *ae* and *r* mutations on starch synthesis furthermore suggest that class I branching enzymes cannot fully compensate for loss of class II branching enzyme activity.

In addition to the distinct biochemical properties of class I and class II branching enzymes there are differences in the primary structures of the proteins. Enzymes from the two families are structurally similar and related to glycogen branching enzymes of bacteria. However, class II branching enzymes contain an extension of ~50 residues at the amino terminal compared to class I enzymes. Very recent work has demonstrated that deletion of 39 residues of this extension in mBEII lowers the specific activity to ~70 % of wild-type levels, whereas the substrate specificity and chain transfer pattern is unaltered (97). These results may indicate this extension is not responsible for the different properties of the two branching enzyme families.

4.3 Structure-Function Relationships.

There is no three-dimensional structure of branching enzyme available, although the crystallization of a truncated *E. coli* branching enzyme has been reported (98). This report was published simultaneously with our work on the limited proteolysis of *E. coli*

branching enzyme (99; Chapter 4). However the study by Hilden *et al* (98) was limited in its biochemical analysis of the truncated branching enzyme, and the poor diffraction quality of the crystal form (4.1 Å at the EPS synchrotron source) makes it an unsuitable candidate for a three-dimensional structure.

Although the structure of a branching enzyme has not been determined, its homology to amylolytic enzymes, defined as enzymes involved in cleavage and/ or transfer of α-glucans, has provided important information about its structure- function relationships. Several structures of amylolytic enzymes including α-amylase, cyclodextrin glucanotransferase, isoamylase, and pullulanase have been solved, and all consist of a central α/β-barrel structure (100-103). Alignments and secondary structure prediction of branching enzyme show this protein also conforms to this structure. This allows for prediction of which residues are involved in catalysis, as the catalytic residues of α/β-barrels are typically found in the loops interconnecting each central β-strand with the following α-helix (104).

Homology between branching enzymes and other amylolytic enzymes was first described by Romeo *et al.* (64). Later it was established that branching enzymes belonged to the family of amylolytic enzymes as they contain four highly conserved regions that are also found in α-amylases, pullulanase, isoamylase and cyclodextrin glucanotransferases (CGTase; 105, 106). Figure 11 shows a schematic representation of some branching enzymes and an alignment of the four conserved regions found in all amylolytic enzymes. The four conserved regions contain seven amino acids invariantly found in all amylolytic enzymes, and these residues have been targeted for site-directed mutagenesis studies.

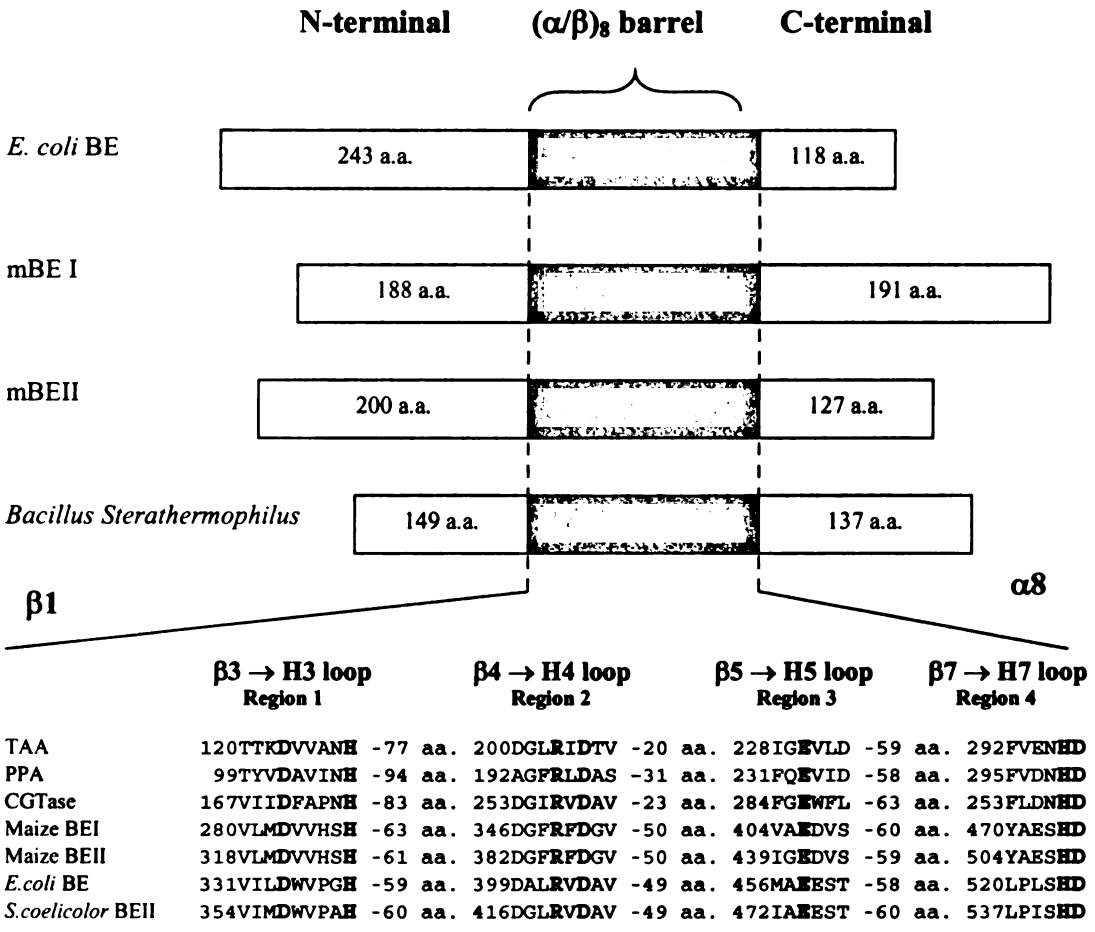

Figure 11. Shematic representation of some branching enzymes from plants and bacteria. The central $(\alpha/\beta)_8$ barrel is shaded gray. The N- and C-terminal extensions relative to the barrel are indicated for each protein. The lower part of the figure shows the four highly conserved regions shared between enzymes of the amylolytic family, including four branching enzymes. The location of each region in the $\beta \rightarrow \alpha$ loops of the $(\alpha/\beta)_8$ barrel is indicated. The 7 residues of region 1-4 that are completely conserved in the α-amylase family, are indicated in bold letters. Key: TAA, Taka α-amylase; PPA, porcine pancreatic α-amylase; CGTase, cyclodextrin glucano-transferase.

Site-directed mutagenesis of the two conserved Asp residues in region 2 and 4 and the Glu residue of region 3 indicate these amino acids are important for branching activity (107, 108). These three residues are proposed to be catalytic residues in the amylolytic family, based on the crystal structures and biochemical evidence from α-amylase, CGTase, and pullulanase (100-102, 109). Although the exact role of these residues in branching enzyme is unknown, the site-directed mutagenesis studies indicate that part of the mechanism in all these enzymes is shared.

Chemical modification of mBEII with phenylglyoxal, a reagent specific for arginine, caused inactivation of the enzyme (110). The phenylglyoxal inactivation could be prevented by the presence of amylose during the experiment, suggesting a potential role in substrate binding. Subsequently, the Arg residue of region 2 (R384 in mBEII) was targeted for site-directed mutagenesis studies (111). All substitutions produced inactive enzymes, except the conservative substitution R384K, which retained 5 % of wild-type activity. However, kinetics of the purified R384K mutant indicated only a minor increase in K_m of the amylose substrate (111). Thus, whereas the Arg of region 2 appears to play an important role in branching enzyme catalysis, it may not be directly involved in substrate binding.

Chemical modification of mBEII with the histidine specific reagent diethylpyrocarbonate caused rapid inactivation of mBEII, but the inactivation could be prevented by the presence of amylose (112). Treatment of the diethylpyrocarbonate-inactivated enzyme with hydroxylamine rapidly restored the enzyme activity. The conserved His residues of regions 1 and 4 (H320 and H508 in mBEII, respectively) were individually substituted by Ala *via* site-directed mutagenesis (112). Kinetic data of the

purified mutants H320A and H508A showed little effect on V_{max}, but a 10-fold increase in K_m. Thus, the results suggested an important role of the conserved histidine residues in substrate binding.

The proposed functions for the conserved residues described above correlate well with site-directed mutagenesis of α-amylase and cyclodextrin glucanotransferase as well as their three-dimensional structures (100, 101, 109). Apart from these regions there is limited sequence homology between various branching enzymes. Typically the similarity is 25-40 % identity across species and 40-70 % between isozymes from the same source.

All branching enzymes contain extension as the N- and C-termini relative to the central α/β-barrel domain (113, 114). In contrast to the central α/β-barrel, these extension are not well conserved between different branching enzymes. For example, between the maize isoforms mBEI and mBEII, the sequence identity is 58 % overall but 67 % in the central α/β-barrel doimain. Kuriki *et al* investigated the roles of these extensions by construction of chimeric enzymes out of mBEI and mBEII (115). A chimeric enzyme with the N-terminal and central α/β-barrel of mBE II and the C-terminal domain of mBEI produced an active enzyme with the chain transfer pattern of mBEII and the substrate specificity of mBEI (115). These results suggest that the C-terminal domain is involved in substrate specificity and the N-terminal and/ or central α/β-barrel region is involved in chain transfer action of branching enzymes. Although the study was limited by the large number of inactive chimeric constructs, these results has provided much insight into which domains are responsible for the properties of branching enzymes.

5. ADP-Glucose Pyrophosphorylase.

5.1 Allosteric Regulation.

The reaction of ADP-Glc PPase was first described in 1962 by Espada in soya bean (116) and was subsequently found in many plant tissues and bacterial extracts (reviewed in ref. 2, 6, and 52). The enzyme is highly regulated but its specificity toward the effectors depends upon the source of the enzyme. ADP-Glc PPase from most bacteria requires the glycolytic intermediate fructose 1,6-bisphosphate (FBP) for optimal activity and is inhibited by adenosine monophosphate (AMP; 58). The presence of FBP may be considered as an indicator of carbon in excess of energy need, acting as a signal that under these circumstances, carbon may be used for an energy storage compound. Conversely, AMP can be considered to indicate a low energy-charge of the cell, where synthesis of energy storage compounds should be repressed. The enzyme from cyanobacteria and almost all higher plant sources is activated by 3-phosphoglyceric acid (3-PGA) and is inhibited by orthophosphate (Pi; 117, 118). A high ratio of 3-PGA/ Pi is observed during photosynthetic carbon fixation, which produces 3-PGA as the first stable product in many plants, meanwhile the Pi concentration is low due to photophosphorylation. Thus, it appears that in many cases there is a correlation between the nature of the activator seen for the organism's ADP-Glc PPase and its major assimilation pathway.

The activator can have multi-fold effect on enzyme activity, either increasing V_{max} and/ or lowering the K_m of the enzyme for the substrates. In addition, the activator can reverse the effect of the allosteric inhibitor. The concentration for half-maximal activation ($A_{0.5}$) and inhibition ($I_{0.5}$) for ADP-Glc PPase is generally of the order of μM.

5.2 ADP-Glucose Pyrophosphorylase is a Tetramer.

Studies on the subunit structure of ADP-Glc PPases have been carried out to some extent (58, 66). For all bacterial and cyanobacterial enzymes studied so far, the native enzyme is a homotetramer (α_4) with a subunit mass of approximately 50 kDa. In contrast, the plant enzyme consists of two related but distinct subunits having masses in the 50-60 kDa range forming a $\alpha_2\beta_2$ structure (119). The smaller subunit (50-55 kDa) is highly conserved with an amino acid sequence identity of 85-95% across plant species. In contrast, different larger subunits (50-60 kDa) are less conserved (50-60%; 120). When the small and large subunit from the same plant are compared, the identity is typically in the range of 50-60%.

Recent experiments indicate that the plant small subunit is the catalytic subunit, as it has enzymatic activity when expressed alone. The large subunit functions by modulating the regulatory properties of the small subunit (Table 1; 66, 121). The large subunit does not have any detectable catalytic activity when expressed in absence of the small subunit.

Table 1: Properties of potato tuber small subunit and the native enzyme.

	Potato small (α_4)	Potato small + large ($\alpha_2\beta_2$)
Specific Activity	50 U/ mg	100 U/ mg
$A_{0.5}$ for 3-PGA	2.4 mM	160 μM
$I_{0.5}$ for Pi (in presence of 3 mM 3-PGA)	80 μM	640 μM

From Ballicora *et al.* (66). Enzymes were purified to homogeneity. Assay was in ADP-Glc synthesis direction.

The potato tuber small subunit expressed in absence of the large subunit forms a stable α_4 structure with high enzymatic activity. The α_4 enzyme is less sensitive to the activator 3-PGA and more sensitive to the inhibitor, Pi, compared to the native enzyme. Thus, a possible role for the plant large subunit in potato tuber is to increase the sensitivity for the activator and decrease the sensitivity for the inhibitor. Table 2 presents a matrix of amino acid sequence identity/ similarity of various ADP-Glc PPases based on pair-wise alignments. The enzymes from heterotrophic bacteria are highly conserved (80-98 %) but only 30-35 % identical to the enzyme from cyanobacteria and plants. However, the enzymes of bacterial and plants do exhibit many conserved domains (Figure 12). There are regions where the relationship between the bacterial and plant enzymes is minimal or nonexistent, and both bacterial and plant enzymes exhibit significant identity among themselves. Examples of this include the extreme N-terminal and C-terminal regions of the enzyme. One might speculate that the universally conserved regions are catalytic while the regions conserved only in plants or bacteria are regulatory elements. As discussed below, a large number of biochemical data supports this argument.

5.3 Structure of the Pyrophosphorylase Domain.

There is no reported structure of ADP-glucose pyrophosphorylase. However, recent work has produced the three-dimensional structure of the *E. coli* N-acetylglucosamine 1-phosphate uridylyltransferase (GlmU) involved in the biosynthesis of peptidoglycan in bacteria (122). The crystal structure of a truncated form of *E. coli* GlmU was solved to 2.25 Å and 2.3 Å resolution for the apo-GlmU and

Table 2: Matrix of amino acid sequence identity/ similarity of ADP-glucose pyrophosphorylases.

	E.coli	*Anabeana*	Ara, small	Ara, large	Pot, small	Pot, large
E.coli	-	0.35/0.47	0.35/0.48	0.27/0.39	0.32/0.43	0.30/0.43
Anabeana	-	-	0.66/0.75	0.61/0.72	0.66/0.75	0.60/0.71
Ara, small	-	-	-	0.50/0.61	0.87/0.88	0.51/0.63
Ara, large	-	-	-	-	0.51/0.63	0.63/0.74
Pot, small	-	-	-	-	-	0.51/0.63

Scores are based on pair-wise sequence comparisons.

Ara, small: Arabidopsis small subunit; Ara, large: Arabidopsis large subunit; Pot, large: Potato tuber small subunit.

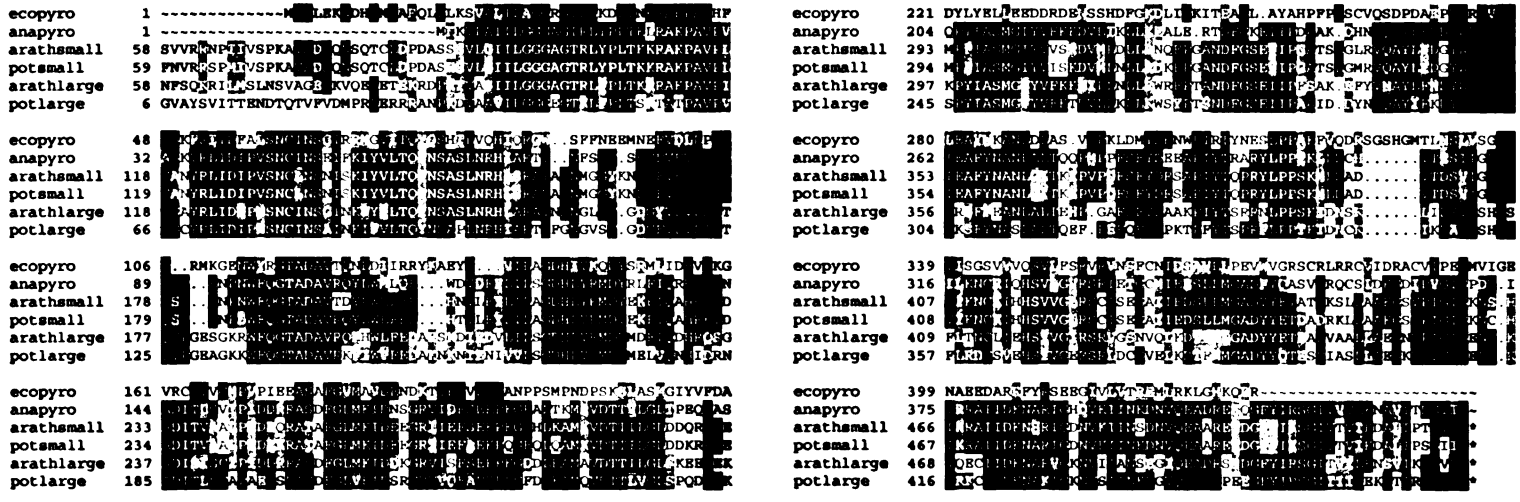

Figure 12. Amino acid alignment of several ADP-glucose pyrophosphorylases. Conserved positions (50 % identity or higher) are highlighted by use of the software Boxshade. A conserved residue is shaded in black and conservative substitutions are shaded in grey. Key to sources of ADP-glucosepyrophosphorylases: ecopyro: *E. coli*; anapyro: Anabaena; arathsmall: *Arabidopsis thaliana* small subunit; arathlarge: *Arabidopsis thaliana* leaf large subunit; potsmall: potato tuber small subunit; potlarge: potato tuber large subunit.

GlmU/UDP-GlcNAc complex, respectively. GlmU is a bifunctional enzyme that catalyzes two reactions in presence of $MgCl_2$:

(1) GlcN-1-P + acetyl-CoA → GlcNAc-1-P + CoA

(2) GlcNAc + UTP → UDP-GlcNAc + PPi

The first reaction involves an acetyltransferase activity, whereas the second reaction involves a pyrophosphorylase activity to synthesize the nucleotide-activated form of N-acetylglucosamine. The truncated GlmU, for which the crystal structure was solved, is defective in acetyltransferase activity but has normal uridylyltransferase activity (122). Biochemical experiments have shown GlmU is organized into two domains (123): The pyrophosphorylase domain is encoded by the N-terminal (Asn3-Asn227) of GlmU and shares homology with other pyrophosphorylases, whereas the C-terminal encodes the acetyltransferase domain with 23 times the hexapeptide repeat (LIV)-(GAED)-X_2-(STAV)-X typical of bacterial acetyltransferases (124). The alignment of *E. coli* GlmU with ADP-Glc PPases from diverse sources shows the conservation of several residues, although the overall homology is weak (Figure 13). However, secondary structure predictions of ADP-Glc PPases closely match the actual structure of the GlmU pyrophosphorylase domain (125), which further validates GlmU as a prototypic template for the pyrophosphorylase superfamily. The alignment only spans the N-terminal part of ADP-Glc PPase, which encompasses the proposed active site (125). The remaining ADP-Glc PPase sequence is probably involved in its allosteric regulation based on biochemical evidence, as discussed in a later section.

Figure 13. Amino acid sequence alignment of ADP-glucose pyrophosphorylases and N-acetylglucoseamine 1-phosphate uridylyltransferase. Only the amino terminal regions that share homology are shown. Several residues of *E. coli* N-acetylglucoseamine 1-phosphate uridylyltransferase with proposed involvement in substrate binding or catalysis are indicated in bold.

GlmU: *E. coli* N-acetylglucoseamine 1-phosphate uridylyltransferase. Sources of ADP-glucose pyrophosphorylases: anabe: *Anabaena*; stuss: Potato tuber small subunit; agrob: *Agrobacterium*; r_sph: *Rhodospirilum*; ecoli: *E. coli*; bst_c: *Bacillus stearothermophilus*. Consen: consensus sequence of ADP-glucose pyrophosphorylases.

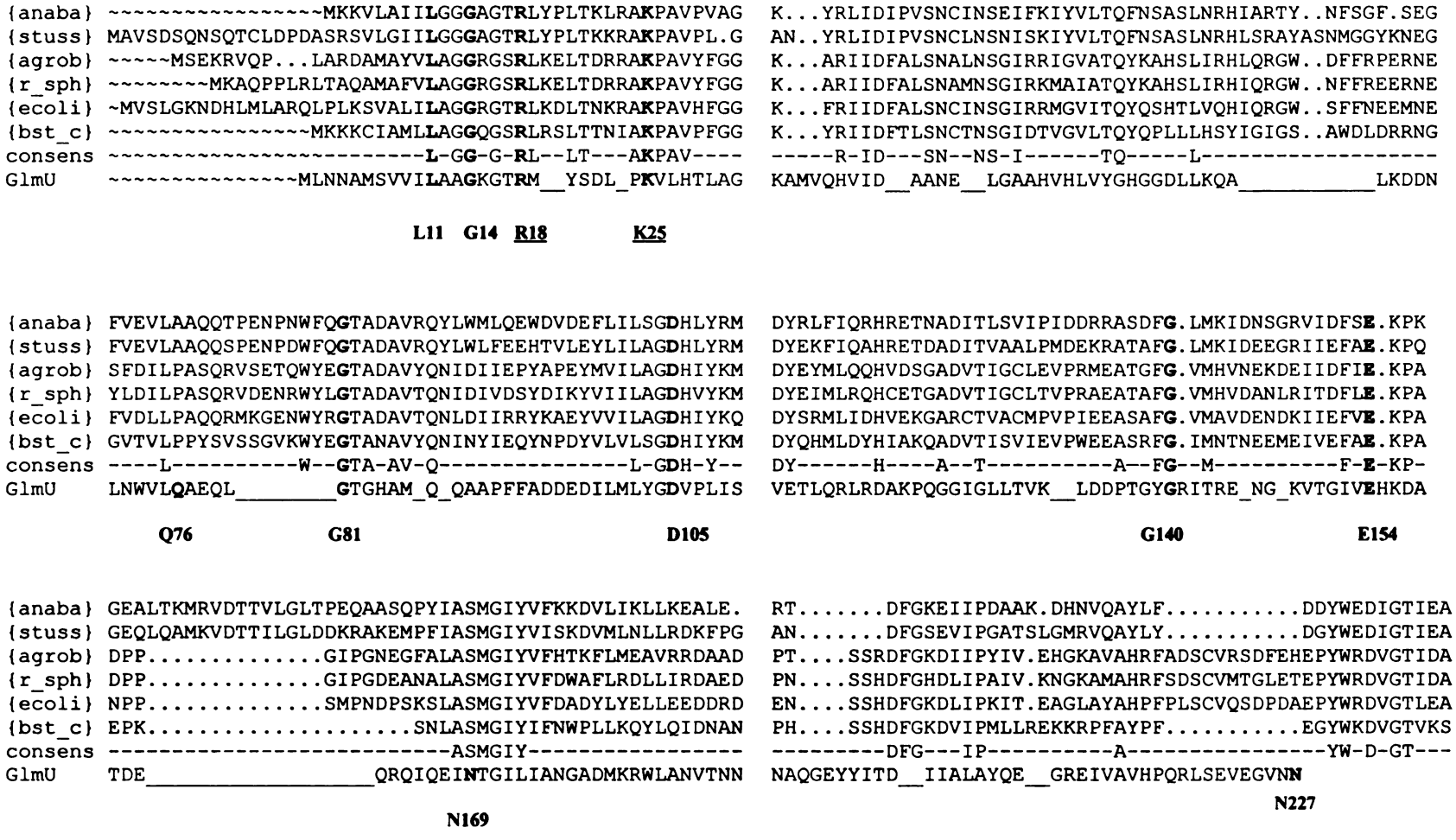
{anaba} ~~~~~~~~~~~~~~~~~MKKVLAIILGGGAGTRLYPLTKLRAKPAVPVAG K...YRLIDIPVSNCINSEIFKIYVLTQFNSASLNRHIARTY..NFSGF.SEG
{stuss} MAVSDSQNSQTCLDPDASRSVLGIILGGGAGTRLYPLTKKRAKPAVPL.G AN..YRLIDIPVSNCLNSNISKIYVLTQFNSASLNRHLSRAYASNMGGYKNEG
{agrob} ~~~~~MSEKRVQP...LARDAMAYVLAGGRGSRLKELTDRRAKPAVYFGG K...ARIIDFALSNALNSGIRRIGVATQYKAHSLIRHLQRGW..DFFRPERNE
{r_sph} ~~~~~~~~MKAQPPLRLTAQAMAFVLAGGRGSRLKELTDRRAKPAVYFGG K...ARIIDFALSNAMNSGIRKMAIATQYKAHSLIRHIQRGW..NFFREERNE
{ecoli} ~MVSLGKNDHLMLARQLPLKSVALILAGGRGTRLKDLTNKRAKPAVHFGG K...FRIIDFALSNCINSGIRRMGVITQYQSHTLVQHIQRGW..SFFNEEMNE
{bst_c} ~~~~~~~~~~~~~~~~MKKKCIAMLLAGGQGSRLRSLTTNIAKPAVPFGG K...YRIIDFTLSNCTNSGIDTVGVLTQYQPLLLHSYIGIGS..AWDLDRRNG
consens ~~~~~~~~~~~~~~~~~~~~~~~~~~L-GG-G-RL--LT---AKPAV---- -----R-ID---SN--NS-I------TQ-----L------------------
GlmU ~~~~~~~~~~~~~~~MLNNAMSVVILAAGKGTRM__YSDL_PKVLHTLAG KAMVQHVID__AANE__LGAAHVHLVYGHGGDLLKQA_____LKDDN
L11 G14 R18 K25
{anaba} FVEVLAAQQTPENPNWFQGTADAVRQYLWMLQEWDVDEFLILSGDHLYRM DYRLFIQRHRETNADITLSVIPIDDRRASDFG.LMKIDNSGRVIDFSE.KPK
{stuss} FVEVLAAQQSPENPDWFQGTADAVRQYLWLFEEHTVLEYLILAGDHLYRM DYEKFIQAHRETDADITVAALPMDEKRATAFG.LMKIDEEGRIIEFAE.KPQ
{agrob} SFDILPASQRVSETQWYEGTADAVYQNIDIIEPYAPEYMVILAGDHIYKM DYEYMLQQHVDSGADVTIGCLEVPRMEATGFG.VMHVNEKDEIIDFIE.KPA
{r_sph} YLDILPASQRVDENRWYLGTADAVTQNIDIVDSYDIKYVIILAGDHVYKM DYEIMLRQHCETGADVTIGCLTVPRAEATAFG.VMHVDANLRITDFLE.KPA
{ecoli} FVDLLPAQQRMKGENWYRGTADAVTQNLDIIRRYKAEYVVILAGDHIYKQ DYSRMLIDHVEKGARCTVACMPVPIEEASAFG.VMAVDENDKIIEFVE.KPA
{bst_c} GVTVLPPYSVSSGVKWYEGTANAVYQNINYIEQYNPDYVLVLSGDHIYKM DYQHMLDYHIAKQADVTISVIEVPWEEASRFG.IMNTNEEMEIVEFAE.KPA
consens ----L----------W--GTA-AV-Q---------------L-GDH-Y-- DY------H----A--T----------A--FG--M----------F-E-KP-
GlmU LNWVLQAEQL_____GTGHAM_Q_QAAPFFADDEDILMLYGDVPLIS VETLQRLRDAKPQGGIGLLTVK__LDDPTGYGRITRE_NG_KVTGIVEHKDA
Q76 G81 D105 G140 E154
{anaba} GEALTKMRVDTTVLGLTPEQAASQPYIASMGIYVFKKDVLIKLLKEALE. RT.....DFGKEIIPDAAK.DHNVQAYLF.....DDYWEDIGTIEA
{stuss} GEQLQAMKVDTTILGLDDKRAKEMPFIASMGIYVISKDVMLNLLRDKFPG AN.....DFGSEVIPGATSLGMRVQAYLY.....DGYWEDIGTIEA
{agrob} DPP.....GIPGNEGFALASMGIYVFHTKFLMEAVRRDAAD PT....SSRDFGKDIIPYIV.EHGKAVAHRFADSCVRSDFEHEPYWRDVGTIDA
{r_sph} DPP.....GIPGDEANALASMGIYVFDWAFLRDLLIRDAED PN....SSHDFGHDLIPAIV.KNGKAMAHRFSDSCVMTGLETEPYWRDVGTIDA
{ecoli} NPP.....SMPNDPSKSLASMGIYVFDADYLYELLEEDDRD EN....SSHDFGKDLIPKIT.EAGLAYAHPFPLSCVQSDPDAEPYWRDVGTLEA
{bst_c} EPK.....SNLASMGIYIFNWPLLKQYLQIDNAN PH....SSHDFGKDVIPMLLREKKRPFAYPF.....EGYWKDVGTVKS
consens ----------ASMGIY---------- ---------DFG---IP----------A----------YW-D-GT---
GlmU TDE_____QRQIQEINTGILIANGADMKRWLANVTNN NAQGEYYITD__IIALAYQE__GREIVAVHPQRLSEVEGVNN
N169 N227

The structure of the GlmU pyrophosphorylase domain consists of a central seven-stranded mixed β-sheet surrounded by 6 α-helices, 3 on each side of the β-sheet (Figure 14A). The uridylyltranserase active site, identified by the presence of soaked UDP-GlcNAc, is in a large open pocket. This 21 Å long and 13 Å deep pocket is formed by two lobes: The first lobe consists of residue Asn3-Val111 and the surface loop His216-Asn227, whereas the second lobe consists of the remaining residues of the pyrophosphorylase domain (Figure 14A,B). The interaction between GlmU and the substrate UDP-GlcNAc is shown in detail in Figure 14C,D. The first lobe exposes Leu11, Gly14, Gly16, Arg18, and Lys25 towards the pocket along with Gln76-Thr82. The second lobe exposes the region Gly138-Asp157 to the pocket, whereas the floor of the active site is made from the regions Tyr103-Asp105 and Val223-Asn227. The sugar and nucleotide moieties of UDP-GlcNAc contacts the protein, whereas the phosphate groups are totally solvent accessible. Based on the structure and biochemical evidence, the authors propose Arg18 and possibly Lys25 as catalytic residues, which are conserved in all ADP-Glc PPases (Figure 13). However, the article does not propose a catalytic mechanism for the enzyme. The assigned amino acids for nucleotide binding are Leu11, Ala13, Gln76, and Asp105, where the leucine and aspartate residues are also found in ADP-Glc PPases. The sugar-binding site of GlmU is composed of Gly81, Asp105, Tyr139, Glu154, Asn169, Tyr197, and Thr199. In ADP-Glc PPase we only find Gly81, Asp105 and Glu154 as being uniquely conserved. It is possible the sequence variations between ADP-Glc PPases and GlmU of the above residues are largely due to their different substrate specificity, whereas catalytic residues and amino acids important for substrate interaction but not sugar- or nucleotide recognition are strictly conserved in the enzyme family. Certainly,

Figure 14. Structure of the pyrophosphorylase domain of N-acetylglucosamine 1-phosphate uridylyltransferase. Adapted from, Brown *et al* (122). This figure is presented in color.

(A) Ribbon diagram of the pyrophosphorylase domain showing the first lobe (Asn3-Val111) in blue and the second lobe (Glu112-Gln213) in magenta, the bound UDP-GlcNAc in orange and the consensus motif including Arg18 and Lys25 in red.

(B) Electrostatic potential mapped on the molecular surface from –7kT (red) to +7kT (blue) with the bound UDP-GlcNAc within the pocket.

(C) A close-up view of the pyrophosphorylase domain (orientation as in Figure 14A) with UDPGlcNAc (orange), and the side chain residues Arg18, Lys25 (catalytic residues; red), Leu11, Ala13, Gln76, and Asp105 (nucleotide binding site; pink), Gly81, Asp105, Tyr139, Glu154, Asn169, Tyr197, and Thr199 (sugar binding site, green) and Gln193, Glu195, Asn227, and Gln231 (yellow).

(D) Superposition of the apo-GlmU (yellow) and the GlmU/UDP-GlcNAc complex (green). Backbone regions that deviate significantly are highlighted with their side chains. A rigid-body motion of regions Val131-Gln166 and Val187-Tyr197 is observed, along with significant movements of Tyr103, Tyr139 and Gln193 side chains within the active site.

A

B

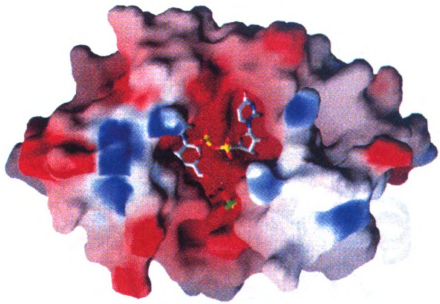

C

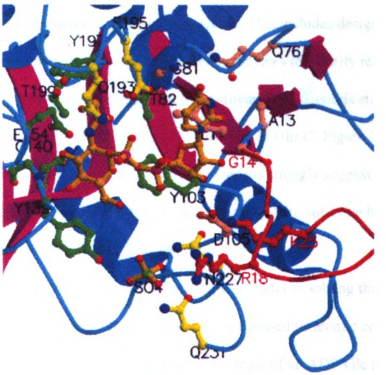
Y197
E195
Q76
S81
T199
Q193
T82
A13
G14
Y105
T27/R18
Q231

D

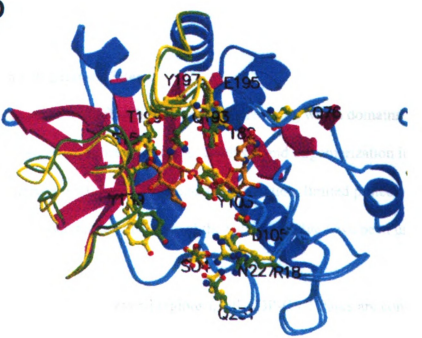
Y197
E195
T27/R18
Q231

the conservation of multiple residues proposed in substrate binding and/or catalysis suggests there is a shared mechanism between XDP pyrophosphorylases and that useful information can be extracted from studying GlmU. This includes design of site-directed mutagenesis experiments of the ADP-Glc PPase enzymes to identify residues important for catalysis and substrate binding. In fact, site-directed mutagenesis studies of *E. coli* ADP-Glc PPase residue D142 that aligns with D105 of GlmU (Figure 13) is currently being performed in our laboratory. Preliminary results strongly suggest that D142 of *E. coli* ADP-Glc PPase has a direct role in catalysis rather than substrate binding as proposed by the authors of the GlmU structure.

The structure of GlmU may even serve as a model in solving the crystal structure of ADP-Glc PPase, although the authors have not released its atomic coordinates. Still, the known topology of GlmU will facilitate the tracing of an ADP-Glc PPase electron density map.

5.4 Active and Regulatory Sites.

A large amount of effort has focused on answering which domains are responsible for allosteric regulation, substrate binding, catalysis, and oligomerization in the ADP-Glc PPases. Site-directed mutagenesis, chemical modification, limited proteolysis, and chimeric enzyme construction are some of the techniques that have been used to address these questions.

As discussed above, several regions in all ADP-Glc PPases are conserved. When the invariant residue K195 (Figure 15) in the *E. coli* enzyme was subjected to site-directed mutagenesis, the apparent affinity ($S_{0.5}$) for Glc-1-P decreased dramatically,

suggesting involvement in Glc-1-P binding (126). When the equivalent position in the potato tuber small subunit (K198) was changed to Arg, Ala or Glu, the $S_{0.5}$ for G-1-P decreased 135-550 fold, while the apparent affinities for allosteric effectors and other substrates were unaffected (127). Of importance is the conservation of this Lys in GlmU (as Lys156; Figure 13) but it has not been assigned a function in this enzyme, nor has the authors described its conservation. However, it is in close proximity to GlmU residue Glu154 involved in binding of the sugar moiety.

ecopyro	EFVE**K**PANPP
anapyro	DFSE**K**PKGEA
arathsmall	EFSE**K**PKGEH
potsmall	EFAE**K**PQGEQ
arathlarge	SFSE**K**PKGDD
potlarge	QFAE**K**PKGFD

Figure 15. G-1-P binding site of ADP-Glc PPase. The *E. coli* ADP-Glc PPase residue K195 and equivalent positions are indicated in bold letters. Refer to legend of Figure 12 for key to sources of ADP-Glc PPases.

Interestingly, mutagenesis of the equivalent lysine, K213, in the *large* subunit of potato tuber had no effect on the $S_{0.5}$ for G-1-P, and thus it seems unlikely that the large subunit participates in Glc-1-P binding (127). These results are consistent with the small subunit being involved in catalysis and the large subunit being a modulator of the regulatory properties of the small subunit of plant ADP-Glc PPases.

The site for ATP binding has been investigated by chemical modification using the substrate analog 8-azido-AMP with the *E. coli* enzyme (128). The major binding site of 8-azido-AMP was found in the region indicated in Figure 16, specifically at the Y114 residue. When the residue Y114 was changed by site-directed mutagenesis to phenylalanine, a 10-20 fold effect on $S_{0.5}$ for ATP was seen, but the apparent affinities for other substrates and allosteric effectors was changed as well (129). Furthermore, this Y114 is not conserved, as the plant ADP-Glc PPases have a Phe residue at this position and GlmU has a deletion in this particular region. These results indicate that Y114 probably is not the ATP binding site, although it may be close to it.

```
ecopyro          Q..RMKGENW YRGTADAVTQ
anapyro          QTP..ENPNW FQGTADAVRQ
arathsmall       QSP..ENPNW FQGTADAVTD
potsmall         QSP..ENPDW FQGTADAVRQ
arathlarge       QTPGESGKRW FQGTADAVRQ
potlarg          QTPGEAGKKW FQGTADAVRK
```

Figure 16. Proposed ATP binding site of ADP-Glc PPase. Residue Y114 of *E. coli* ADP-Glc PPase and the equivalent positions are indicated in bold letters. Refer to legend of Figure 12 for key to sources of ADP-Glc PPases.

Pyridoxal phosphate (PLP) has been found to be an activator of many ADP-Glc PPases (52, 130, 131). PLP probably mimics the 2 phosphate groups of FBP and the phosphate and carboxylate group of 3-PGA, respectively (132). Using PLP in chemical modification experiments it was found that residue K39 in the *E. coli* enzyme, K440 in the small subunit of spinach leaf enzyme and K419 of the *Anabaena* enzyme was

involved in the binding of their respective activators. Further studies by PLP modification showed that also K382 of the *Anabaena* enzyme (131) and the equivalent lysine in the spinach leaf *large* subunit (130) was involved in activation. In conclusion, there appears to be two activator sites for 3-PGA in the C-terminal (Figure 17). Site-directed mutagenesis studies on the potato tuber enzyme have showed that the activator sites in the small subunit are more important than the equivalent sites in the large subunit (121).

	Activator site 1	Activator site 2
ecopyro	NAEEDARRFY RSEEGIVLVT	~~~~~~~~~~ ~~~~~~
anapyro	IRRAIIDKNA RIGHDVKIIN	VVVLKNAVIT DGTII~
arathsmall	IKRAIIDKNS RIGDNVKIIN	VTVIKDALIP TGTVI*
potsmall	IKRAIIDKNA RIGDNVKIIN	VTVIKDALIP SGIII*
arathlarge	IQECIIDKNA RVGKNVIIAN	TVILKNSVIK DGVVI*
potlarge	IRKCIIDKNA KIGKNVSIIN	IIILEKATIR DGTVI*

Figure 17: Activator sites of cyanobacterial and plant ADP-Glc PPases. Refer to legend of Figure 12 for key to sources of ADP-Glc PPases.

Limited proteolysis by proteinase K of *E. coli* ADP-Glc PPase in presence of Mg^{2+}, ADP-Glc, and FBP, generated an enzyme with 10 to 13 amino acids removed at the N-terminal and 2 amino acids removed at the C-terminal (133). This truncated enzyme was almost independent of FBP for maximal activity and insensitive to AMP inhibition, whereas the apparent affinities for substrates were unaltered. Using genetic engineering, an enzyme (N_{d1-11}, Figure 18) lacking the first 11 amino acids was constructed and found to have properties identical to the proteolyzed enzyme (134).

```
                    1         10
E. coli native      MVSLEKNDH LMLARQLP
E. coli Nd1-11                LARQLP
```

Figure 18: *E. coli* ADP-Glc PPase N_{d1-11}.

The 11 amino acids that appear to be important for allosteric regulation contain a lysine residue (K6 of *E. coli* enzyme) found in several bacterial ADP-Glc PPases which are activated by FBP. It remains to be determined by site-directed mutagenesis if this lysine residue can be changed with resulting loss of allosteric regulation. However, the above results suggest that elements at the N-terminal are involved in allosteric regulation of bacterial enzymes.

In a study by Sheng and Preiss (135), the *Anabaena* enzyme was treated with the arginine specific reagent phenylglyoxal, which resulted in a time- and concentration dependent loss of activity. The inhibitor phosphate most effectively protected the enzyme from phenylglyoxal inactivation. Five arginine residues conserved in higher plant- and cyanobacterial ADP-Glc PPases (but not in bacterial enzymes) were individually changed to alanine. This approached produced a mutant R294A with 100-fold lower affinity for the inhibitor in the presence of activator, 3-PGA, and 40-fold in absence of activator. Because the R294A substitution had little impact on the kinetic constants for substrates and activator, these results suggest that R294 is specifically involved in inhibitor binding (Figure 19). However, when the potato tuber small subunit was subjected to site-directed mutagenesis at the equivalent position (Figure 19), the resulting mutant showed no effect on phosphate sensitivity but unexpectedly lowered 5-10 fold the apparent affinity for

3-PGA (136). Clearly, more work is needed in order to locate exactly what the phosphate binding site is, and why the effect of changing this residue apparently differs between cyanobacteria and plants.

```
ecopyro          YNESLPPAKF
anapyro          RARYLPPTKL
arathsmall       QPRYLPPSKM
potsmall         QPRYLPPSKM
arathlarge       SRRNLPPSKI
potlarge         SPRFLPPTKI
```

Figure 19: Proposed *Anabaena* Phosphate binding site. Residue R294 and conserved equivalent positions are indicated in bold letters. Refer to legend of Figure 12 for key to sources of ADP-Glc PPases.

The ADP-Glc PPases of a number of allosteric mutants have been cloned (137-139). In almost all cases these mutations occur at sites different from the allosteric and substrate binding sites. Thus the regions where the mutations occur may be involved in maintaining the conformation of the inactive WT enzyme (T state in Monod's allosteric model; 140). Here, I will only describe the ADP-Glc PPase mutant deduced from *E. coli* strain 618, which accumulates 300 % more glycogen than the WT (*E. coli* K-12) strain (138). The nucleotide sequence of the ADP-Glc PPase gene showed a mutation, resulting in a substitution of G336 to aspartate (Figure 20). The single mutation G336D was solely responsible for the altered allosteric properties, as determined by site-directed mutagenesis of the WT enzyme to G336D. G336D had identical kinetics to the enzyme of

strain 618 (139). G336D has a 5-fold lower $A_{0.5}$ for FBP and a 12-fold higher $I_{0.5}$ for AMP compared to the WT enzyme. In addition, only a 2-fold activation by FBP was observed compared to a 35-fold activation as seen by the WT enzyme (141). Thus, the substitution G336D appears to result in "conformational steering" towards the active form (R-state) compared to the WT enzyme.

E.coli G336D	TLNSLVS**D**GC
E.coli WT	TLNSLVS**G**GC
anapyro	VTESIIGEGC
arathsmall	VTDSVIGEGC
arathlarge	LIDSIISHGS

Figure 20: Position of G336 of *E. coli* ADP-Glc PPase, indicated in bold. Refer to legend of Figure 12 for key to sources of ADP-Glc PPases.

References

1. Hizukuri S. (1995) *in* Carbohydrates in Food (Elliasson, A.C, Ed.) Acad. Press, NY. pp. 347-428.
2. Preiss, J. and Sivak, M.N. (1998) *in* Comprehensive Natural Products Chemistry (Pinto, B.M, Ed.) Pergamon Press, Oxford, Vol. 3, pp. 441-495.
3. Sivak, M.N. and Preiss, J. (1998) Advances in Food and Nutrition Research, Academic Press, San Diego, CA., Vol 41.
4. Smith, A.M., Denyer, K., and Martin, C. (1997). *Annu. Rev. Plant Phisiol. Plant. Mol. Biol.* **48**, 67-87.
5. Nelson, O.E. and Pan, D. (1995) *Plant Mol. Biol.* **46**, 475-496.
6. Preiss, J. (1991) *Oxf. Surv. Plant. Mol. Cell Biol.* **7**, 59-114.
7. Lin, T.P., Casper, T., Sommerville, C. Preiss, J. (1988). *Plant Physiol.* **86**, 1131-1135.
8. Heldt, H.W., Flugge, U.I. and Borchert, S. (1991) *Plant Physiol.* **95**, 341-343.
9. Heldt, H.W. and Flugge, U.I. (1987) *in* Biochemistry of Plants (Stumpf, P.K. and Conn, E.E., Eds.) Academic Press, NY, Vol. 12, pp. 49-85.
10. Badenhuizen, N.P. (1965) *in* The Biogenesis of Starch Granules in Higher Plants. Appleton-Century Crofts, NY.
11. Tyson, R.H. and ap Rees, T. (1988) *Planta* **175**, 33-38.
12. Hill, L.M. and Smith, A.M. (1991) *Planta* **185**, 91-96.
13. Viola, R., Davies, H.V. and Chudeck, A.R. (1991) *Planta* **183**, 202-208.
14. Preiss, J. (1988) *in* The Biochemistry of Plants. (Preiss, J., Ed.) Academic Press, NY. Vol. 14, pp. 181-254.
15. Okita, T.W. (1992) *Plant Physiol.* **100**, 560-564.

16. Liu, T.T. and Shannon, J.C. (1981) *Plant Physiol.* **67**, 525-529.

17. MacDonald, F.D. and ap Rees, T. (1983) *Phytochemistry* **22**, 1141-1143.

18. Keeling, P.L., Wood, J.R., Tyson, R.H., and Bridges, I.G. (1988) *Plant Physiol.* **87**, 311-319.

19. Pozueta-Romeo, J., Ardila, F. and Akazawa, T. (1991) *Plant Physiol.* **97**, 1565-1572.

20. Ball, S., Marianne, T., Dirick, L., Fresnoy, M., Delrue, B., and Decq, A. (1991) *Planta* **185**, 17-26.

21. Muller-Rober, B., Sonnewald, U. and Willmitzer, L. (1992) *EMBO J.* **11**, 1229-1238.

22. Stark, D.M., Timmerman, K.P., Barry, G.F., Preiss, J., and Kishore, G.M. (1992) *Science* **258**, 287-292.

23. Preiss, J. Sivak, M. (1995) *in* Seed Development and Germination 1st ed., Marcel Dekker, NY. pp. 139-168.

24. Manners, D.J. (1989) *Carbohydr. Polym.* **11**, 87-112.

25. Detherage, W.L., MacMasters, M.M., and Rist, C.E. (1955) *Trans. Am. Assoc. Cereal. Chem.* **13**, 31-42.

26. Gallant, D.J., Bouchet, B., and Baldwin, P.M. (1997) *Carbohydr. Polym.* **32**, 177-191.

27. Jenkins, P.J., Cameron, R.E., and Donald, A.M. (1993) *Starke* **45**, 417-420.

28. Nikuni, Z., *Chorikagaku* **2**, 6-23.

29. French, D. (1972) *Denpun Kagaku* **19**, 8-33.

30. Hizukuri, S. (1986) *Carbohydr. Res.* **147**, 342-347.

31. Lineback, D. R. (1984) *Baker's Dig.* **58**, 16-21.

32. Katz, J.R. and Van Italie, T.B. (1930) *Z. Phys. Chem. Abt.* **A150**, 90-100.

33. Hizukuri, S. (1985) *Carbohydr. Res.* **141**, 295-306.

34. Buleon, A., Gallant, D.J., Bouchet, B., Mouille, G., D'Hulst, C., Kossman, J., and Ball, S.G. (1998) *Plant Physiol.* **115**, 949-957.

35. Smith, A.M. and Martin, C. (1993) *in* Biosynthesis and Manipulation of Plant Products (Grierson, D., Ed.) Blackie Academic and Prof. Pub. Glascow. Vol. 3, pp. 1-54.

36. Ball, S., Guan, H.P., James, M., Myers, A., Keeling, P., Mouille, G., Buleon, A., Colonna, P., and Preiss, J. (1996) Cell **86**, 349-352.

37. Correns, C. (1901) *Bibl. Bot.* **53**, 1-161.

38. Sumner, J.B. and Somer, G.F. (1944) *Arch Biochem.* **4**, 4-7.

39. Erlander, S. (1958*) Enzymologia* **19**, 273-283.

40. Nakamura, Y., Umemoto, Y., Takahata, Y., Komae, K., Amano, E., and Satoh, H. (1996) *Plant Physiol.* **97**, 491-498.

41. James, M.G., Robertson, D.S., and Myers, A.M. (1995) *Plant Cell* **7**, 417-429.

42. Mouille, G., Maddelein, M.L., Libessart, N., Talaga, P., Decq, A., Delrue, B., and Ball, S. (1996) *Plant Cell* **8**, 1353-1366.

43. Nakamura, Y. (1996) *Plant Sci.* **121**, 1-18.

44. Van de Wal, M. D'Hulst, C., Vincken, J.P., Buleon, A., Visser, R., and Ball, S. (1998) *J. Biol. Chem.* **273**, 22232-22240.

45. Maddelein, M.L., Libessart, N., Bellanger, F., Delrue, B., D'Hulst, C., Koornhuyse, N., Bossu, J.P., Fontaine, T., Wieruszeski, J.M., Decq, A., and Ball, S. (1994) *J. Biol. Chem.* **269**, 25150-25157.

46. Kram, A.M., Ooertergetel, G.T., and Van Bruggen, E.F.J. (1993) *Plant Physiol.* **101**, 237-243.

47. Nakamura, T., Yamamori, M., Hirano, H., Hirada, S., and Nagamine, T. (1995) *Mol. Gen. Genet.* **248**, 253.

48. Delrue, B., Fontaine, T., Routier, F., Decq, A., Wieruszeski, J.M., Koornhuyse, N., Maddelein, M.L., Fournet, B., and Ball, S. (1992) *J. Bacteriol.* **174**, 3612-3620.

49. Weatherwax, P. (1922) *Genetics* **7**, 568-572.

50. Murata, T., Sugiyama, T., and Akazawa, T. (1965) *Biochem. Biophys. Res. Comm.* **18**, 371-376.

51. Takeda, Y. and Hizukuri, S. (1982) *Carbohydr. Res.* **102**, 312-327.

52. Preiss, J. (1984) *Ann. Rev. Microbiol.* **38**, 419-458.

53. Holme, T. (1957) *Acta Chem. Scand.* **11**, 763-775.

54. Strange, R.E. (1958) *Nature* **220**, 606-607.

55. Slock, J.A. and Stahly, D.D. (1974) *J. Bacteriol.* **120**, 399-406.

56. Geddes, R. (1985) *in* The Polysaccharides (Aspinall, G.O., Ed) Academic Press, Sandiego, CA. Vol. 3, pp. 283-336.

57. Recondo, E. and Leloir, L.F. (1961) *Biochem Biophys Res. Comm.* **6**, 85-88.

58. Preiss, J., Shen, L., Greenberg, E. and Gentner, N. (1966). *Biochemistry* **5**, 1833-1845.

59. Barengo, R., Flawia, M., and Krisman, C.R. (1975) *FEBS Lett.* **53**, 274-278.

60. Kawaguchi, K., Fox, J., Holmes, E., Boyer, C., and Preiss, J. (1978) *Arch. Biochem Biophys.* **190**, 385-397.

61. Hestrin, S. (1960) *in* The Bacteria (Gunsalus, I.C., Stanier, R.Y, Eds.) Academic Press, NY. Vol. 3, pp. 373-388.

62. Preiss, J. and Walsh, D.A. (1981) in Biology of Carbohydrates (Ginsburg, V., Robbins, P., Eds) Wiley, NY, pp. 199-314.

63. Okita, T.W., Rodriguez, R.L. and Preiss, J, (1981) *J. Biol. Chem.* **256**, 6944-6952.

64. Romeo, T., Kumar, A. and Preiss, J. (1988) *Gene* **70**, 363-376.

65. Iglesias, A.A., Barry, G.F., Meyer, C., Bloksberg, L., Nakata, P.A., Greene, T., Laughlin, M.J., Okita, T.W., Kishore, G.M. and Preiss, J. (1993). *J. Biol. Chem.* **268**, 1081-1086.

66. Ballicora, M.A., Laughlin, M.J., Fu, Y., Okita, T.W., Barry, G.F. and Preiss, J. (1995). *Plant Physiol.* **109**, 245-251.

67. Imparl-Radosevich, J.M., Nichols, D.J., Li, P., McKean, A.L., Keeling, P. and Guan, H.P. (1999) *Arch. Biochem. Biophys.* **362**, 131-138.

68. Guan, H.P., Baba, T. and Preiss, J. (1994) *Plant Physiol.* **104**, 1449-1453.

69. Guan, H.P., Baba, T. and Preiss, J. (1994) *Cell. Mol. Biol.* **40**, 981-988.

70. Guan, H.P., Kuriki, T., Sivak, M., Preiss, J. (1995) *Proc. Natl. Acad. Sci.* **92**, 964-967.

71. Kumar, A., Larsen, C. E., Preiss, J. (1986). *J. Biol. Chem.* **261**, 16256-16259.

72. Cao, H., Imparl-Radosevich, J.M., Guan, H.P., Keeling, P., James, M., and Myers, A.M. (1999) *Plant Physiol.* **120**, 205-216.

73. Martin, C. and Smith, A.M. (1995) *Plant Cell* **7**, 971-985.

74. Myers, A.M., Morell, M.K., James, M.G., and Ball, S.G. (2000) *Plant Physiol.* **122**, 989-997.

75. Okita, T.W., Rodriquez, R.L. and Preiss, J. (1981) *J. Biol. Chem.* **256**, 6944.

76. Furukawa, K., Tagaya, M., Inouye, M., Preiss, J. and Fukui, T. (1990) *J. Biol. Chem.* **265**, 2086-2090.

77. Furukawa, K., Tagaya, M., Tanaziwa, K., and Fukui, T. (1993) *J. Biol. Chem.* **268**, 23837-23842.

78. Furukawa, K., Tagaya, M., Tanaziwa, K., and Fukui, T. (1994) *J. Biol. Chem.* **269**, 868-871.

79. Holmes, E. and Preiss, J (1982). *Arch. Biochem. Biophys.* **216**, 736-740.

80. Krisman, C.R. (1962) *Anal. Biochem.* **4**, 17-23.

81. Hawker, J. S, Ozbun, J. L., Ozaki, H., Greenberg, E., Preiss, J. (1974). *Arch. Biochem. Biophys.* **160**, 530-551.

82. Takeda, Y., Guan, H. P. and Preiss, J. (1993). *Carbohydr. Res.* **240**, 253-263.

83. Hizukuri, S, Takeda, Y., Yasuda, M., and Suzuki, A. (1981) *Carbohydr. Res.* **205**-213.

84. Boyer, C. and Preiss, J. (1977). *Biochem.* **16**, 3693-3699.

85. Baecker, P.A., Greenberg, E. and Preiss, J. (1986). *J. Biol. Chem.* **261**, 8738-8743.

86. Boyer, C. and Preiss, J. (1978). *Carbohydr. Res.* **61**, 321-334.

87. Singh, B. K. and Preiss, J. (1985). *Plant Physiol.* **79**, 34-40.

88. Mizuno, K., Kawasaki, M., Shimada, H., Satoh, H., Kobayashi, E., Okumura, S., Arai, Y. and Baba, T. (1993). *J. Biol. Chem.* **268**, 19084-19091.

89. Nakamura, A., Haga, K., Ogawa, S., Kuwano, K., Kimura, K., and Yamane, K. (1992). *FEBS Lett.* **296**, 37-40.

90. Dang, P. L., and Boyer, C. D. (1988) *Phytochem.* **27**, 1255-1259.

91. Guan, H. P. and Preiss, J. (1993). *Plant Physiol.* **102**, 1269-1273.

92. Mendel, G. (1865) *Vehr. Nat. Forsh. Ver. Brunn.* **4**, 3-47.

93. Kooistra, E. (1962) *Euphytica* **11**, 357-373.

94. Bhattacharyya, M.K., Martin, C. and Smith, A.M. (1990) *Plant Mol. Biol.* **22**, 525-531.

95. Shannon, J.C. and Garwood, D.L. (1984) in Starch: Chemistry and Technology (Whistler, R.L., BeMiller, J.N., Pascall, E.F. Eds) Academic Press, Orlando, FL. pp. 25-86.

96. Mizuno, K., Kawasaki, T., Shimada, H., Satoh, H., Kobayashi, E., Okumura, S., Arai, Y. and Baba, T. (1993) *J. Biol. Chem.* **268**, 19084-1919091.

97. Hong, S., Mikkelsen, R. and Preiss, J. (2000) *Arch. Biochem Biophys.* In Press.

98. Hilden, I. Leggio, L., Larsen, S. and Poulsen, P. (2000) *Eur J Biochem.* **267**, 2150-2155.

99. Binderup, K., Mikkelsen, R. and Preiss, J. (2000) *Arch. Biochem. Biophys.* **377**, 366-371.

100. Matsuura, Y., Kusunoki, M., Harada, W. and Kakudo, M. (1984). *J. Biochem.* **95**, 697-702.

101. Buisson, G., Duee, E., Haser, R. and Payan, F. (1987). *EMBO J.* **6**, 3909-3916.

102. Klein, C. and Schulz, G. E. (1991). *J. Mol. Biol.* **217**, 737-750.

103. Katsuya, Y., Mezaki, Y., Kubota, M. and Matsuura, Y. (1998) *J. Mol. Biol.* **281**, 885-897.

104. Farber, G. and Petsko, G.A. (1990) *Trends. Biochem. Sci.* **15**, 228-234.

105. Baba, T., Kimura, K., Mizuno, K., Etoh, H., Ishida, Y., Shida, O. and Arai, Y., (1991). *Biochem. Biophys. Res. Commun.* **181**, 87-94.

106. Svensson, B. (1994). *Plant. Mol. Bio.* **25**, 141-157.

107. Kuriki, T., Takata, H., Okada, S. and Imanaka, T. (1991). *J. Bacteriol.* **173**, 6147-6152.

108. Takata, H., Kuriki, T., Okada, S.,Takesada, Y., Iizuka, M., Minamiura, N. and Imanaka, T. (1992). *J. Biol. Chem.* **267**, 18447-18452.

109. Uitdehaag, J.C.M., Mosi, R., Kalk, K.H., Van der Veen, B.A., Dijkhuizen, L., Withers, S.G. and Dijkstra, B.W. (1999) *Nat. Struc. Biol.* **6**, 432-436.

110. Cao, H. and Preiss, J. (1996) *J. Protein Chem.* **15**, 291-304.

111. Libessart, N. and Preiss, J. (1998) *Arch. Biochem. Biophys.* **360**, 135-141.

112. Funane, K., Libessart, N., Stewart, D., Michishita, T. and Preiss, J. (1998) *J. Protein Chem.* **17**, 579-590.

113. Jespersen, H.M., MacGregor, E.A., Sierks, M.R. and Svennson, B. (1991) *Biochem. J.* **280**, 51-55.

114. Janecek, S., Svennson, B. and Henrissart, B. (1997) *J. Mol. Evol.* **45**, 322-331.

115. Kuriki, T., Stewart, D.C. and Preiss, J. (1997) *J. Biol. Chem.* **272**, 28999-29004.

116. Espada, J. (1962). *J. Biol. Chem.* **237**, 3577-3581.

117. Ghosh, H.P. and Preiss, J. (1966). *J. Biol. Chem.* **241**, 4491-4504.

118. Plaxton, W. C. and Preiss, J. (1987). *Plant Physiol.* **83**, 105-112.

119. Preiss, J. (1997). *In* Engineering Improved Carbon and Nitrogen Resources. Taylor and Francis, London, pp 81-104.

120. Smith-White, B. S. and Preiss, J. (1992). *J. Mol. Evol.* **34**, 449-464.

121. Ballicora, M.A., Fu, Y., Nesbitt, N. M. and Preiss, J. (1998). *Plant Physiol.* **118**, 265-274.

122. Brown, K., Pompeo, F., Dixon, S., Mengin-Lecreulx, D., Cambillau, C. and Bourne, Y. (1999) *EMBO J.* **18**, 4096-4107.

123. Gehring, A.M., Lees, W.J., Miniola, D.J., Malsh, C.T. and Brown, E.D. (1996) *Biochemistry* **35**, 579-585.

124. Vaara, M. (1992) *FEMS Microbiol Lett.* **76**, 249-254.

125. Ballicora, M.A., Fu, Y., Wu, M., Sheng, J., Nesbitt, N.M. and Preiss, J. (1996) *in* Regulation and Manipulation of Starch and Sucrose Metabolism in Plants. (Nakamura, Y., Ed.) Tsukuba, Japan. pp 5-11.

126. Hill, M. A., Kaufmann, K., Otero, J., Preiss, J. (1991). *J. Biol. Chem.* **266**, 12455-12460.

127. Fu, Y., Ballicora, M.A. and Preiss, J. (1998). *Plant Physiol.* **117**, 989-996.

128. Lee, Y.M. and Preiss, J. (1986). *J. Biol. Chem.* **261**, 1058-1064.

129. Kumar A., Tanaka, T., Lee Y.M. and Preiss, J. (1988). *J. Biol. Chem.* **263**, 14634-14639.

130. Morell, M., Bloom, M, Preiss, J. (1988). *J. Biol. Chem.* **263**, 633-637.

131. Charng, Y., Iglesias, A.A. and Preiss, J. (1994). *J. Biol. Chem.* **261**, 1058-1064.

132. Preiss, J. (1996). Regulation of Glycogen Synthesis. In *Escherichia coli* and *Salmonella typhimurium*: Cellular and Molecular Biology, second edition, Amer. Soc. Microbiol., Washington, D.C. Vol. 1, pp. 1015-1024.

133. Wu, M. and Preiss, J. (1998). *Arch. Biochem. Biophys.* **358**, 182-188.

134. Wu, M. and Preiss, J. (2000) *Arch. Biochem. Biophys.* In Press.

135. Sheng, J., Preiss and J. (1997). *Biochemistry*, **36**, 13077-13084.

136. Ballicora, M. and Preiss, J. Unpublished results

137. Preiss, J. Romeo, T. (1989). *In* Advances in Microbial Physiology, vol. 30, pp 183-238. Academic Press, New York/ London.

138. Leung, P., Lee, Y.M., Greenberg, E., Esch, K., Boylan, S., Preiss, J. (1986). *J. Bacteriol.* **167**, 82-88.

139. Meyer, C.R., Ghosh, P., Nadler, S., Preiss, J. (1993). *Arch. Biochem. Biophys.* **302**, 64-71.

140. Monod, J., Wyman, J., Changeux, J. P. (1965). *J. Mol. Biol.* **12**, 88-118

141. Meyer, C.R., Bork, J.A., Nadler, S., Yirsa, J., Preiss, J. (1998*). Arch. Biochem. Biophys.* **353**, 152-159.

CHAPTER 2

SITE-DIRECTED MUTAGENESIS STUDIES OF TYR-300, GLU-459, and GLU-527 in *ESCHERICIA COLI* BRANCHING ENZYME.

This data has been published in two separate articles:

Binderup, K. and Preiss, J. (1998)." Glu-459 is Important for *E. coli* Branching Enzyme Function", *Biochemistry* **37**, 9033-9037.

Mikkelsen, R., Binderup, K. and Preiss, J. (2001) " Tyrosine Residue 300 is Important for Activity and Stability of Branching Enzyme from *Escherichia coli*". *Arch. Biochem. Biophys.* Accepted for publication- in press.

Abstract.

The branching enzyme belongs to the amylolytic family, a group of enzymes that cleave and/ or transfer chains of glucan. The amylolytic enzymes are homologous and all contain 4 conserved regions, proposed to contain the active site.

By primary structure analysis the 3 conserved residues Tyr-300, Glu-459, and Glu-527 in *E. coli* branching enzymes were identified. These residues are near the conserved regions 1, 2 and 4, respectively, and hence map to the active site. We used site-directed mutagenesis of the Glu-459, Tyr-300 and Glu-527 residues in the *E. coli* branching enzyme in order to determine the significance of these conserved positions. A substitution of Glu-459 to Asp resulted in increased specific activity compared to wild type, suggesting that the mutation had created a more efficient enzyme. Changing Glu-459 to Ala, Lys or Gln lowered the specific activities and altered the preferred substrate from amylose to amylopectin. Mutagenesis of Glu-527 and in particular Tyr-300 affected the enzymatic activity, indicating these residues are important for obtaining maximal branching activity. In addition, substitution of Tyr-300 to Phe was found to affect the thermal stability of branching enzyme.

Introduction

Branching enzymes catalyze the formation of α-1,6-glucosidic linkages of glycogen in bacteria (1) and of starch in plants (2). The enzyme hence plays an important role in the biosynthesis of starch and glycogen (2). Branching enzymes from a variety of sources have been identified and described including *E. coli* (3-5), maize (6-8), and rice endosperm (9, 10).

Homology between the branching enzymes and other amylolytic enzymes was first described by Romeo *et al.* (11). Subsequently, Baba *et al.* (12) established that branching enzymes contain four highly conserved regions in the central portion of the enzyme, which are thought to constitute the active site. These regions now define the amylolytic enzyme family, which includes α-amylase, pullulanase, isoamylase, cyclodextrin glucanotransferase and branching enzyme. Jespersen *et al.* (13) predicted all of the above enzymes to fold into a $(\alpha/\beta)_8$ barrel similar to that observed in the crystal structures of α-amylases (14-16) and cyclodextrin glucanotransferases (17, 18). Site-directed mutagenesis studies of the active center of neopullulanase (19) suggested that the catalytic mechanism of the amylolytic enzymes was similar (20). In branching enzyme, most of the seven amino acids invariantly found in the four conserved regions have been subjected to site-directed mutagenesis and found crucial for catalysis or substrate binding (21-23).

Even though the members of the amylolytic family may share structural features and regions of conserved amino acids, they catalyze different reactions and this poses the question of which residues are responsible for the distinct catalytic properties. This work describes studies on three conserved amino acids in branching enzymes. We investigated

the two residues Glu-459 and Glu-527, located immediately after the catalytic residues Glu-458 (region 3) and Asp-526 (region 4), respectively, hereby forming two acid pairs near the proposed catalytic site. These amino acids are not conserved in the other members of the amylolytic family. For Glu-459, we investigate the properties of the constructed *E. coli* branching enzyme mutants E459D, E459A, E459K, and E459Q and conclude that the efficiency of catalysis as well as the preferred substrate for branching activity is affected. Substitution of Glu-527 resulted in enzymes with 10-25 % of wild-type branching enzyme activity. Tyr-300 is found in all amylolytic enzymes prior to region 1, and has been proposed to play a role in substrate binding based on the crystal structures of α-amylase, isoamylase, and cyclodextrin glucanotransferase (24). We have investigated the function of this Tyr in *E. coli* branching enzyme by its replacement to Ala, Asp, Phe, Ser, and Trp. The major finding here is the dramatic loss of activity and the decreased thermal stability upon substitution of Tyr-300 with Phe.

Materials and methods

***E. coli* BE expression vector**. H.P. Guan kindly provided the plasmid pEXSB, the construction of which has been described previously (5). The pEXSB plasmid is a pET-23d derived plasmid containing the origin p15A, T7 promotor, T7 terminator, kanamycin resistance, and the *E. coli glgB* gene encoding the *E. coli* BE.

Construction of mutants. The pEXSB plasmid purified from Epicurian Coli XL2-Blue cells (Stratagene Corp., La Jolla, CA) was used as dsDNA template in site-directed mutagenesis (Quickchange site-directed mutagenesis kit, Stratagene Corp.). Oligonucleotides were synthesized using an Applied Biosystems model 380A DNA synthesizer (Macro-molecular Facility, Department of Biochemistry, Michigan State University). The mutations were confirmed by DNA sequencing and secondary mutations were ruled out by sequencing the entire gene for all constructions. DNA sequencing was done by the dideoxy chain-terminating method (25) using the dsDNA as template. The primers used were the T7 universal primers or synthetic 21-mer oligonucleotides.

Expression of wild type (WT) and mutant *E. coli* BE. An overnight culture of the transformed cells (BL21[DE3]) carrying the recombinant plasmid encoding the gene for WT BE or the constructed mutants was diluted 1:20 (v/v) in fresh Luria Broth medium containing 50 $\mu g \cdot ml^{-1}$ kanamycin. The cells were grown at 37°C to $A_{600} = 0.5$ and allowed to cool down to 25°C. Flasks were transferred to a shaker at room temperature and T7 RNA polymerase expression induced by adding isopropyl-D-thiogalactoside to 0.5 mM. After 2 hrs incubation endogenous expression was turned off by adding rifampicin to 150 $\mu g \cdot ml^{-1}$. Incubation was continued for 16 hrs at room temperature and cells were then harvested in a refrigerated centrifuge.

Purification of *E. coli* BE wild-type and mutants. The cell pastes obtained were about 1.5 g per 1 l of culture. The purification of the *E. coli* BE WT and the mutants was performed as described by Guan *et al.* (5). Protein concentration was measured with the BCA protein assay reagent (26), using BSA as the standard.

Assay of BE activity. BE activity was measured by three different assays as described by Guan and Preiss (8).

Assay A. The phosphorylase A stimulation assay is based on the stimulation by BE of the synthesis of α-D-glucan from α-D-Glc-1-P catalyzed by rabbit phosphorylase a (27). Reaction mixtures contained, in a final volume of 100 μl, 100 mM citrate (pH 7.0), 10 mM AMP, 0.2 mg phosphorylase a (Sigma Chemical Co.) and 50 mM D-[^{14}C]-Glc-1-P (50 DPM·nmol^{-1}) and were initiated by adding an appropiate amount of BE. One unit is defined as 1 μmol of Glc incorporated into α-D-glucan per min at 30°C.

Assay B. The branching linkage assay determines the number of branching points introduced by BE into the substrate, reduced amylose (28). Substrates were prepared by the reduction of enzymatically synthesized amylose (AS-320, degree of polymerization (d.p.) 1815) as described by Takeda *et al.* (28). Reaction volumes contained 25 mM MOPS (pH 7.5) and an appropriate amount of substrate in a final volume of 100 μl. The reaction was initiated by adding BE. One unit is defined as 1 μmol of branching linkages formed per min at 30°C.

Assay C. The iodine stain assay is based on measuring the decrease in absorbance of the glucan-iodine complex resulting from the branching of the substrate, amylose (potato type III [d.p. 1176, chain length (c.l.) 884]) or amylopectin (corn, Sigma Chemical Co.) (6, 8). Reaction mixtures contained 50 mM citrate (pH 7.0) and 0.1 mg

substrate in a final volume of 500 µl. The reaction was initiated by the addition of an appropriate amount of enzyme. One unit is defined as the decrease in absorbance of 1.0 per min at 30°C.

Analysis of the chain length distribution by high performance anion exchange chromatography. Reduced amylose (5 mg, AS-320, d.p. 1815) was incubated in 25 mM MOPS, pH 7.5 (500 µl) at 30°C with BE (5 mU of *E. coli* BE WT and mutants by assay b). After 1 and 4 hrs, the reaction in a 200 µl aliquot was terminated by boiling for 2 min. The synthesized α-glucan was then debranched by adding 1 M acetate buffer (pH 3.5, 20 µl) and isoamylase (10 µl, 1180 U/µl). After 90 min at 45°C the solution was boiled for 5 min. The solution was filtered through a 0.22 µm membrane and 25 µl samples injected in the HPAEC (BioLC, Dionex, Sunnyvale, CA), using a CarboPac PA-1 column (250 • 4 mm). Eluent A was 150 mM sodium hydroxide; eluent B was 150 mM sodium hydroxide containing 500 mM sodium acetate. The gradient program was: 25% eluent B (75 % eluent A) at Time 0, 45% at 15 min, 60% at 45 min, 70% at 80 min, and 80% at 100 min, with a flow rate of 0.3 $\mu l \cdot min^{-1}$. The standard was 25 µl of 5 $mg \cdot \mu l^{-1}$ maltodextrin (d.p. 1-20, Aldrich, WI).

Results

Identification of targets for mutagenesis. Figure 1 shows a partial sequence alignment of several branching enzymes from a variety of bacteria and plants. Only the sequences in the vicinity of the regions 1, 3 and 4, conserved in the amylolytic family as defined by Baba *et al.* (12), are shown. The residue immediately following E458 (*E. coli* BE numbering) in region 3 is a conserved acid in all branching enzymes, a fact first pointed out by Jespersen *et al.* (13). For prokaryotes this acid is most frequently Glu, while higher plants have Asp in this position. This residue, Glu-459, is located in the β5-H5 loop of the (α/β) barrel based on secondary structure prediction using the software PHD (29). The mutants E459A, E459D, E459K, and E459Q were constructed as described in materials and methods.

We also identified a conserved residue located immediately after the active site in region 4 (Figure 1). Position 527 in *E. coli* BE is conserved as a Glu in all bacterial branching enzymes, whereas the equivalent position in plant and other eucaryotic enzymes is conserved as Gln. Predictions show E527 maps to the center of the β7-H7 loop. The mutants E527A, E527D, E527N, and E527Q were constructed in order to probe the role of this amino acid. Finally, The Y300 residue of *E. coli* branching enzyme was targeted due to its conservation in all amylolytic enzymes, where is has been proposed to play a role in substrate binding (24). Y300 is located in the β2-H2 loop of the central (α/β) barrel domain. The mutants constructed at this site were Y300A, Y300D, Y300F, Y300L, Y300S, and Y300W.

Expression and purification of mutant enzymes. The BL21(DE3) strain used for expression of the *E. coli* BE WT and mutants is *glgB*+. This poses the problem that

		Region 3		Region 4
		E		HD
Eschericia coli (4)	296 GSWG**Y**QPTG	454	VTMAE**E**STDF	521 LPLSHD**E**VVH
Streptomyces aureofaciens (34)	331 GSWG**Y**QVTG	489	VTIAE**E**STAW	556 LPISHD**E**VVH
Bacillus stearothermophilus (35)	223 RSWG**Y**QGTG	347	LMIAE**D**STDW	428 LPFSHD**E**VVH
Bacillus caldolyticus (36)	200 RSWG**Y**QGTG	348	WMIAE**D**STDW	415 LPFSHD**E**VVH
Maize isoform I (12)	238 ASFG**Y**HVTN	403	TVVAE**D**VSGM	470 YAESHD**Q**SIV
Maize isoform II (37)	275 GSFG**Y**HVTN	437	VTIGE**D**VSGM	495 YAESHD**Q**ALV
Arabidopsis isoform II (38)	370 ASFG**Y**HVTN	533	ITVGE**D**VSGM	601 YAESHD**Q**ALV
Rice isoform I (39)	296 ASFG**Y**HVTN	460	TIVAE**D**VSGM	578 YAESHD**Q**SIV
	↓		↓	↓
	E. coli **Y300**		*E. coli* **E459**	*E. coli* **E527**

Figure 1. Partial sequence alignment of several branching enzymes from various organisms. The conserved Glu constituing region 3 and the invariant His-Asp of region 4 as defined by Baba *et al.*, (*12*) are underlined. The amino acids targeted for site-directed mutagenesis in the *E. coli* branching enzyme (Y300, E459 and E527) and their equivalent residues, are indicated in bold.

the recorded activity from the constructed mutants potentially could arise from the endogenous *E. coli* BE. Therefore, we used rifampicin during the induction to inhibit endogenous transcription. Rifampicin is a potent inhibitor of bacterial RNA polymerases (30) but does not affect the T7 RNA polymerase that transcribes the recombinant plasmid. An immunoblot with 0.2 μg crude extract of *E. coli* BE WT and the mutants showed for each, one distinct band, while the negative control (BL21[DE3] carrying plasmid pET23d) even when loaded with excess crude extract , i.e. 5 μg or even 15 μg, showed no bands (data not shown). Furthermore, the negative control lacked any detectable BE activity in the crude extract. These observations indicate rifampicin blocked the expression of endogenous branching enzyme and the detected BE activity arose solely from the expressed mutant plasmids. When compared to the original method published by Guan *et al.* (5), this method increased the specific activity of the crude extract three-fold due to less endogenous expression (data not illustrated).

The WT *E. coli* BE and the constructed mutants were purified to near homogeneity to compare their properties. All the purified proteins showed one band of about 85 kDa on a SDS PAGE gel when 1 μg was loaded on the gel. The specific activity of the WT enzyme in the phosphorylase A assay was similar compared to the 1111 $U \cdot mg^{-1}$ obtained by Guan *et al.* (5) (Tables 1 and 3).

Replacement of Glu-459. Table 1 compares the specific activities of the *E. coli* BE WT and the E459D, E459D, E459K, and E459Q mutants. Interestingly, the E459D showed a higher specific activity when compared to the WT in all assays (185%, 160%, 145%, and 140% relative to wild-type activity in the phosphorylase A assay, branching

Table 1. Specific activities of E459 mutants measured using assay A, B and C.

Assay		WT	E459D	E459A	E459K	E459Q
Phosphorylase *a*,	A	1009	1862	312	66	126
Branching linkage,[a]	B	1.1	1.8	0.21	<0.01	0.16
Iodine stain,[b]	C					
With amylose	C_1	95	139	11	1.1	10
With amylopectin	C_2	55	77	22	3.3	14.5
Ratio of activity						
	A/B	926	1064	1521	>6000	800
	A/C_1	10.6	13.4	29.4	58	12.6
	A/C_2	18.4	24.4	14.3	20.0	8.7
	C_2/C_1	0.58	0.55	2.1	2.9	1.5

[a] In the branching linkage assay the concentration of substrate AS-320 was 17 μM.
[b] C_1 and C_2 denotes the iodine stain assay with amylose and amylopectin, respectively.

linkage assay, iodine assay with amylose, and iodine assay with amylopectin, respectively).

Table 1 includes the ratios of activity for the three different assays. Guan and Preiss (8) showed that these ratios are useful for differentiation of the properties of branching enzymes. The WT and E459D enzymes have essentially similar ratios of activity, indicating that the properties of the E459D mutant are similar to the WT. The other mutants show lower specific activities as compared to WT, the E459K being the less active especially in the branching linkage assay. The C_2/C_1 ratio increases from a 0.58 in the WT to 2.1, 2.9, and 1.5 in E459A, E459K, and E459Q, respectively, meaning these mutations altered the substrate preference from amylose to amylopectin.

The kinetic properties of *E. coli* BE had not been studied previously, and a full characterization was needed for this study. Using reduced amylose AS-320 as substrate, we investigated the kinetic parameters of *E. coli* BE WT and the E459D mutant. The computed K_m values displayed in Table 2 show a lower K_m (11.7 μM) for the WT as compared to that of the E459D mutant (23.5 μM). The specific activities (V_{max} per mg of protein) were 3.7 U/mg for the wild-type and 5.9 U/mg for the E459D. The estimated specific activities as well as the high K_m of E459D are approximate due to the low solubility of amylose that does not allow the use of high concentrations of substrate. Based on this fact, the indicated specific activity of the E459D mutant is a low estimate.

The K_m and specific activities for the maize branching enzymes have been published previously with assays using AS-320 as substrate (31). The reported K_m values were 59 μM for both mBEI and mBEII but due to a computational error in amount of substrate, these numbers are off by a factor of 7. The corrected values for K_m are 8.4 μM

for both mBEI and mBEII. The specific activity was 3.3 U/mg for mBEI and 0.62 U/mg for mBEII. Therefore, the kinetic parameters of *E. coli* BE WT closely resembles the mBEI. Fersht (32) defined the substrate specificity as K_{cat}/ K_m. This ratio is similar for WT and E459D ($4.5 \cdot 10^5$ $s^{-1} \cdot M^{-1}$ and $3.5 \cdot 10^5$ $s^{-1} \cdot M^{-1}$ respectively, Table 2).

Table 2. Kinetic parameters of WT *E. coli* and mutant E459D BEs.

	WT	E459D
Specific activity[a] (μmol x min^{-1} x mg^{-1})	3.7±0.2	5.9±0.8
K_m (μM)	11.7±0.7	23.5±5.6
k_{cat}/K_m (s^{-1} x M^{-1})	4.5 x 10^5	3.5 x 10^5

[a] Activity was measured by the branching linkage assay (assay b) using reduced amylose AS-320 as substrate.

Modification of the structure of reduced amylose AS-320 by BE was analyzed for the WT and all mutants except E459K, due to its low activity. Figure 2 shows the HPAEC pulsed amperiometric detector (PAD) response chromatograms of WT and E459D after 4 hrs of branching as described in Materials and Methods. The mutant enzymes E459A and E459Q yielded similar results to the WT (data not illustrated). The only significant difference in the chromatograms in Figure 2 is presence of a d.p. 4 peak in the chain length distribution of E459D which is not observed for WT enzyme. Therefore the HPAEC chromatogram was rerun with 1.5 μg of maltotetraose included in the sample to test if the retention time of the maltotetrose corresponded to that of the observed peak. This increased the proposed d.p. 4 peak two-fold in size and we

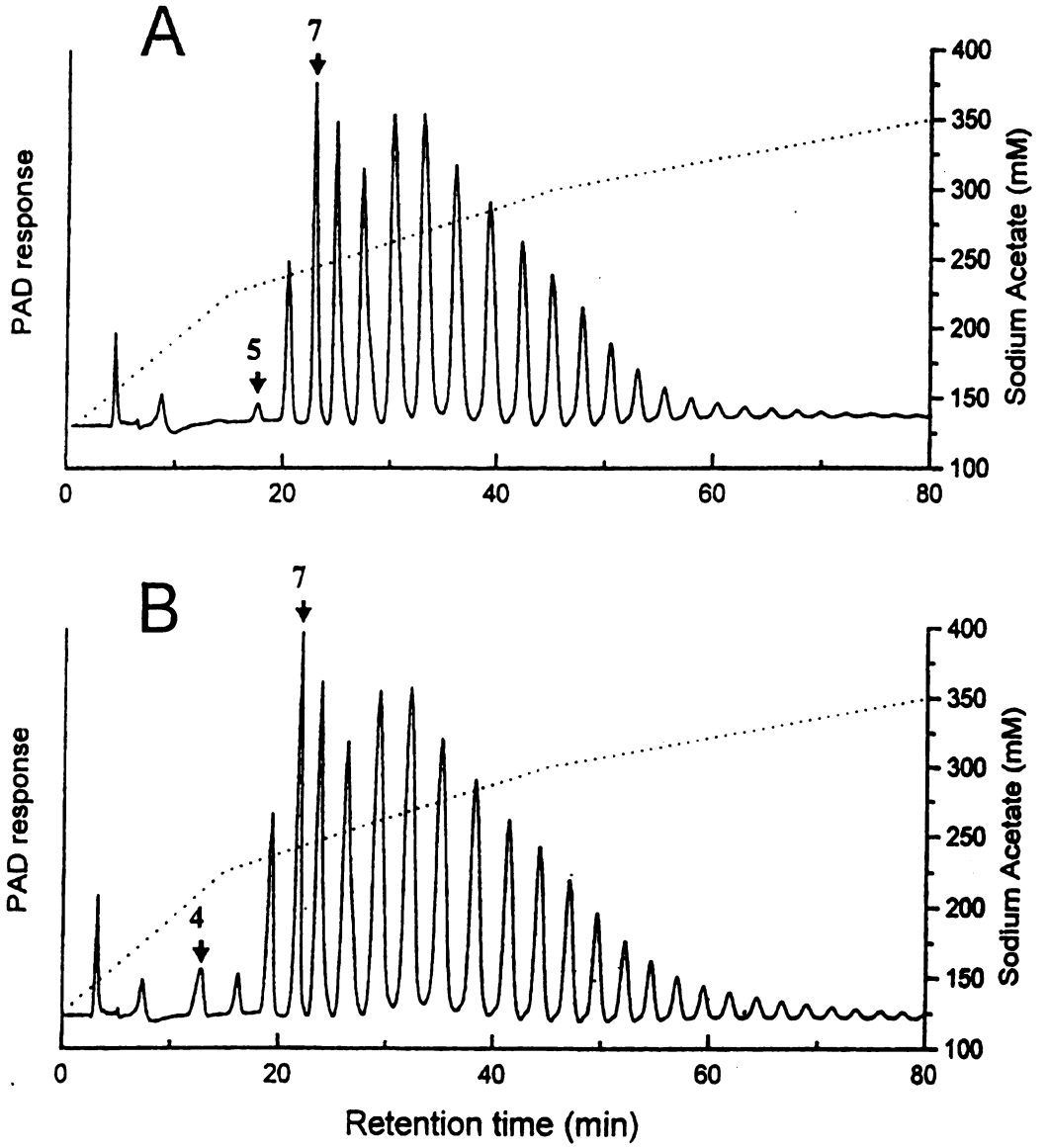

Figure 2. HPAEC analysis of the debranched α-glucan formed by action of *E. coli* BE WT on reduced amylose AS-320 (**A**) and of E459D (**B**). Number on peak indicates the corresponding c.l. The sodium acetate gradient is superposed on chromatogram.

concluded the E459D does differ from WT in transferring this particular chain length. A similar study of the *E. coli* BE WT was done recently by Guan *et al.* (5) were they registered d.p. 4 and even d.p. 3, however without presenting the corresponding PAD chromatograms. The relative peak area for all E459 mutants based on the PAD response chromatograms were calculated and showed that there is little difference in the branching products of the enzymes tested, the most commonly transferred chain length being 11 (data not shown).

As the focus of our study is a conserved acid in the branching enzymes, we studied the activity over a pH range for the *E. coli* BE WT and E459A (Figure 3). The effect of pH on *E. coli* BE activity had not been reported previously. Figure 3 indicates that the activity profile of the WT and E459A are similar over the pH range tested with an optimum near pH 7.7. The reported pH optimum for the maize branching enzyme isoforms is 7.5 (28). If the Glu-459 was involved in acid-base catalysis, a substitution would create a shift in the relative activity at a particular pH, but this is not the case. Thus, a role of Glu459 as destabilizing the de-protonated form of the neighboring Glu-458, proposed to be a catalytic residue, can be ruled out.

Replacement of Glu-527. Glu-527 was substituted with Ala, Asp, Asn, and Gln as described above and the corresponding mutant enzymes purified to homogeneity. All the E527 mutants showed lower activity than the wild-type enzyme varying from 10 % (E527N) to 25 % (E527D) (Table 3). As for E459 we find that the C_2/C_1 ratios change significantly for E527N and E527Q, indicating a shift in the preference of substrate in assay B from amylose to amylopectin. However, this did not affect the chain transfer

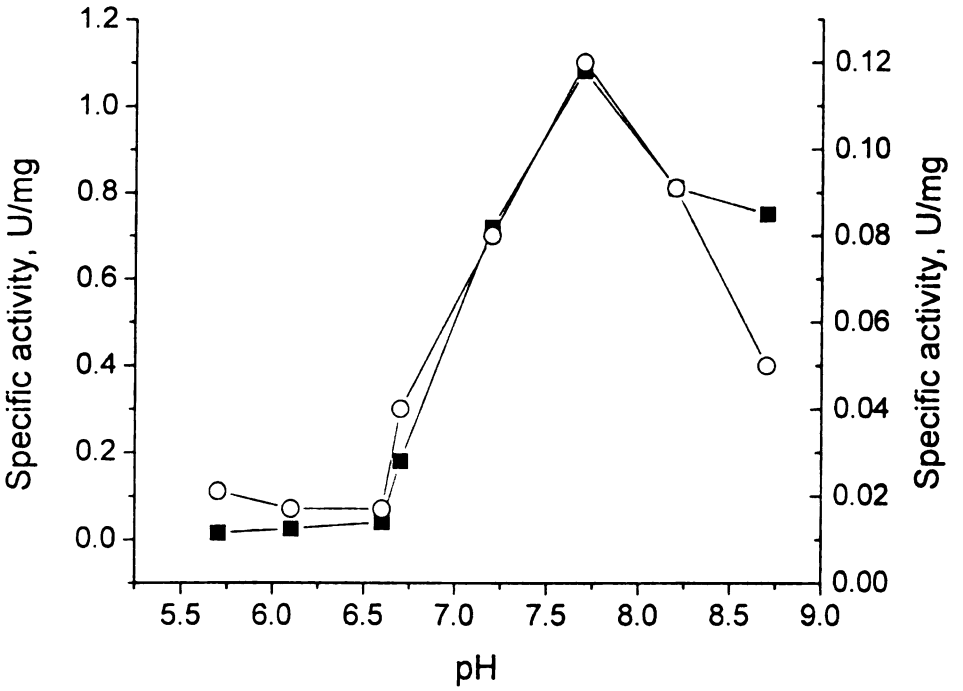

Figure 3. pH profile of *E. coli* BE WT (■) and E459A (○) mutant. Left Y-axis is specific activity for WT and right Y-axis for E459A as defined by the branching linkage assay (assay B).

Table 3. Specific activities of E527 mutants measured using assay A, B and C.

Assay		WT	E527A	E527D	E527N	E527Q
Phosphorylase *a*,	A	1100	158	267	112	128
Branching linkage,[a]	B	1.11	0.25	0.46	0.19	0.20
Iodine stain,[b]	C					
amylose	C_1	91.5	23.2	47.3	4.9	7.2
amylopectin	C_2	51.2	10.8	35.9	10.4	15.6
Ratio of activity						
	A/B	1000	632	581	588	640
	A/C_1	12.0	6.8	5.7	22.8	17.8
	A/C_2	21.5	14.6	7.4	10.7	8.2
	C_2/C_1	0.56	0.47	0.76	2.12	2.17

[a] In the branching linkage assay the concentration of substrate AS-320 was 17 μM.

[b] C_1 and C_2 denotes the iodine stain assay with amylose and amylopectin, respectively.

pattern, as all the E527 mutants had chain transfer patterns identical to BE WT as determined by HPAEC. Using the branching linkage assay the K_m for E527A was measured to 14.2 μM ±1.7 compared to 11.7 μM ±0.7 for the wild-type enzyme, and therefore E527 is not likely to be involved in substrate binding.

Replacement of Tyr-300. Several mutants of Y300 were constructed and the corresponding enzymes purified and analyzed with respect to the three assays available for detecting branching activity (Table 4). The majority of the mutants had levels of branching activities below the detection level of assays B and C. In particular, for mutant Y300W the activity was at background levels even in the more sensitive assay A. Only Y300F with 25 % of BE WT activity could be analyzed in further detail. The possible involvement of Y300 in substrate binding was investigated through the kinetic parameters of this mutant. The specific activities of BE WT and Y300F were 3.2 U/mg and 0.8 U/mg, respectively. The computed K_m value of 17.5 μM for Y300F was very similar to the WT BE K_m of 14.2 μM, indicating the Y300 is not directly involved in the binding of substrate in branching enzyme.

From the crystal structure of isoamylase, is has been suggested the conserved Tyr may form a hydrogen bond in the active site to the catalytic Asp in region 1 (24). The inability to form such a hydrogen bond could result in lower heat stability and enzymatic activity at elevated temperatures compared to the wild-type enzyme. Therefore, we measured the heat stability of *E. coli* BE, which has not been studied previously. We measured the heat stability of WT BE and Y300F by heating samples to temperatures between 30 and 65°C for 10 min. Residual enzymatic activity was assayed by the phosphorylase *a* assay

Table 4. Specific activities of Y300 mutants measured using assay A, B and C.

Assay		WT	Y300A	Y300D	Y300F	Y300L	Y300S	Y300W
Phosphorylase *a*,	A	1100	11.7	2.2	271	1.9	11.4	<0.1
Branching linkage,[a]	B	1.11	<0.04	<0.03	0.24	<0.02	<0.03	<0.01
Iodine stain,[b]	C							
amylose	C_1	91.5	n.d.	n.d.	16.3	n.d.	n.d.	n.d.
amylopectin	C_2	51.2	n.d.	n.d.	14.3	n.d.	n.d.	n.d.
Ratio of activity								
	A/B	1000	>293	>73	1130	>95	>380	-
	A/C_1	12.0			16.3			
	A/C_2	21.5			19.0			
	C_2/C_1	0.56			0.88			

[a] In the branching linkage assay the concentration of substrate AS-320 was 17 μM.

[b] C_1 and C_2 denotes the iodine stain assay with amylose and amylopectin, respectively.

n.d. not detectable

(Figure 4). These results show that the heat stability of Y300F is lowered by approximately 5 degrees compared to the WT enzyme, indicating that the hydroxyl group of the Tyr is important for stability of the enzyme. To analyze this further we measured the relative activity of WT BE and Y300F at temperatures between 30 and 50°C using the branching linkage assay, assay B (Figure 5). Y300F showed a significantly lower relative activity at higher temperatures compared to WT. Both WT and Y300F were stable at 50°C for at least 30 min in the presence of substrate (data not shown). Combined, these measurements demonstrate the importance of the hydroxyl group on the Tyr residue for stability of the active site.

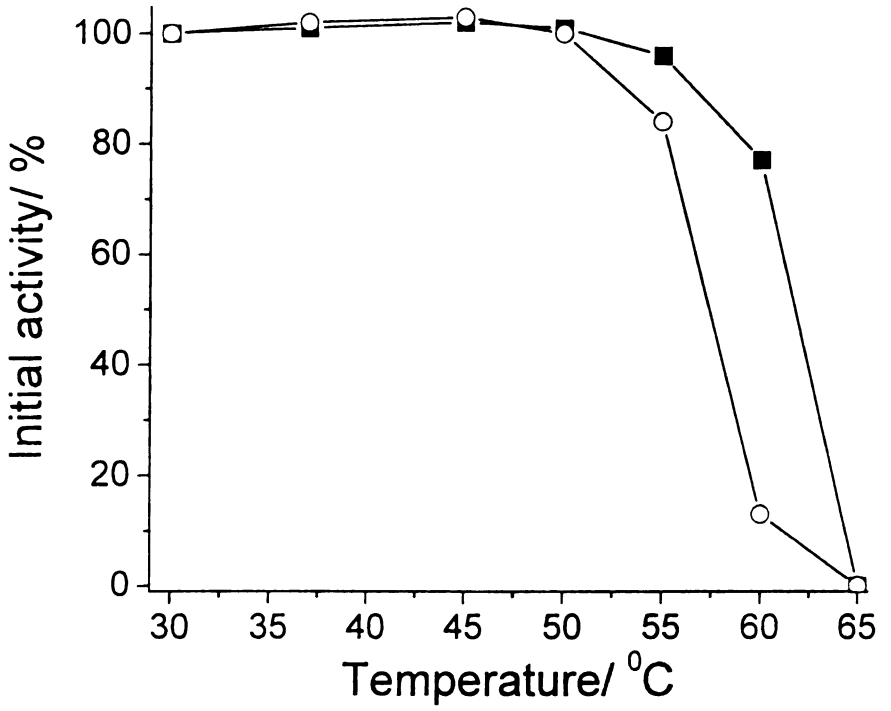

Figure 4. Heat stability curve of BE WT (■) and Y300F (○). Samples were heated to the indicated temperature for 10 min followed by cooling on ice for 5 min. The remaining activity was determined by the phosphorylase A stimulation assay (assay A). The activity obtained at 30°C was set to 100 %.

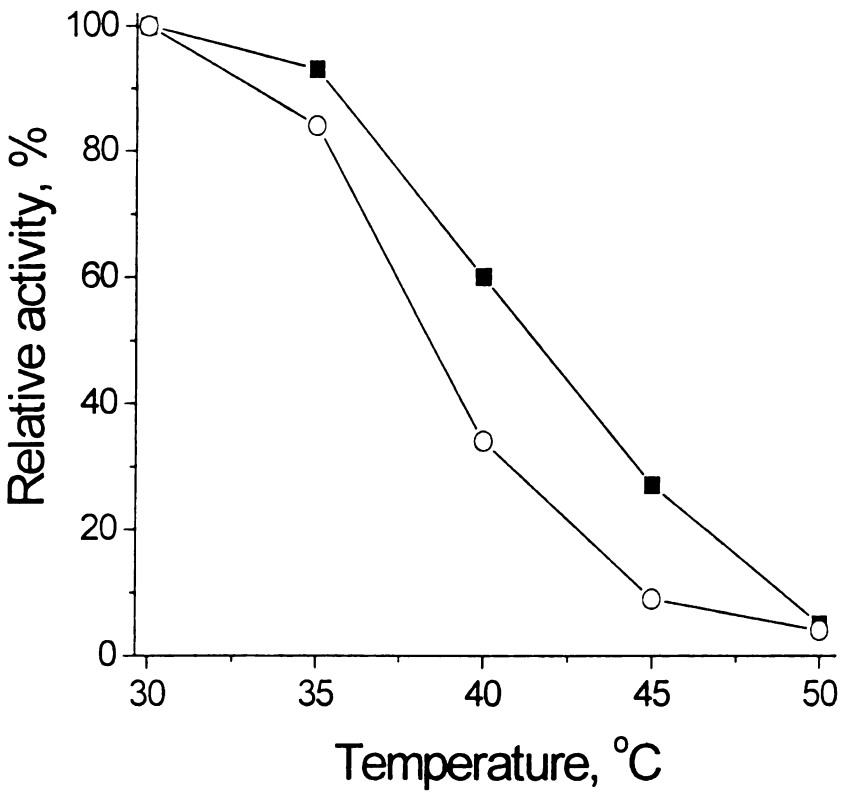

Figure 5. Relative activity of BE WT (■) and Y300F (○) at elevated temperatures. Specific activities of BE WT and Y300F were determined at the indicated temperature using the branching linkage assay (assay B). The activity obtained at 30°C was set to 100%.

Discussion.

Based on the results presented here, we conclude that Glu-459, located in the conserved region 3, is important for the function of the *E. coli* BE. When Glu-459 is changed to other amino acids, a significant change in the properties of the enzyme is seen with respect to specific activities, kinetic parameters and substrate specificity. The conservative change from Glu to Asp even led to higher specific activities compared to the WT in all three assays available. It is worth noting that all higher plant branching enzymes (as well as a few from prokaryotes) have an Asp at this position. It would be interesting to study the consequences of the reciprocal conservative substitution at this position in a plant branching enzyme.

Glu-459 is not likely to be involved in chain transfer, as the HPAEC-PAD chromatograms were virtually identical for all constructed mutants. It is also evident that Glu-459 is not an essential catalytic residue, as some activity remained even when it was substituted with an amino acid of opposite charge (E459K). However, Glu-459 could be involved in catalysis of a step which is not rate limiting, based on our observations of altered specific activity and substrate preference. The pH profiles of the WT and the E459A mutant rules out the possibility that Glu-459 is involved in acid-base catalysis as the pH profiles as the profiles can be superimposed.

The residues Y300 and E527 are both required for maximum branching activity, although they are evidently not catalytic residues. Previously it has been suggested that Y300 plays a role in substrate binding (24), but kinetic analysis of BE WT and Y300F revealed similar K_m values. These findings rule out any direct involvement of the hydroxyl group of Y300 in binding of substrate. However, the Tyr could participate in

binding and stabilization of the substrate via hydrophobic stacking interactions with the aromatic ring. Such stacking interactions between the substrate and the corresponding Tyr residue have been reported in cyclodextrin glucanotransferase (33). We did see an effect on heat stability of approximately 5°C and branching activity at elevated temperatures when analyzing the Y300F mutant. These findings indicate the formation of a hydrogen bond between Y300 and another residue in or near the active site as being important for the enzyme stability.

A three-dimensional structure is required before we can assign specific roles for the residues investigated here by site-directed mutagenesis, and in turn, the reason for these positions being conserved in all known branching enzymes.

References.

1. Preiss, J. (1984) *Annu. Rev. Microbio.* **38**, 419-458.
2. Preiss, J. (1991) in *Plant Molecular and Cell Biology* (Mifflin, B., Ed), vol 7, pp 59-114, Oxford University Press, Oxford.
3. Boyer, C., and Preiss, J. (1977) *Biochem.* **16**, 3693-3699.
4. Baecker, P.A., Greenberg, E., Preiss, J. (1986) *J. Biol. Chem.* **261**, 8738-8743.
5. Guan, H.P, Li, P., Imparl-Radosevich, J., Preiss, J., Keeling, P. (1997) *Arch. Biochem. Biophys.* **342**, 92-98.
6. Boyer, C., and Preiss, J. (1978) *Carbohydr. Res.* **61**, 321-334.
7. Singh, B.K. and Preiss, J. (1985) *Plant Physiol.* **79**, 34-40.
8. Guan, H.P, and Preiss, J. (1993) *Plant Physiol.* **102**, 1269-1273.
9. Nakamura, A., Haga, K., Ogawa, S., Kuwano, K., Kimura, K., Yamane, K. (1992) *FEBS Lett.* **296**, 37-40.
10. Mizuno, K., Kawasaki, M., Shimada, H., Satoh, H., Kobayashi, E., Okumura, S., Arai, Y., Baba, T. (1993) *J. Biol. Chem.* **268**, 19084-19091.
11. Romeo, T., Kumar, A., Preiss, J. (1988) *Gene* **70**, 363-376.
12. Baba, T., Kimura, K., Mizuno, K., Etoh, H., Ishida, Y., Shida, O., Arai, Y., (1991) *Biochem. Biophys. Res. Commun.* **181**, 87-94.
13. Jespersen, H.M, Ann MacGregor, E., Henrissat, B., Sierks, M.R., Svensson, B. (1993) *J. Protein Chem.* **12**, 781-805.
14. Matsuura, Y., Kusunoki, M., Harada, W., Kakudo, M. (1984) *J. Biochem.* **95**, 697-702.
15. Buisson, G., Duee, E., Haser, R., Payan, F. (1987) *EMBO J.* **6**, 3909-3916.

16. Boel, E., Brady, L., Brozozowski, A.M., Derewenda, Z., Dodson, G.G., Jansen, V.J., Petersen, S.B., Swift, H., Thim, L., Woldike, H.F. (1990) *Biochem.* **29**, 6244-6249.

17. Klein, C., and Schulz, G.E. (1991) *J. Mol. Biol.* **217**, 737-750.

18. Kubota, M., Matsuura, Y., Sakai, S., Katsube, Y. (1991) *Denpun Kagaku* **38**, 141-146.

19. Kuriki, T., Takata, H., Okada, S., Imanaka, T. (1991) *J. Bacteriol.* **173**, 6147-6152.

20. Takata, H., Kuriki, T., Okada, S.,Takesada, Y., Iizuka, M., Minamiura, N., Imanaka, T. (1992) *J. Biol. Chem.* **267**, 18447-18452.

21. Kuriki, T., Guan, H.P., Sivak, M., Preiss, J. (1996) *J. Protein Chem.* **15**, 305-313.

22. Funane, K., Libessart, N., Stewart, D., Michishita, T., Preiss, J. (1998). *J. Prot. Chem.* **17**, 579-590.

23. Libessart, N., Preiss, J. (1998). *Arch. Biochem. Biophys.* **360**, 135-141.

24. Katsuya, Y., Mezaki, Y., Kubota, M., Matsuura, Y. (1998). *J. Mol. Biol.* **281**, 885-897.

25. Sanger, F., Nicklen, S., Coulson. (1977) *Proc. Natl. Acad. Sci. USA* **74**, 5463-5467.

26. Smith, P.K., Krohn, R.I., Hermanson, G.T., Mallia, A.K., Gartner, F.H., Provenzano, M.D., Fujimoto E.K., Goeke, N.M., Olson, B.J., Klenk, D.C. (1985) *Anal. Biochem.* **150**, 76-85.

27. Hawker, J.S, Ozbun, J.L., Ozaki, H., Greenberg, E., Preiss, J. (1974) *Arch. Biochem. Biophys.* **160**, 530-551.

28. Takeda, Y., Guan, H.P., Preiss, J. (1993) *Carbohydr. Res.* **240**, 253-263.

29. Burkhard, R., Sander, C. (1993). *J. Mol. Biol.* 232, 584-599.

30. Fromageot, H.P., and Zinder, N.D. (1968) *Prod. Natl. Acad. Sci.* **61**, 184-191.

31. Kuriki, T., Stewart, D.C., Preiss, J. (1997) *J. Biol. Chem.* **272**, 28999-29004.

32. Fersht, A.R. (1985) in *Enzyme structure and Mechanism*, Freeman, New York.

33. Uitdehaag, J. C. M., Mosi, R., Kalk, K. H., Van der Veen, B. A., Dijkhuizen, L., Withers, S. G., Dijkstra, B. W. (1999) *Nature Struc. Biol.* **5**, 432-436.

34. Homerova, D., and Kormanec, J. (1994) *Biochem. Biophys. Acta* **1200**, 334-336.

35. Takata, H., Takaha, T., Kuriki, T., Okada, S., Takagi, M., Imanaka, T. (1994) *Appl. Envir. Microbio.* **60**, 3096-3104.

36. Kiel, J. A., Boels, J. M., Beldman, G. and Venema, G. (1992) *DNA seq.* **3**, 221-232.

37. Fisher, D.K., Gao, M., Kim, K.N., Boyer, C.D., Guiltinan, M.J. (1996*) Plant Mol. Bio.* **30**, 97-108.

38. Fisher, D.K., Boyer, C.D., Hannah, L.C. (1993) *Plant Physiol.* **102**, 1045-1046.

39. Mizuno, K., Kimura, K., Arai, Y., Kawasaki, M., Shimada, H., Baba, T. (1992) *J. Biochem.* **112**, 643-651.

CHAPTER 3

SLOW-BINDING INHIBITION OF BRANCHING ENZYME BY THE PSEUDOOLIGOSACCHARIDE BAY-e4609.

This data has been published.

Binderup, K., Libessart N., and Preiss, J. (2000) "BAYe4609, a Slow-Binding Inhibitor of Branching Enzyme. Functional Evidence for Relationship with Amylolytic Enzymes." *Arch. Biochem Biophys.* **374**, 73-78.

Abstract.

Branching enzyme from *E. coli* is shown to be inhibited by the pseudo-oligosaccharide BAY e4609. The mechanism of binding is studied in detail by kinetics using reduced amylose as substrate. Lineweaver-Burk plots suggest the mechanism of a non-competitive or slow-binding inhibitor. Further studies by progress curves and rate of loss of branching activity allows us to conclude BAY e4609 as being a slow-binding inhibitor of branching enzyme. We discuss how these results parallel the inhibition of α-amylase by acarbose and the significance for branching enzyme as belonging to the amylolytic family.

Introduction.

Branching enzyme catalyzes the formation of α-1,6-glucosidic linkages of glycogen in bacteria (1) and starch in plants (2-4). Hence, the enzyme plays an important role in the biosynthesis of starch and glycogen (2-4). Many starch/ glycogen hydrolases and related enzymes have been assigned to the α-amylase family as they contain a characteristic $(\alpha/\beta)_8$ barrel domain (5-7). It has been suggested that branching enzymes belong to the family of amylolytic enzymes (5-7) by virtue of containing in the central portion of the enzyme, four conserved regions also present in other amylolytic enzymes, amylase, pullulanase, isoamylase, and cyclodextrin transferase. By site-directed mutagenesis of branching enzymes it was suggested that in addition to structural similarities of the amylolytic enzymes, the catalytic mechanisms among them are shared (8). Moreover, the variations in substrate specificities and products can be ascribed to the relationship between their catalytic centers and different subsite structures (9, 10).

Several inhibitors of α-amylases have been reported including tendamistate/ Hoe 467 (11), trestatins (12), and acarbose (13, 14). Investigation of carbohydrate-splitting enzyme inhibitors have largely been driven through medical interest in the treatment of metabolic diseases such as diabetes (For a review of inhibitors of α-glucosidases see Truscheit *et al.* (15)). In particular, the pseudo-tetrasaccharide acarbose has been found to inhibit CGTases as well as α-amylases (15), and recently X-ray structures of porcine pancreatic α-amylase and *Bacillus circulans* CGTase both with bound acarbose have been solved (16, 17). In both cases acarbose was found at the catalytic site of the enzyme. Whereas Qian and co-workers proposed acarbose to be a transition state analog (16), Strokopytov found it more likely to be a substrate analog (17) even though the mode of

binding of the inhibitor in the two structures was very similar. Despite these differences, the interpretation of the roles of amino acids surrounding the catalytic cleft including identifying residues involved in substrate binding and direct catalysis was very similar.

To date no published study has reported any inhibitors of BE. The present study reports the identification of an acarbose-like inhibitor of BE, BAY e4609 (Figure 1).

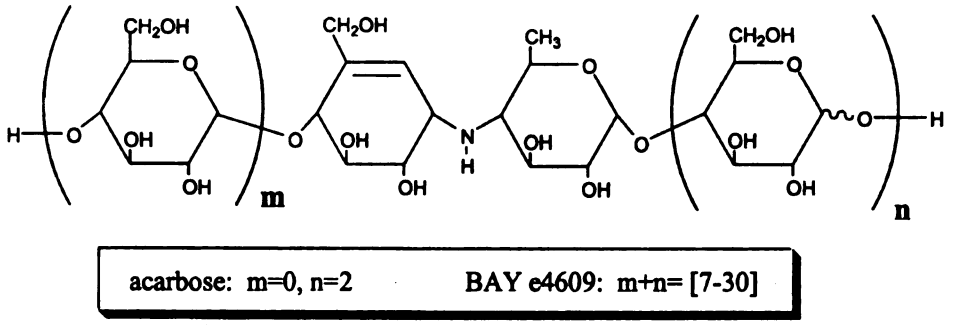

Figure 1: Structures of the pseudo-oligosaccharides acarbose and BAY e4609. m and n designates the number of glucose units at the non-reducing and reducing end, respectively. Acarbose is a pseudo-maltotetrose, whereas BAY e4609 is a pseudo-oligosaccharide of chain length ranging from 9 to 32.

BAY e4609 is a pseudo-oligosaccharide resembling amylose with a hydroxymethylconduritol unit and a 4-amino-4-deoxy-D-chinovose residue linked to a varying number of α-D-glucose units from 7 to 30. It is a secondary metabolite purified from *Actinoplanes* strain 50/13 (13) and has been shown to be an even more potent inhibitor of pig pancreatic α-amylase than acarbose (15). We investigate the mode of binding of the inhibitor to BE and discuss how our results strengthen the hypothesis of BE belonging to the amylolytic family beyond sequence conservation.

Materials and Methods.

Expression and purification of *E. coli* BE. An overnight culture of the transformed cells (BL21[DE3]) carrying the recombinant plasmid encoding the gene for BE was diluted 1:20 (v/v) in fresh Luria broth medium containing 50 μg ml^{-1} kanamycin. The cells were grown at 37°C to A_{600} = 0.5 and allowed to cool down to 25°C. Flasks were transferred to shaker at room temperature and T7 RNA polymerase expression induced by adding isopropyl-D-thiogalactoside to 0.5 mM. After 2 hrs incubation endogenous expression was turned off by adding rifampicin to 150 μg ml^{-1} as described by Binderup and Preiss (18). Incubation was continued for 16 hrs at room temperature and cells were then harvested in a refrigerated centrifuge. The purification of the *E. coli* BE was performed as described by Guan *et al.* (19) with some modifications: The cell paste (about 1.5 g per 1 l of culture) was resuspended in 10 ml buffer A (50 mM Tris-acetate pH 7.5; 10 mM ethylenediaminetetracetic acid [EDTA]; 2.5 mM dithiothreitol [DTT]) and lysed by sonication. The homogenate was centrifuged at 10000 g for 15 min at 4° followed by precipitation with 1.6 M ammonium sulfate by addition of a 3.8 M stock solution. After centrifugation the pellet was resuspended in 10 ml buffer A and dialyzed overnight in buffer A. The sample was then loaded on MonoQ HR 10/10 column and eluted with 0-0.3 M KCl in buffer A. Fractions containing branching enzyme activity were pooled and BE precipitated with 1.6 M ammonium sulfate. The precipitate was resuspended in 10 ml buffer B (10 mM triethanolamine pH 8.0; 1 mM EDTA; 2.5 mM DTT) and dialyzed overnight in buffer B. The sample was loaded on a MonoQ HR 5/5 column and eluted with 0-0.4 M KCl in buffer B. Fractions were pooled and

concentrated to 2 mg ml^{-1}. Protein concentration was measured with the bicinchoninic acid protein assay reagent (20), using bovine serum albumin as the standard.

Assay of BE activity. BE activity was measured using the phosphorylase A stimulation assay (assay A) and the branching linkage assay (assay B) as described previously (21).

Assay A. The phosphorylase A stimulation assay is based on the stimulation by BE of the rate of synthesis of α-D-glucan from α-D-Glucose-1-P catalyzed by rabbit phosphorylase a (22). Reaction mixtures contained in a final volume of 100 μl, 100 mM citrate (pH 7.0), 10 mM adenosine monophosphate, 0.2 mg phosphorylase a (Sigma Chemical Co.) 50 mM D-[^{14}C]-Glucose-1-P (50 DPM $nmol^{-1}$), and various amounts of inhibitor. The reaction was initiated by adding an appropiate amount of BE. One unit is defined as 1 μmol of glucose incorporated into α-D-glucan per min. at 30°C.

Assay B. The branching linkage assay determines the number of branching points introduced by BE into the substrate, reduced amylose (23). Substrates were prepared by the reduction of enzymatically synthesized amylose (AS-320, degree of polymerization 1815) as described (23). Reaction mixtures contained 25 mM MOPS (pH 7.5) and an appropriate amount of substrate (35 μM unless stated otherwise) and inhibitor in a final volume of 100 μl. The reaction was initiated by adding an appropiate amount of BE. Debranching was performed by using isoamylase from *Pseudomonas amyloderamosa* (Hayashibara Biochemical Laboratories, Japan). One unit is defined as 1 μmol of branching linkages formed per min. at 30°C.

Gel filtration. A column (1.6 x 55 cm) was packed with Fractogel TSK HW-50F resin (EM Science) and equilibrated with H_2O. BAY e4609 (15 mg) was applied on the

column and 2-ml fractions were collected at a flow rate of 20 ml/hr. The average degree of polymerization (d.p.) was determined by the ratio of total carbohydrate to reducing sugar, as measured by the phenol-H_2SO_4 assay (24) and Park-Johnson method (25), respectively.

Results.

Activity of *E. coli* BE in presence of inhibitor was initially performed by the phosphorylase a stimulation assay (Figure 2). The phosphorylase a incorporates glucose units into the nonreducing ends of a glucose polymer. In contrast to acarbose, BAY e4609 has a nonreducing end (Figure 1) which will serve as substrate for phosphorylase a, so all experiments were performed with controls lacking BE. Figure 2 shows how residual activity was reduced to less than 10% after 30 min incubation when using a BAY e4609 concentration of 250 $\mu g\ ml^{-1}$ (BAY e4609 covers a range of sizes corresponding to a molecular weight (MW) of 1500 to 5000, for which reason the concentration of BAY e4609 is designated in $\mu g\ ml^{-1}$).

The high sensitivity and ease of the phosphorylase a assay makes it ideal for a qualitative estimate of branching activity, however it is not suitable for kinetic studies as substrate concentration cannot be varied. In contrast, the branching linkage assay allows for detailed kinetic studies but is complicated by the fact that it utilizes the enzyme isoamylase [E.C. 3.2.1.68] (a α-[1,6] glucosidic-linkage hydrolyzing enzyme) which is homologous to BE (6, 7). The lower branching activity when using inhibitor could be due in part to BAY e4609 interaction with isoamylase. Consequently, the activity of isoamylase in presence of BAY e4609 was measured using glycogen as substrate and found to be unaffected (data not shown).

A Lineweaver-Burk plot was used to identify the type of inhibition. Figure 3 shows the *E. coli* BE in presence of various concentrations of BAY e4609. When fitted to linear equations, the lines appear to intersect on the X-axis, indicative of a non-competitive type of inhibitor, for which the inhibitor does not affect the binding of

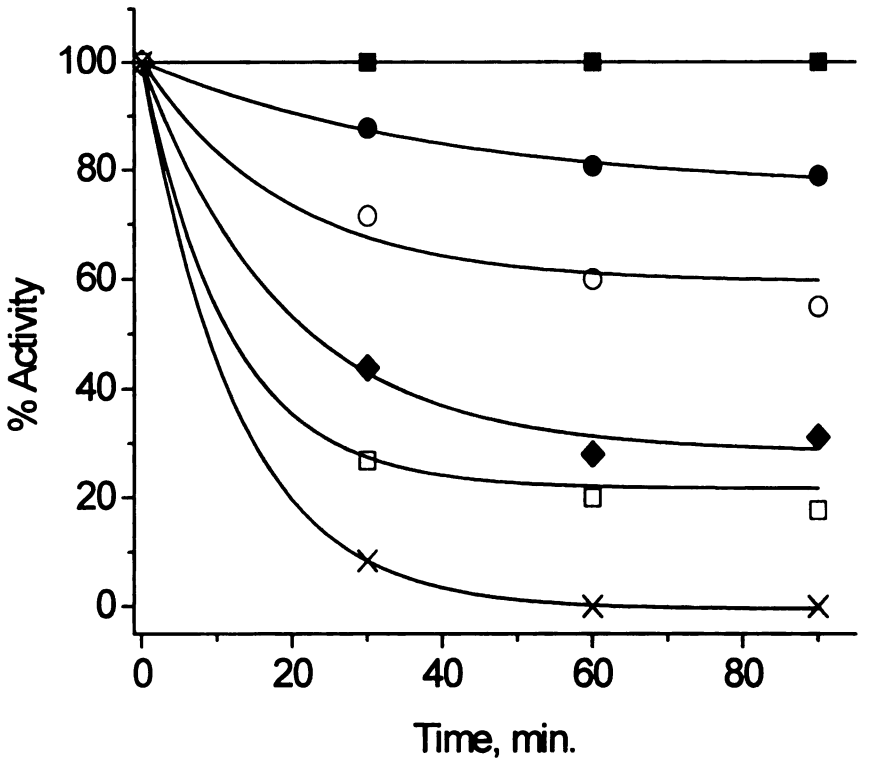

Figure 2: Inhibition of *E. coli* BE by BAY e4609. (■) no inhibitor; (●) 2.5 μg/ml; (○) 10 μg/ml (◆) 25 μg/ml; (□) 100 μg/ml; (×) 250 μg/ml. Activity was measured by phosphorylase a stimulation assay. The activity of BE without inhibitor was set as 100 % activity for each time point. 1 unit (U) by assay A of BE was used. T = 30 °C, pH = 7.0.

substrate to enzyme, but reduces the V_{max}. The reaction pathway for such a system can be written as in equation 1.

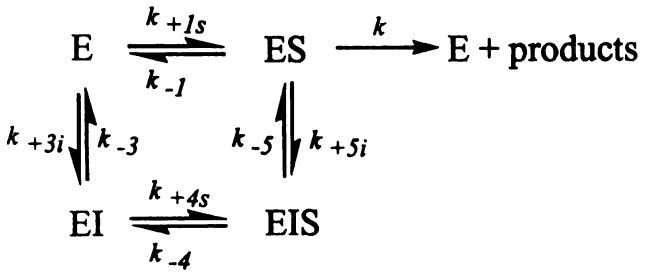

(1)

Two distinct types of non-competitive inhibitors exit depending on the fate of the complex EIS. For a fully non-competitive inhibitor, EIS does not break down and the effect is equivalent to a reduction in the amount of active enzyme. In case of a partially non-competitive inhibitor EIS breaks down at a velocity different of ES and the rate of reaction is the sum of the two.

However, an irreversible inhibitor may appear as a noncompetitive inhibitor in a Lineweaver-Burk plot. EI is a complex which is fully active and rapidly reversible during the reaction, whereas EI* is the inactive BE-inhibitor complex which is very slowly reversible ($k_{-2} << k_2$). A true irreversible inhibitor has a k_{-2} value of zero (for example, when a covalent E-I bond is formed) whereas a slow-binding inhibitor is defined as having a slow release rate as seen by a low k_{-2} value (26). Thus, the differentiation of an inhibitor as being irreversible or slow-binding is merely a matter of degree.

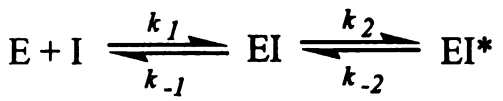

(2)

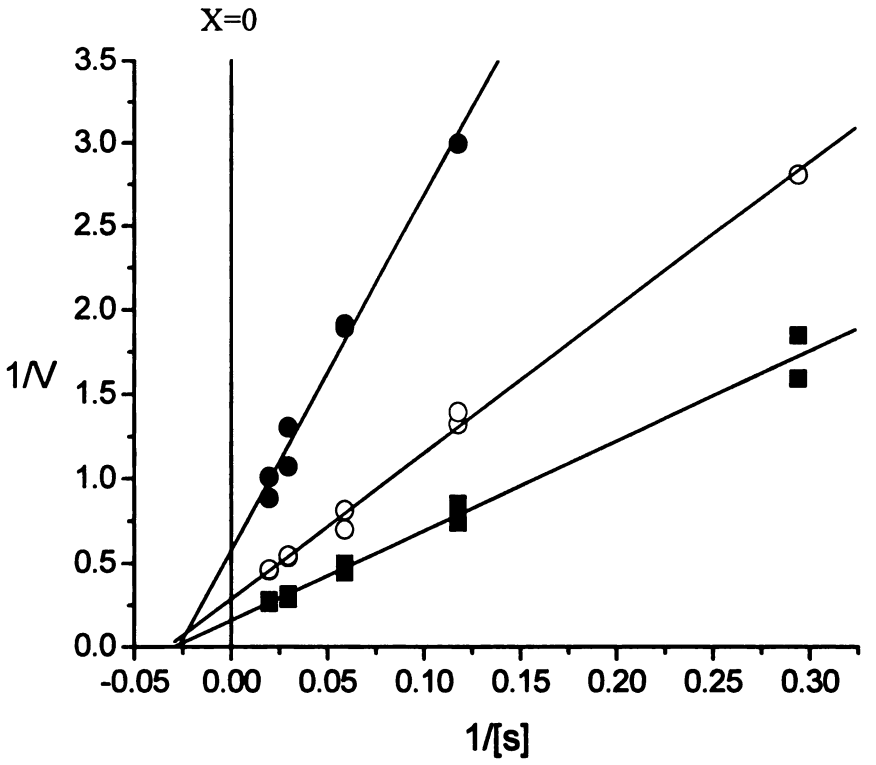

Figure 3: Lineweaver-Burk plot of *E. coli* BE in presence of BAY e4609. (■) no inhibitor; (○) 25 μg/ml; (●) 50 μg/ml. Activity was measured by branching linkage assay (assay B) using reduced amylose AS-320 as substrate. Reactions were started with 1 mU of BE (assay B) diluted into substrate containing inhibitor. Product was measured after 30 min incubation. T = 30 °C, pH = 7.5.

As analysis of primary plots does not allow differentiation between these models, additional information was sought by monitoring the rate of loss of activity.

The rate of BAY e4609 inactivation of *E. coli* BE was investigated by incubating BE with excess inhibitor at 30 °C for up to 5 min. At various times, aliquots were removed into tubes containing reduced amylose AS-320 without added inhibitor and branching activity measured by assay B for 30 min as described in materials and methods. Figure 4 shows the rate of loss of branching activity being of first order. This suggests dissociation of the inactive BE-inhibitor complex is slow, fitting reaction pathway 2 (27, 28).

Continuous kinetic assays using BAY e4609 were done by pre-incubating BE with inhibitor on ice and starting the reaction with substrate. A classical reversible competitive inhibitor in this type of experiment will show linear product formation as the initial enzyme-inhibitor complex readily will establish a dynamic equilibrium. In contrast, Figure 5 shows an initial velocity less than the steady state velocity with a significant lag period characteristic of a slow-binding inhibitor (26). As shown in Figure 5, the progress curve for BE in absence of inhibitor is linear as expected, but clearly the initial inhibitor-enzyme complex dissociates slowly as the steady state velocity is not reached until about 30 min of incubation with 35 μM substrate. This also points towards reaction pathway 2 being the most plausible mechanism of BAY e4609 and furthermore indicates that it is a slow-binding inhibitor rather than irreversible ($k_{-2}>0$). This was confirmed by the observation that *E. coli* BE does not bind BAY e4609 covalently as determined by the lack of a gel-shift when enzyme pre-incubated with inhibitor is run on a SDS-PAGE gel under denaturing conditions (data not shown).

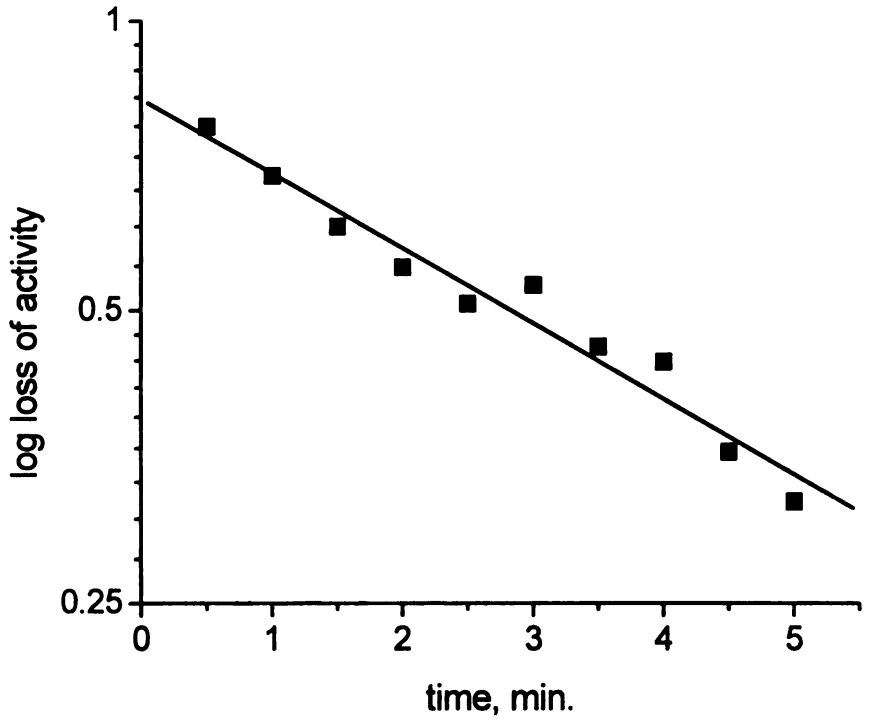

Figure 4: Rate of loss of branching enzyme activity. 0.5 mU of *E. coli* BE was pre-incubated with a final concentration of 50 µg/ml of BAY e4609 at 30 °C. At various times, aliquots were taken and diluted into 35 µM substrate lacking inhibitor. The activity of BE without inhibitor is defined as 100 %. Activity was measured by the branching linkage assay after 30 min incubation. T = 30 °C, pH = 7.5. There was no loss of activity during incubation of the BE in the absence of inhibitor.

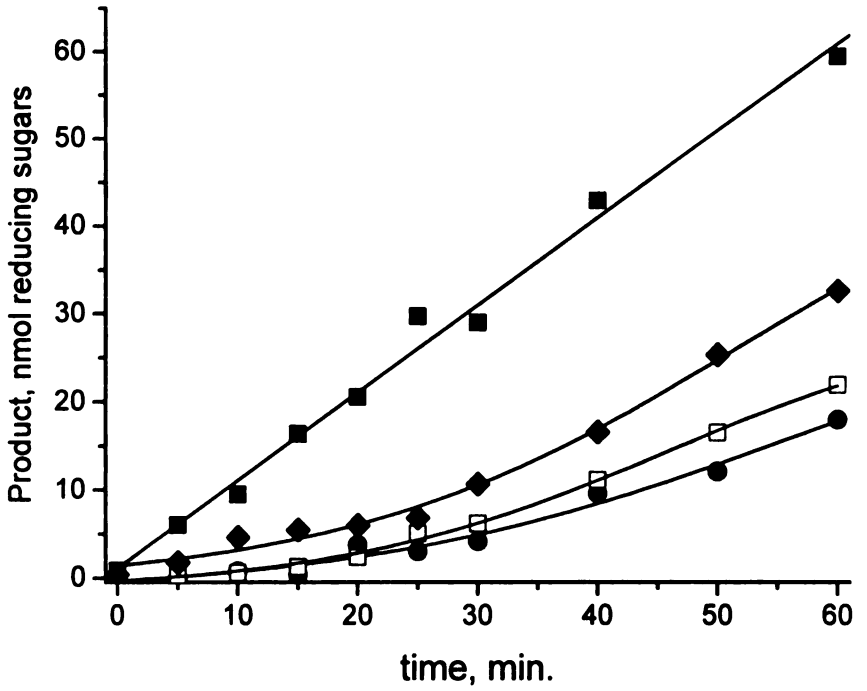

Figure 5: Preincubation of *E. coli* BE with BAY e4609. (■) no inhibitor; (◆) 25 μg/ml; (□) 37.5 μg/ml; (●) 50 μg/ml. 0.5 mU (assay B) of *E.coli* BE was incubated for 90 min on ice with inhibitor and diluted into the substrate amylose AS-320 lacking additional inhibitor. Branching activity was measured by assay B after 0 to 60 min incubation at 30 °C. pH = 7.5, [AS-320] = 35 μM.

Progress curves for the inhibition of BE by BAY e4609 was performed by starting the reaction with enzyme diluted into the substrate containing inhibitor (Figure 6). In the presence of a classical rapid reversible inhibitor the reaction rates will remain linear during the period where there is no substrate depletion. For a slow-binding inhibitor there will be an initial burst of reaction followed by a lower steady-state rate, reflecting the slow establishment of equilibrium between enzyme and inhibitor. The curves presented in figure 6 show in presence of inhibitor an initial rapid formation of product, which after a few minutes drops to a much reduced rate. The rate of reaction in absence of inhibitor is linear throughout the time of incubation. In conclusion, the data presented in this report is consistent with BAY e4609 being a slow binding inhibitor of *E. coli* BE.

Fractionation of BAY e4609. In order to determine if a subset of the BAY e4609 chains enriched in inhibitory activity could be isolated, we performed fractionation of the oligosaccharide mixture by gel filtration (Figure 7). Fractions 29-35 (pool 1), 36-39 (pool 2) and 40-45 (pool 3) were combined and concentrated as described under materials and methods. The average oligosaccharide size was determined to be d.p. 33 for pool 1, d.p. 17 for pool 2, and d.p. 10 for pool 3, indicating fractionation according to chain size of BAY e4609. Inhibition experiments using assay B with a constant amount of each of the three pooled inhibitor fractions showed that all chain sizes of BAY e4609 inhibited branching enzyme. The population of average d.p. 33 inhibited branching enzyme 1.4 and 3.4 times more efficiently than the average d.p. 17 and d.p. 10 populations, respectively (data not shown). This suggests that whereas all chain sizes of BAY e4609 inhibit branching enzyme, the longer chains constitute a more active portion of BAY e4609.

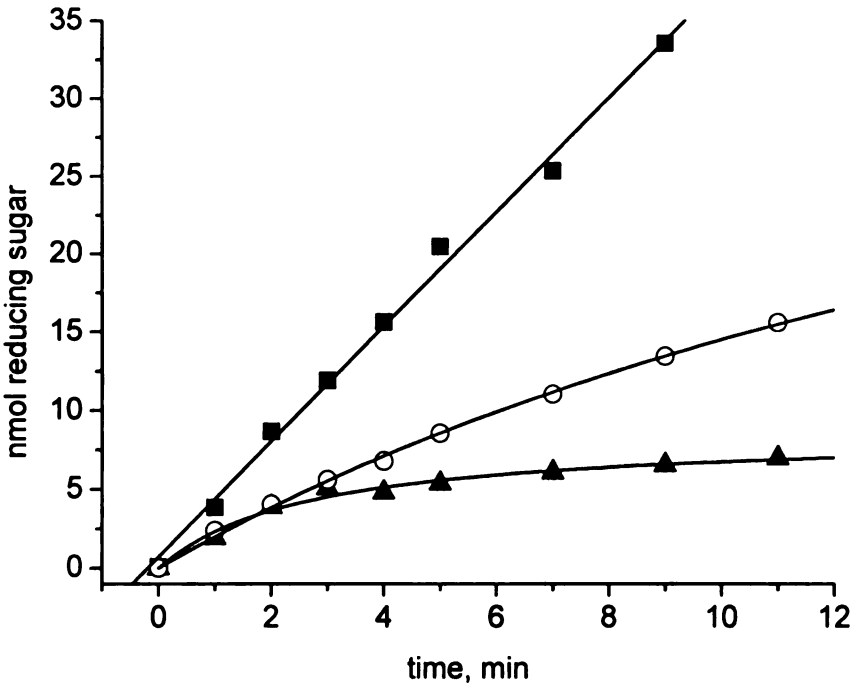

Figure 6: Progress curve of *E. coli* BE with BAY e4609. (■) no inhibitor; (○) 0.5 μg/ml, (▲) 1.5 mg/ml. Concentration of substrate reduced amylose AS-320 was 10 μM. Reaction was started with 2.5 mU of BE and branching activity measured by the branching linkage assay (assay B) at 30 °C. pH = 7.5.

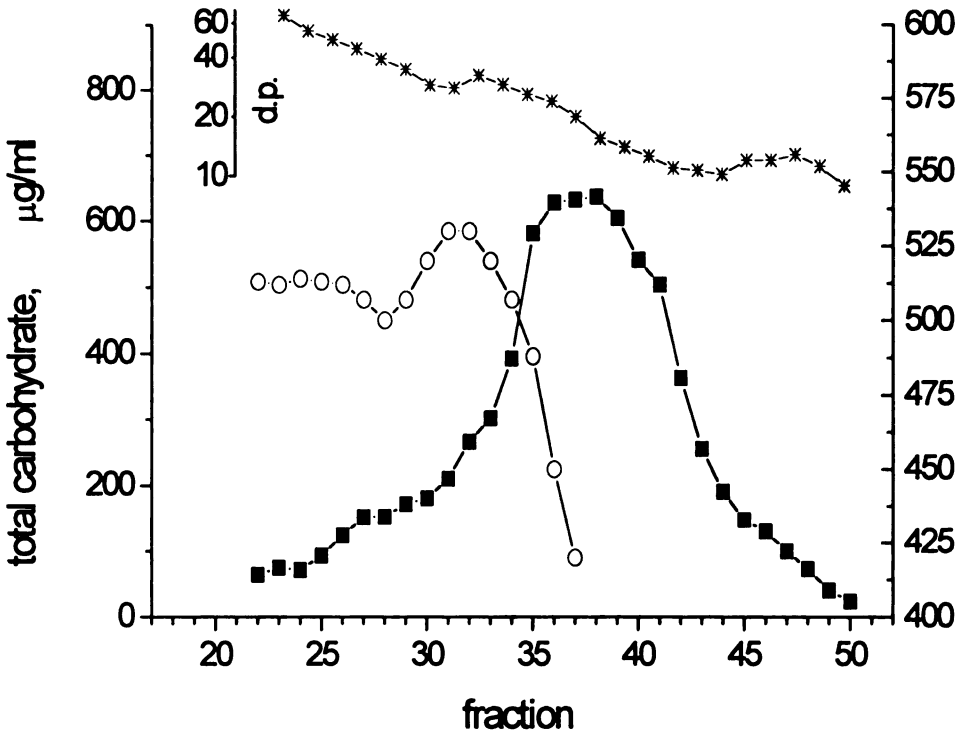

Figure 7. Gel filtration of BAY e4609. The X-axis shows the fraction number. Total carbohydrate (■) was measured by the phenol-sulfuric acid method. The total carbohydrate scale (µg/ml) is shown on the left Y-axis. λ_{max} values of the iodine-oligosaccharide complex (○) is shown on the right Y-axis. The degree of polymerization (d.p., ✳) was determined as described under materials and methods.

Discussion.

We have investigated the mechanism of inhibition of *E. coli* BE by the pseudo-oligosaccharide BAY e4609 and found it to belong to the class of slow-binding inhibitors. The nitrogenous sugars acarbose and deoxynojirimycin had no inhibitory effect on branching enzyme, although both are potent inhibitors of other enzymes of the α-amylase family. This can be thought to be due to their smaller size relative to BAY e4609, as the minimum chain length required for *E. coli* BE branching activity has been found to be of 12 glucose residues (19). BAY e4609 is a mixture of oligosaccharides of ranging size, and the efficiency of inhibition was found to vary according to the number of glucose units present in the inhibitor, the longer chains being more effective. In addition, the relative position of the hydroxymethylconduritol and 4-amino-4-deoxy-D-chinovose residues in a BAY e4609 molecule of a given chain length might be essential for effective inhibition. We have also seen the inhibition of maize branching enzyme II by BAY e4609, although it is inhibited to a lesser extend than BE from *E. coli* (data not shown). The analysis was limited to construction of a Lineweaver-Burk plot, which appeared similar to that of *E. coli* BE with BAY e4609. However, it leaves the exact mode of binding undetermined. It would be interesting to characterize various BE's with respect to BAY e4609 and acarbose to see if relationship with inhibition and enzymatic properties (e.g. substrate preference, chain length transfer) would emerge.

The BE belongs to the family of amylolytic enzymes, which all cleave and/ or transfer chains of α-(1,4)-glucan. This relationship has been based on sequence conservation in the central part of the BE, thought to fold as an $(\alpha/\beta)_8$ barrel as well as site-directed mutagenesis studies of the proposed active site residues. Interestingly,

Wilcox and Whitaker (29) investigated the mechanism of inhibition of bovine pancreatic α-amylase by acarbose and concluded it to be slow, tight-binding. Our observation that the mechanism of inhibition of BE by BAY e4609 is similar to that of α-amylase by acarbose thus provides direct functional evidence for BE being an amylolytic enzyme. Furthermore, it suggests that one or more steps in the reaction path could be shared between α-amylase and BE, as the crystal structure of porcine pancreatic α-amylase complexed with acarbose concluded acarbose to be a transition state analog (16). Interestingly, we found no inhibitory effect of *Pseudomonas amyloderamosa* isoamylase by BAY e4609. This is significant, as isoamylase has been proposed to belong to the family of amylolytic enzymes based on sequence comparison (6, 7). In effect, acarbose/ BAY e4609 can be speculated to be useful in further differentiating the groups of enzymes considered to be in the α-amylase family.

References.

1. Preiss, J. (1984). *Annu. Rev. Microbio.* **38**, 419-458.

2. Preiss, J. (1991). in *Plant Molecular and Cell Biology* (Mifflin, B., Ed), vol 7, pp 59-114, Oxford University Press, Oxford.

3. Preiss, J. and Sivak, M. N. (1986). *in* Genetic engineering (Stelow, J. K., Ed.), Vol. 20, pp 177-223, Plenum, New York.

4. Preiss, J. and Sivak, M. N. (1996). *in* Photoassimilate Distribution in Plants and Crops: Source-Sink Relationships (Zamski, E. and Shaffer, A. A., Eds.), pp 63-96, Dekker, New York.

5. Baba, T., Kimura, K., Mizuno, K., Etoh, H., Ishida, Y., Shida, O. and Arai, Y., (1991). *Biochem. Biophys. Res. Commun.* **181**, 87-94.

6. Jespersen, H. M., MacGregor, A. E., Svennson, B. (1991). *Biochemistry* **280**, 51-55

7. Jespersen, H. M, MacGregor, A. E., Henrissat, B., Sierks, M. R., Svensson, B. (1993). *J. Protein Chem.* **12**, 781-805.

8. Kuriki, T., Takata, H., Okada, S. and Imanaka, T. (1991). *J. Bacteriol.* **173**, 6147-6152.

9. Nakamura, Y., Takeichi, T., Kawaguchi, K., and Yamanouchi, H. (1992). *Plant Physiol.* **84**, 329-335.

10. Holm, L., Koivula, A. K., Lehtovaara, P. M., Hemminki, A., and Knowles, J. K. C. (1990). *Protein Eng.* **3**, 181-191.

11. Meyer, B. H., Muller, F. O. and Clur, B. K. (1983) *J. Clin. Pharmac.* **16**, 145-148.

12. Mayo, J. W. and Carlson, D. M. (1974). *Arch. Biochem. Biophys.* **163**, 498.

13. Frommer, W., Puls, W., Schafer, D. and Schmidt, D. D. (1970). German priority, December 28, BAYER AG.

14. Puls, W., Keup, U, Krause, H. P., Muller, L., Schmidt, D. D., Thomas, G. and Truscheit, E. (1980). *Front. Horm. Res.* **7**, 235.

15. Truscheit, E., Frommer, W., Junge, B., Muller, L, Scmidt, D. D. and Wingender, W. (1981). *Angew. Chem. Int. Ed. Engl.* **20**, 744-761.

16. Qian, M., Haser, R., Buisson, G., Duee, E. and Payan, F. (1994). *Biochemistry* **33**, 6284-6294.

17. Strokopytov, B., Penninga, D., Rozeboom, H. J., Kalk, K. H., Dijkhuizen, L. and Dijkstra, B. W. (1995). *Biochemistry* **34**, 2234-2240.

18. Binderup, K. and Preiss, J. (1998). *Biochemistry* **37**, 9033-9037.

19. Guan, H. P., Li, P., Imparl-Radosevich, J., Preiss, J. and Keeling, P. (1997). *Arch. Biochem. Biophys.* **342**. 92-98.

20. Smith, P.K., Krohn, R.I., Hermanson, G.T., Mallia, A.K., Gartner, F.H., Provenzano, M.D., Fujimoto E.K., Goeke, N.M., Olson, B.J. and Klenk, D.C. (1985). *Anal. Biochem.* **150**, 76-85.

21. Guan, H.P. and Preiss, J. (1993). *Plant Physiol.* **102**, 1269-1273.

22. Hawker, J.S, Ozbun, J.L., Ozaki, H., Greenberg, E. and Preiss, J. (1974). *Arch. Biochem. Biophys.* **160**, 530-551.

23. Takeda, Y., Guan, H.P. and Preiss, J. (1993). *Carbohydr. Res.* **240**, 253-263.

24. Dubois, M., Gilles, K. A., Hamilton, J. K., Rebers, P. A., and Smith, F. (1956). *Anal. Chem.* **28**, 350.

25. Park, J. T., and Johnson, M. J. (1949). *J. Biol. Chem.* **181**, 149.

26. Morrison, J. F. and Walsh C. T. (1988). *Adv. Enzymol.* **62**, 201-301.

27. Uehara, Y., Tonomure, B. and Hiromi, K. (1980). *Arch. Biochem. Biophys.* **202**, 250-258.

28. Gutfreund, H. (1972). in *Enzymes: Physical Principles* pp. 20. Wiley-Interscience, New York.

29. Wilcox, E. R. and Whitaker, J. R. (1994). *Biochemistry* **23**, 1783-1791.

CHAPTER 4

LIMITED PROTEOLYSIS OF *ESCHERICIA COLI* BRANCHING ENZYME.

Part of this data has been published:

Binderup, K., Mikkelsen, R., and Preiss, J. (2000) " Limited Proteolysis of Branching Enzyme from *Escherichia coli*". *Arch. Biochem. Biophys.* **377**, 366-371.

Abstract

Branching enzyme is involved in determining the structure of starch and glycogen. It catalyzes the formation of branch points by cleavage and transfer of α-(1,4) glucan chains to α-(1,6) branch points. Limited proteolysis of the branching enzyme from *E. coli* (84 kDa) by proteinase K produced a truncated protein of 70 kDa, which still retained 40-60 % of branching activity, depending on the type of assay used. Amino acid sequencing showed that the 70 kDa protein lacked 111 or 113 residues at the amino terminal, whereas the carboxy terminal was still intact. We purified this truncated enzyme to homogeneity and analyzed its properties. The enzyme had a 3- to 4-fold lower catalytic efficiency compared to the native enzyme, whereas the substrate specificity was unaltered. Furthermore, a branching enzyme with 112 residues deleted at the amino terminal was constructed by recombinant technology and found to have properties identical to the proteolyzed enzyme. We have obtained high-resolution diffracting crystals of this truncated branching enzyme form and have collected a complete native data set to 2.3 Å.

Introduction

Branching enzyme (1,4-α-D-glucan:1,4-α-D-glucan 6-α-D-(1,4-α-D-glucano)-transferase; EC 2.4.1.18) catalyzes the cleavage of an α-1,4 glucosidic linkage and the subsequent transfer of α-1,4-glucan to α-1,6 branch points. The enzyme hence plays an important role in determining the structure of starch and glycogen (1). Several bacterial branching enzymes have been identified and characterized (2). Also, multiple isoforms of the branching enzyme encoded by distinct genes have been reported for many plants, including maize, rice and spinach (3-5). The investigation of the mode of chain transfer and substrate specificity in the maize endosperm isoforms BE I (mBEI) and BE II (mBEII) led to the hypothesis that these enzymes have different roles in the synthesis of amylopectin *in vivo* (6,7). The mBEI can transfer long branches (d.p. 40 to 100) whereas mBEII transfers shorter chains (d.p. 6 to 14). Furthermore, the preferred substrate for mBEI is amylose, whereas mBEII prefers amylopectin. The differences between mBEI and mBEII isoforms suggest that mBEI first branches the amylose transferring long chains and mBEII, in turn, uses this product for further branching to amylopectin.

BE has been shown to belong to the amylolytic family of enzymes by amino acid sequence alignments and site-directed mutagenesis experiments. The amylolytic family, consisting of enzymes that cleave and/or transfer chains of glucan, contains a central $(\alpha/\beta)_8$-barrel as observed in α-amylase and cyclodextrin glucano transferase (8). Branching enzymes have variable extensions at the amino- and carboxy termini relative to the conserved $(\alpha/\beta)_8$-barrel region with little sequence conservation across sources. Our knowledge of the function and significance of these domains is limited. A study using hybrid enzyme construction of two maize branching enzyme isoforms produced a

chimeric enzyme with the N-terminal and central $(\alpha/\beta)_8$-barrel of mBEII and the C-terminal domain of mBEI. This approach produced an active enzyme with the chain transfer pattern of mBEII and the substrate specificity of mBEI (9), suggesting that the C-terminal domain is involved in substrate specificity. Another chimeric enzyme construction with the mBEI sequence at the N-terminal and the central $(\alpha/\beta)_8$-barrel plus the C-terminal domain of mBEII gave an active enzyme having an alteration in size of oligosaccharide chain transfer (9). Thus it was suggested that the N-terminal and/ or central α/β-barrel region is involved in determining the size of chain transferred.

Here, we use the technique of limited proteolysis in order to study the role of the amino- and carboxy-terminal of *E. coli* branching enzyme. The major finding of this investigation was a branching enzyme truncated at the amino terminal with altered activity. Furthermore, crystallization experiments of the truncated *E. coli* branching enzyme formed single well-diffracting crystals which is allowing us to pursue the first three-dimensional structure of a branching enzyme.

Materials and methods

***E. coli* BE expression vector**. H. P. Guan kindly provided the plasmid pEXSB. The pEXSB plasmid is a pET-23d (Novagen) derived expression vector containing the origin p15A, T7 promotor, T7 terminator, kanamycin resistance, and the *E. coli glg*B gene encoding the *E. coli* BE (10).

Limited proteolysis of branching enzyme. All proteases were obtained from Boehinger Mannheim except carboxypeptidase Y from Pierce. Purified branching enzyme (0.5 mg/ml) was digested with the various proteases under the following conditions: 25 °C, 1 mM $CaCl_2$ and 50 mM Tris-Cl pH 7.5 for proteinase K, chymotrypsin, trypsin, and subtilisin. Papain: 25 °C, 1 mM $CaCl_2$ and 50 mM Na citrate pH 6.5. Protease V8 : 25 °C, 1 mM $CaCl_2$ and K-PO_4 or NH_4HCO_3 (50 mM, pH 7.8). Elastase: 25 °C, 1 mM $CaCl_2$ and 50 mM Tris-Cl pH 8.0. Carboxypeptidase Y: 37 °C, 1 mM $CaCl_2$ and 50 mM Na citrate pH 6.5. Time of incubation and concentration of the proteases were varied as indicated in each experiment. Proteolysis was stopped by adding phenylmethylsulfonylfluoride to 0.5 mM and aliquots assayed for activity.

Purification of proteinase K treated branching enzyme. Purified *E. coli* BE was digested by proteinase K as described above for 90 min at 1:1000 molar ratio. The proteolyzed enzyme was loaded on a Mono Q HR 5/5 column equilibrated in 50 mM Tris-Acetate pH 8.0, 5 mM EDTA and 2.5 mM DTT (buffer A). The enzyme eluted at 0.1 M KCl by a gradient of 0-50 % buffer B (buffer A + 1 M KCl).

Construction of Nd_{1-112} truncated BE. The pEXSB plasmid purified from Epicurian Coli XL2-Blue cells (Stratagene) was used as dsDNA template for PCR using the following primers: 5'- GAT GCC TGG CCC ATG GCT GAA GGT ACT CAC CTG

CG -3' and 5'- GCT AGT TAT TGC TCA GCG G -3'. The resulting DNA fragment and pET23d vector were both digested with NcoI and SalI restriction enzymes (New England Biolabs). The PCR fragment and the purified major DNA band from the pET23d digestion were subsequently ligated using the T4 ligase (Boehinger Mannheim). This produced plasmid pTRC1, encoding a 112 amino acid deleted branching enzyme (Nd_{1-112}) with a serine to alanine mutation at position 2 due to construction of the NcoI restriction site. The construct was confirmed by restriction enzyme analysis and DNA sequencing of the entire coding region.

Expression of WT and truncated *E. coli* BE. A 200 ml overnight culture of the transformed cells (BL21[DE3]) carrying pEXSB or pTRC1 was added to a Biostat E10 fermentor containing 12 l fresh LB with 25 $\mu g \cdot ml^{-1}$ kanamycin or 100 $\mu g \cdot ml^{-1}$ ampicillin, respectively. The cells were grown at maximum aeration with 200 rpm stirring at 37°C to A_{600} = 0.4. The temperature was adjusted to 25°C and expression of the T7 RNA polymerase induced by adding isopropyl-D-thiogalactoside to 0.5 mM. After 5 hrs induction, the cells were harvested by centrifugation at 100,000 g · min.

Expression of seleno-methionine substituted Nd_{1-112}. The gene encoding the truncated branching enzyme was excised from pTRC1 and ligated into a pET28a vector using the NcoI/SalI restriction sites. The plasmid was transformed into *E. coli* strain CT-13, kindly provided by Dr. Honggao Yan, Michigan State University. *E. coli* strain CT-13 is a methionine-auxotroph BL21(DE3) derivative and tetracyclin resistant. The culture medium (minimal medium) consisted of 1X Eagle Basal medium (GibcoBRL), 0.2 % glucose, 0.5 mM $MgSO_4$, 100 μM $CaCl_2$, 10 μM $ZnCl_2$, 10 μM $FeCl_3$, 0.4 mg/l thiamine, 4 mg/l d-biotin, 50 μg/ml kanamycin, and 10 μg/ml tetracyclin. Cells from 500 ml

minimal medium overnight culture containing 100 μg/ml L-methionine were washed and added to a Biostat E10 fermentor containing 12 l fresh minimal medium with 50 μg/ml selenium-methionine (Sigma). The cells were grown at maximum aeration with 200 rpm stirring at 37°C to A_{600} = 0.5 before addition of 1 mM isopropyl-D-thiogalactoside and selenium-methionine to 100 μg/ml. After 15 hrs induction at 25°C, cells were harvested and stored at -80°C.

Purification of BE WT and Nd_{1-112}. The purification procedure was modified from Guan *et al.* (10). After sonication the BE WT was precipitated with 40 % $(NH_4)_2SO_4$, whereas the Nd_{1-112} enzyme was precipitated with 30 % $(NH_4)_2SO_4$. The MonoQ HR 16/10 pH 7.5 column was replaced with a DEAE fractogel column (EM science) equilibrated in 50 mM Tris-Acetate pH 8.0, 10 mM EDTA and 2.5 mM DTT (buffer C). The enzyme was eluted with a gradient of 0-50 % buffer D (buffer C + 1 M KCl). The remaining part of the purification was identical to that reported previously (10). BE-WT and Nd_{1-112} eluted at 0.25 M KCl and 0.1 M KCl, respectively, for both the DEAE fractogel and Mono Q column. For truncated branching enzyme substituted with selenium-methionine the sample was concentrated after the MonoQ column to 1 ml. Then 200 μl batches were injected onto a Superose 12 size exclusion column (Pharmacia, Sweden) pre-equilibrated with buffer E (25 mM HEPES pH 7.5 and 5 mM DTT), and eluted with 1.5 bed volume buffer E. The fractions with highest BE purities were pooled and concentrated to 5 mg/ml.

SDS-PAGE and Western Blotting. SDS-PAGE was performed by 4-15 % polyacrylamide gels according to the method of Laemmli (11). Western blotting was carried out according to the method of Burnette (12). The primary rabbit antibody anti-BE

was diluted 1:1000 in 25 mM K-PO_4 pH 7.2, 150 mM NaCl and 3 % gelatin. The antigen- antibody complex was detected using anti-rabbit IgG conjugated with alkaline phosphatase (US Biochemicals, diluted 1:10000) with a chromogenic substrate (Boehinger Mannheim). Molecular weights were determined using Perfect Protein markers (M_r 15, 25, 35, 50, 75, 100, and 150 kDa) for both SDS-PAGE and western blots.

Protein sequencing. N-terminal and C-terminal protein sequencings were performed by Joe Leykam at the Macro-molecular Facility, Department of Biochemistry, Michigan State University.

Assay of BE activity. BE activity was measured by three different assays as described by Guan and Preiss (7).

Assay A. The phosphorylase A stimulation assay is based on the stimulation by BE of the synthesis of α-D-glucan from α-D-Glc-1-P catalyzed by rabbit phosphorylase a (5). Reaction mixtures contained in a final volume of 100 µl, 100 mM citrate (pH 7.0), 10 mM adenosine monophosphate, 0.2 mg phosphorylase a (Sigma) and 50 mM D-[^{14}C]-Glc-1-P (50 DPM · $nmol^{-1}$) and the assay was initiated by an appropriate amount of BE. One unit is defined as 1 µmol of Glc incorporated into α-D-glucan per min at 30°C.

Assay B. The branching linkage assay determines the number of branching points introduced by BE into the substrate, reduced amylose (6). Substrates were prepared by the reduction of enzymatically synthesized amylose (AS-320, d.p. 1815) as described by Takeda *et al.* (6). Reaction volumes contained in a final volume of 100 µl, 25 mM MOPS (pH 7.5) and an appropriate amount of substrate. The reaction was initiated by adding an

appropriate amount of BE. One unit is defined as 1 μmol of branching linkages formed per min at 30°C.

Assay C. The iodine stain assay is based on the monitoring the decrease in absorbance of the glucan-iodine complex resulting from the branching of the substrate, amylose or amylopectin (potato type III [d.p. 1176, chain length 884] and corn respectively, Sigma) (3,7). Reaction mixtures contained in a final volume of 500 μl, 50 mM citrate (pH 7.0) and 0.1 mg substrate. The reaction was initiated by the addition of an appropriate amount of enzyme. One unit is defined as the decrease in absorbance of 1.0 per min at 30°C.

Protein assay. Protein concentration was measured with the BCA protein assay reagent (13), using BSA as the standard.

Mass spectrometry. Protein samples were dialyzed against H_20 and analyzed by mass spectrometry by Stacy Trzos at the Macro-molecular Facility, Department of Biochemistry, Michigan State University.

Protein crystallization. Initial crystallization experiments were carried out at 4°C and 25°C by the sparse-matrix approach using the hanging drop vapor-diffusion method described by Jancarik and Kim (14). Drops contained 2 μl precipitant solution (100 mM HEPES pH 7.2) and 2 μl protein solution at 5 mg/ml.

X-ray diffraction analysis. Crystals were transferred to a cryo-protectant solution containing 25 % (v/v) 2-methyl-2,4-pentanediol, 2 % (w/v) polyethylene glycol 4000 and 100 mM HEPES pH 7.5. Crystals were mounted in nylon cryo-loops (Hampton, CA) and stored in liquid N_2. High resolution data were collected at the Advanced Photon Source at Argonne on the Structural Biology Center ID-19 beamline. Intensity data was collected in

a 3x3 (3072x3072 pixel) CCD area detector to a resolution of 2.3 Å. The crystal to detector distance was set to 220 mm and 160° of data was collected with an oscillation range of 0.5°. Diffraction data was indexed and integrated using DENZO and scaled by the software SCALEPACK (15).

Table 1. Purification table of BE-WT.

Purification step	Volume	Protein	Activity	Specific activity	Yield
	ml	*mg*	*units*	*units · mg^{-1} protein*	*%*
Crude extract	228	4500	891500	198	100
0-40 % $(NH_4)_2SO_4$	180	2200	750100	341	84
DEAE-fractogel	330	701	526000	750	59
Mono Q	128	250	272500	1090	31

Enzyme activity was measured by the phosphorylase a stimulation assay (Assay A).

Results

Purification of *E. coli* BE-WT. The expression and purification procedure detailed in materials and methods greatly improved the yield of *E. coli* branching enzyme (Table 1). The BE-WT enzyme constituted 20 % of total protein in crude extract and appeared as the major band on a SDS-PAGE gel (data not shown). A total yield of 250 mg BE-WT was obtained from a single 12 l batch representing a 20-fold improvement of that reported previously (10).

Proteolysis of *E. coli* branching enzyme. The action of proteinase K on BE was monitored by SDS-PAGE and branching activity. Initial proteolysis experiments were performed using 1:50 molar ratio of proteinase K to branching enzyme (data not shown). These experiments showed a rapid digestion of the native enzyme (84 kDa) to yield a truncated enzyme (70 kDa) subsequently degraded to several smaller fragments. Branching activity under these conditions was rapidly lost. Use of a 1:1000 molar ratio of proteinase K to BE produced the 70 kDa fragment as the major product in 90 min (Figure 1A), with small amounts of fragments of 42, 35, 32, and 13 kDa. Although branching enzyme activity decreased during the proteolysis experiment, 30 % activity remained (Assay A) when no native enzyme was apparent on a SDS-PAGE gel after 90 min (Figure 1B). To test if branching enzyme could be protected from proteinase K cleavage by substrate, we performed digestion experiments in presence of glycogen, amylopectin or amylose, but neither changed the proteolytic rate or the cleavage pattern (data not shown). In an effort to produce alternative digestion patterns, we subjected branching enzyme to several proteases with a range of specificities (Figure 2). Whereas branching enzyme was found sensitive to proteinase K and subtilisin, the other proteases utilized had low rates of

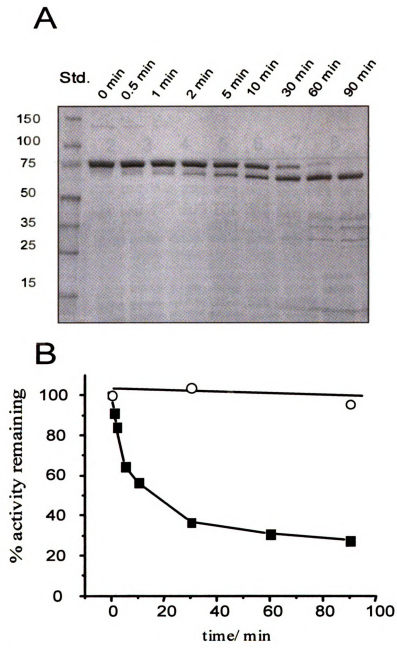

Figure 1. SDS-PAGE (**A**) and branching activity (**B**) of *E. coli* BE treated with 1:1000 molar ratio of proteinase K to BE at various incubation times. **A**: 3 μg of total protein was loaded per lane. The gel has been stained with coomasie brilliant blue. **B**: Branching activity of BE-WT control (O) and proteinase K treated BE (■) by phoshorylase a stimulation assay (Assay A).

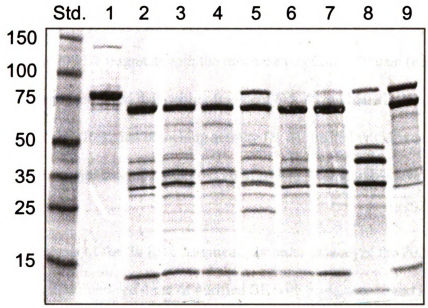

Figure 2. SDS-PAGE of BE-WT treated with various proteases as described in materials and methods. 3 μg of total protein was loaded per lane and the gel stained with coomasie brilliant blue. The ratio of protease to BE-WT and incubation time is indicated in parentheses. Control BE-WT (lane 1). Proteinase K (lane 2; 1:1000; 90 min). Protease V8 w. PO_4 buffer (lane 3; 1:30; 1 hr). Protease V8 w. NH_4HCO_3 buffer (lane 4; 1:20; 2 hrs). Elastase (lane 5; 1:2; 3 hrs). Chymotrypsin (lane 6; 1:30; 2 hrs). Subtilisin (lane 7; 1:500; 90 min). Trypsin (lane 8; 1:10; 3 hrs). Carboxypeptidase Y (lane 9; 1:3; 2 hrs).

digestion. Even 3 hours of treatment using a 1:2 molar ratio of elastase to BE failed to cleave the native enzyme completely. Carboxypeptidase Y also had a low proteolytic effect on branching enzyme and high concentrations (1:3 molar ratio) produced a digestion pattern of an endopeptidase, probably due to small contaminations of other proteases (Figure 2, lane 9). All proteases tested displayed similar digestion patterns, producing a 70 kDa fragment with the notable exception of trypsin (Figure 2, lane 8). For the latter, assays showed that neither fragment (45, 40, and 30 kDa) exhibited branching enzyme activity. Residual branching activity for BE treated with the remaining proteases indicated the major fragment (approx. 70 kDa) had a comparable level of activity in all cases.

Analysis of the 70 kDa fragment. In order to analyze the 70 kDa fragment in greater detail, we cleaved 4 mg of purified BE with proteinase K and subsequently purified 1.6 mg of the truncated enzyme, PK-BE, as described in materials and methods (Figure 3). N-terminal microsequencing of purified PK-BE yielded a 1:1 molar ratio of Leu-Leu-Ser-Glu-Gly-Thr-His-Leu- and Ser-Glu-Gly-Thr-His-Leu-Arg-Pro-, indicating proteinase K performed a staggered cut cleaving either at position Trp^{111}-↓-Leu^{112} or Leu^{113}-↓-Ser^{114}. C-terminal sequencing of both wild-type BE and PK-BE yielded Glu-Ala-Glu-Arg-, indicating the C-terminal of PK-BE was still intact. This gives PK-BE a calculated MW of 71.6 kDa. In order to confirm the results from limited proteolysis, we subsequently generated a truncated BE by inserting a start codon at position 113 *via* recombinant DNA techniques as described in materials and methods. This truncated enzyme, Nd_{1-112}, was expressed and purified to near-homogeneity (Figure 3, Table 2).

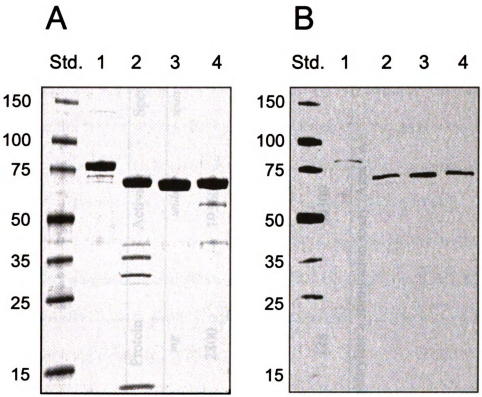

Figure 3. SDS-PAGE (A) and western blot analysis (B) of wild-type and truncated branching enzymes. Control BE-WT (lane 1). Proteinase K treated BE-WT (lane 2). Purified PK-BE (lane 3). Purified Nd_{1-112} (lane 4). Loading per lane was 3 μg total protein in A and 100 ng total protein in B.

Table 2. Purification table of Nd_{1-112}.

Purification step	Volume	Protein	Activity	Specific activity	Yield
	ml	*mg*	*units*	*units · mg^{-1} protein*	*%*
Crude extract	260	2800	193600	69.2	100
0-30 % $(NH_4)_2SO_4$	145	839	193200	230	100
DEAE-fractogel	360	266	143200	538	74
Mono Q	80	128	80300	627	41

Enzyme activity was measured by the phosphorylase a stimulation assay (Assay A).

Both SDS-PAGE and western blot analysis indicate PK-BE and Nd_{1-112} have similar migration patterns and are free of any native BE.

Activity of PK-BE and Nd_{1-112}. Activities of pure PK-BE, Nd_{1-112} and BE-WT were characterized with respect to three assays available for branching enzyme (Table 3). Specific activities of PK-BE and Nd_{1-112} were very similar and consistently lower than BE-WT (60 % of wild-type activity for assay A and 40 % for assay B and assay C). Calculating the ratio of activity has been useful in comparing the properties of various branching enzymes (7,16). In particular the iodine assay has been employed to establish a measure of preference between the two substrates amylose and amylopectin. Here, the enzymes have a similar C_2/C_1 ratio (iodine assay with amylopectin and amylose, respectively), suggesting the substrate preference is unaltered for both PK-BE and Nd_{1-112} relative to BE-WT. As for BE-WT, both truncated branching enzymes showed negligible levels of amylolytic activity.

Kinetic parameters of the enzymes were determined using the branching linkage assay (Assay B) with reduced amylose AS-320 as substrate (Table 4). Whereas the K_m values were essentially unchanged, both PK-BE and Nd_{1-112} have a 3-4 fold lower specific activity and catalytic efficiency than BE-WT.

Crystallization of *E. coli* branching enzyme. Previous attempts to *crystallize E. coli* BE WT were unsuccessful in providing single protein crystals suitable for X-ray diffraction analysis. When subjecting Nd_{1-112} to crystallization trials by the sparse matrix screening, we were able to produce single protein crystals of maximum size 0.3x0.1x0.1

Table 3. Specific activities of *E. coli* BE WT, PK-BE and Nd_{1-112}.

Specific Activities, (U/mg)			
Assay	WT	PK-BE	Nd_{1-112}
Phosphorylase A, **A**	1100	650	684
Branching linkage, **B**	1.10	0.39	0.47
Iodine Stain[a], **C**			
Amylose, $\mathbf{C_1}$	91.5	34.9	35.1
Amylopectin, $\mathbf{C_2}$	51.2	22.1	21.6
Ratio of activity			
A/B	1000	1667	1455
$\mathbf{A/C_1}$	12.0	18.6	19.5
$\mathbf{A/C_2}$	21.5	29.4	31.7
$\mathbf{C_2/C_1}$	0.56	0.63	0.62

[a]The $\mathbf{C_1}$ and $\mathbf{C_2}$ denotes the iodine staining assay with amylose and amylopectin as substrate, respectively.

Table 4. Kinetic parameters of *E. coli* BE WT, PK-BE and Nd_{1-112}.

	WT	PK-BE	Nd_{1-112}
Specific activity, ($\mu mol \times min^{-1} \times mg^{-1}$)	3.7 +/- 0.2	0.98 +/- 0.05	1.25 +/- 0.04
K_m, (μM)	11.7 +/- 0.7	12.7 +/- 1.6	12.6 +/- 1.2
k_{cat}/ K_m, ($s^{-1} \times M^{-1}$)	4.5×10^5	1.1×10^5	1.4×10^5

Activity was measured by the branching linkage assay (Assay B) using reduced amylose

Table 5. Statistics for the branching enzyme X-Ray diffraction data collection[a]

Wavelength (Å)	0.97794
Resolution range (Å)	35.0 – 2.3 (2.38 – 2.30)
Number of measured reflections	1,671,259
Number of independent reflections	152,002
Completeness (%)	99.6 (98.6)
Rmerge (I)[b] (%)	8.6 (30.3)
$\langle I \rangle / \langle \sigma I \rangle$ (%)	10.43 (2.57)

[a] Values in parenthesis refer to the lowest resolution shell

[b] Rmerge = $\Sigma I \, |II - \langle I \rangle| \, / \, \Sigma \langle I \rangle$, where II is an individual intensity measurement and $\langle I \rangle$ is the average intensity for this reflection, with summation over all data

mm (Figure 4). A high-resolution native data set was collected at the Argonne Advanced Photon Source complete to 2.3 Å (Table 5). The branching enzyme crystals belong to the $P2_1$ space group with unit cell parameters a = 91.44, b = 102.58, c = 185,41 Å, and β = 91.38°. Based on these results and the size of the enzyme (71.6 kDa monomer in solution), we assume to have 4 molecules in the assymmetric unit. The corresponding crystal volume per protein mass (V_m) and solvent content are within the range of values observed for protein crystals (17). The crystal properties are summarized in Table 6. The data was 99.6% complete in a 35.0 to 2.3 Å resolution range with a R_{merge} of 0.086 for 152002 unique reflections derived from a total of 1617259 individual reflections.

Table 6. Branching enzyme crystal properties.

Unit cell (Å, °)	A = 91.44, b = 102.58, c = 185.41
	β = 91.38
Space group	$P2_1$
Z	4
V_m ($Å^3$/Da)	3.1
Solvent content (%)	56.5

Production of selenium-methionine Nd_{1-112}. In order to solve the structure we decided to obtain phasing information *via* multiple anomalous dispertion data derived from selenium-methionine substituted branching enzyme crystals. Using the pTRC1 plasmid we measured that 10 % of the final branching enzyme yield was obtained prior to induction, which would hinder full incorporation of selenium-methionine into Nd_{1-112}

Figure 4. Crystal of the truncated *E. coli* branching enzyme.

(data not shown). Furthermore, methionine auxotroph CT-13 cells did not grow when transformed with pTRC1. The construct based on the double-repressed pET28 vector as described in materials and methods effectively solved these problems. The yield from 12 l minimal media was 5 mg of highly pure branching enzyme which was fully substituted as determined by mass spectrometry (Table 7).

Table 7. Mass spectrometry of truncated branching enzyme.

	Experimental MW[a]	Theoretical MW	Error
Native Nd_{1-112}	71681.2 Da	71588.2 Da	0.130 %
Se-Met Nd_{1-112}	72406.5 Da	72338.6 Da	0.094 %

[a]Average of three individual experiments.

Crystals of selenium-methionine substituted truncated branching enzyme have now been produced and will be analyzed at the Argonne Advanced Photon Source.

Discussion.

Branching enzyme is important for determining the structure of glycogen and starch. There is considerable variation with respect to specific activities, chain transfer patterns and substrate preferences of branching enzymes from diverse sources, but little is known of what structural features are responsible for these observations. By deleting 111 to 113 amino acids at the N-terminal of *E. coli* branching enzyme by either proteolysis or recombinant techniques, we have produced an active enzyme with altered specific activity. We found that most proteases produced the same proteolytic pattern with a relatively stable fragment of 70 kDa. This suggests part of the amino terminal region is exposed to the surface of the protein as proteolysis occur at flexible loci along the peptide chain (18). Secondary structure prediction by the program PHD (19) indicates proteinase K cleaves the *E. coli* branching enzyme at the carboxy end of an α helix covering residues 105-113, but with a low reliability index. The region of residues Phe^{100} to Pro^{243} of *E. coli* BE has been shown to share homology with the amino terminal (domain N) of isoamylase from *Pseudomonas amyloderamosa* and these regions are proposed to share a common structural domain (8, 20). The recent three-dimensional structure of isoamylase shows domain N contains 160 residues, where residues 1-83 form six β strands and one α helix, whereas residue 83-160 has no secondary structure (21).

It was concluded by Kuriki *et al.* (9) that the substrate specificity of the maize branching enzyme isoforms is determined by the C-terminal region. Our analysis of the N-terminal truncated *E. coli* BE indicates substrate binding is unaffected by the deletion as the K_m was essentially constant between PK-BE, $Nd_{1\text{-}112}$ and BE-WT. Also, glycogen, amylopectin or amylose could not protect the N-terminal region from digestion by

proteinase K. The data from iodine assay furthermore indicate the substrate preference of PK-BE and Nd_{1-112} is unaltered from the native enzyme. These observations support the argument that the N-terminal 111-113 amino acids have limited involvement in substrate binding for *E. coli* branching enzyme. The N-terminal has been proposed to be involved in the chain transfer pattern of branching enzyme based on construction of a hybrid enzyme from the maize isoforms (9). We are currently investigating if the N-terminal 112 amino acids are involved in chain transfer by analyzing the branching pattern of the truncated branching enzyme relative to the native enzyme.

A schematic representation of several branching enzymes constructed by amino acid sequence alignments and secondary structure predictions, illustrates the diversity of the amino and carboxy termini of branching enzymes (Figure 5). *E. coli* BE is homologous to *Bacillus Stearothermophillus* BE (45 % identity/ 57 % similarity) and the two enzymes differ at least with respect to thermostability and temperature optima at 30°C and 50°C, respectively (7,22). As the *B. Stearothermophillus* BE has a shorter N-terminal by 94 residues but otherwise is very similar to *E. coli* BE, we measured if the truncated *E. coli* branching enzymes had altered thermostability compared to BE-WT. However, we found the enzymes were identical in this respect. There appears to be considerable variation of the lengths of both the N- and C-terminal regions between various branching enzymes (Figure 5). The enzyme from *Bacillus stearothermophilus* has the shortest amino terminal region (149 amino acids) of any known branching enzyme. Interestingly, PK-BE has only 130 amino acids at the N-terminal, but still has branching activity. It would be of interest to construct a series of deletion mutants of branching enzyme at the N-terminal toward the conserved $(\alpha/\beta)_8$-barrel to investigate if branching

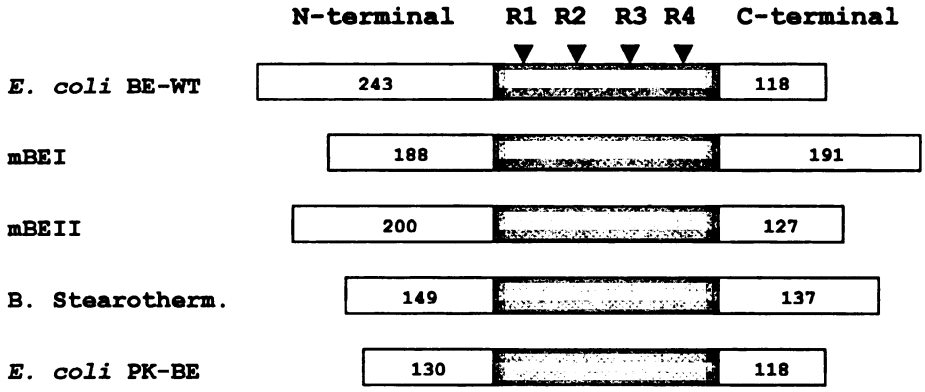

Figure 5. Schematic diagram of several branching enzymes. Location of the conserved $(\alpha/\beta)_8$-barrel (grey) containing the four conserved regions (R1-R4) was determined by alignment to amylolytic enzymes of known structure and secondary structure prediction by PHD (19). The number of amino acids at the amino- and carboxy terminals are indicated. mBEI: maize BE isoform I. mBEII: maize BE isoform II. B. Stearotherm.: *Bacillus Stearothermophilus* BE.

enzyme activity will be further altered or lost, and these experiments are currently in progress in our laboratory. Several enzymes involving cleavage or formation of α-1,6 glucan linkages including branching enzyme, isoamylase and pullulanase, have an amino terminal extension relative to the conserved $(\alpha/\beta)_8$-barrel region. Other amylolytic enzymes, including several α-amylases, do not possess any N-terminal region, leading to speculation if a branching enzyme could be altered in its function by truncation experiments.

There is currently no structure available of branching enzyme. Considerable efforts have concentrated on crystallizing the native enzyme from *E. coli* with limited success. We were hopeful that the truncated enzyme's resistance to further proteolysis indicated a more compact and stable enzyme hereby enabling us to crystallize it. The results from crystallizing the $Nd_{1\text{-}112}$ truncated enzyme are very promising and although much future work is needed we believe this work ultimately will lead us to the first three-dimensional structure of branching enzyme.

References

1. Guan, H. P., Kuriki, T., Sivak, M. N. and Preiss, J. (1995) *Proc. Natl. Acad. Sci.* **92**, 964-967.

2. Preiss, J. (1984) *Annu. Rev. Microbiol.* **38**, 419-458.

3. Boyer, C. D. and Preiss, J. (1978) *Carbohydr. Res.* **61**, 321-334.

4. Nakamura, Y., Takeichi, T., Kawaguchi, K and Yamanouchi, H (1992) *Plant Physiol.* **84**, 329-335.

5. Hawker, J. S., Ozbun, J. L., Ozaki, H., Greenberg, E. and Preiss, J (1974) *Arch. Biochem. Biophys.* **160**, 530-551.

6. Takeda, Y., Guan, H. P. and Preiss, J. (1993) *Carbohyd. Res.* **240**, 253-263.

7. Guan, H. P. and Preiss, J. (1993) *Plant Physiol.* **102**, 1269-1273.

8. Jespersen, H. M., MacGregor, A. E., Henrissat, B., Sierks, M. R. and Svensson, B. (1993) *J. Prot. Chem.* **12**, 791-805.

9. Kuriki, T. Stewart, D. C. and Preiss, J. (1997) *J. Biol. Chem.* **272**, 28999-29004.

10. Guan, H. P., Li, P., Imparl-Radosevich, J., Preiss, J. and Keeling, P. (1997) *Arch. Biochem. Biophys.* **342**, 92-98.

11. Laemmli, U. K. (1970) *Nature* **227**, 680-685.

12. Burnette, W. W. (1981) *Anal. Biochem.* **112**, 195-203.

13. Smith, P. K., Krohn, R. I., Hermanson, G. T., Mallia, A. K., Gartner, F. H., Provenzano, M. D., Fujimoto, E. K., Goeke, N. M., Olson, B. J. and Klenk, D. C. (1985) *Anal. Biochem.* **150**, 76-85.

14. Jancarik, J, Kim, S-H 1991. *J. Appl. Cryst.* **24**; 409-411.

15. Otwinowski, Z, Minor, W (1997). *Methods Enzymol.* **276**; 307-326.

16. Binderup, K. and Preiss, J. (1998) *Biochemistry* **37**, 9033-9037.

17. Matthews, B. (1968). *J. Mol. Biol.* **33**, 491-497.

18. Fontana, A., Fassina, G., Vita, C., Dalzoppo, D., Zamai, M. and Zambonin, M. (1986) *Biochemistry* **25**, 1847-1851.

19. Burkhard, R. and Sander, C. (1993) *J. Mol. Biol.* **232**, 584-599.

20. Svenson, B. (1994) *Plant Mol. Biol.* **25**, 141-157.

21. Katsuya, Y., Mezaki, Y., Kubota, M. and Matsuura, Y. (1998) *J. Mol. Biol.* **281**, 885-897.

22. Takata, H., Takaha, T, Kuriki, T., Okada, S., Takagi, M. and Imanaka, T. (1994) *Appl. Environ. Microbiol.* **60**, 3096-3104.

CHAPTER 5

TRUNCATION OF THE AMINO TERMINAL DOMAIN RESULTS IN ALTERED CHAIN TRANSFER PATTERN OF BRANCHING ENZYME.

Patent pending: Binderup, K. and Preiss, J. "Truncation of the amino terminal domain results in the altered chain transfer pattern of branching enzyme."

Abstract

Previous work has reported the production of an *E. coli* branching enzyme with a 112 residue deletion at the amino terminal by limited proteolysis. Here, we investigate the chain transfer pattern by *in vitro* branching of amylose using purified truncated or native branching enzyme. Gel permeation chromatography of the synthesized α-glucan after 2 and 4 hours of branching shows the truncated branching enzyme transfers fewer short chains (degree of polymerization [d.p.] < 20) and a greater proportion of intermediate size chains (d.p. 30-90) than the native enzyme. High performance anion exchange chromatography (HPAEC) of the branching limited product indicates the truncated branching enzyme transfers a smaller proportion of chains d.p. 5-11 and more chains longer than d.p. 12. Also, the genes encoding native or truncated branching enzyme were individually expressed in a branching enzyme deficient mutant, AC71 (*glgB*$^-$). By HPAEC analysis of the purified α-glucan we find that truncated branching transfers relatively fewer chains of d.p. 4-11 and more chains d.p. longer than d.p. 12. These observations allow us to conclude that truncation of the amino terminal has produced an enzyme with altered branching pattern. Our results are consistent with the construction of hybrid branching enzymes from the maize isoforms.

Introduction

The biosynthesis of plant starch and bacterial glycogen requires the involvement of at least three enzymes: ADPglucose pyrophosphorylase, starch synthase or glycogen synthase (GS) and branching enzyme (BE; 1, 2). The rate of glycogen and starch synthesis is allosteric regulated at the step of ADPglucose pyrophosphorylase. However, the structures of glycogen and starch are mainly determined by the properties of glycogen synthase or starch synthase and branching enzyme (3), although other enzymes are involved (4, 5).

BE catalyzes the cleavage of a α-(1,4) glucosidic linkage and subsequent transfer to a α-(1,6) branch point (6). The enzyme has been identified and characterized from a variety of sources including *E. coli*, maize and rice endosperm (7-9). In many plants multiple isoforms of the enzyme encoded by distinct genes have been reported including maize, rice and pea seed (8-10). The characterization of maize endosperm BE isoforms I (mBEI) and II (mBEII) with respect to chain transfer pattern and substrate specificity, led to the hypothesis that these enzymes have different roles in amylopectin synthesis *in vivo* (8, 11). mBEI transfers long chains (d.p. 40 to 100), whereas mBEII transfers short chains (d.p. 6 to 14). Also, the preferred substrate for mBEI was amylose whereas mBEII showed higher activity with amylopectin. These observations led researchers to suggest that *in vivo*, mBEI transfers long chains which are then further branched by mBEII. Homology in the primary structure between BE and other enzymes cleaving and/or transferring chains of glucan, suggests a central catalytic $(\alpha/\beta)_8$ barrel domain (12, 13). This domain contains seven residues located in four regions that are invariably found in branching enzymes, α-amylases, pullulanases, isoamylases, and cyclodextrin

glucanotransferases (13). In contrast, the size of extensions at the amino- and carboxy termini vary greatly between the amylolytic enzymes (14). By constructing a hybrid branching enzyme out of mBEI and mBEII, an enzyme containing the amino terminal region and central $(\alpha/\beta)_8$ barrel of mBEII and carboxy terminal from mBEI was obtained (15). This resulted in an active branching enzyme with the chain transfer pattern of mBEII and a substrate specificity of mBEI, suggesting the amino terminal being involved in the branching pattern.

Recently, we have reported the construction of a truncated *E. coli* branching enzyme by limited proteolysis using proteinase K (16). This produced an enzyme (PK-BE) with 111 or 113 residues at the N-terminal, whereas the C-terminal was intact. The truncated enzyme had 40-60 % activity of the native *E. coli* BE depending on the type of assay and unaltered substrate specificity. Furthermore, a N-terminal 112 residue deletion of *E. coli* BE constructed by recombinant DNA technology (Nd_{1-112}) was found to have properties identical to PK-BE. In this study we investigate the chain transfer pattern of the truncated *E. coli* branching enzyme using either *in vitro* branching of amylose or expression in AC71 (*glgB*$^-$) followed by analysis of the synthesized α-glucans.

Materials and methods

Plasmids. *glgB* was excised from plasmid pEXSB (17) with restriction enzymes *NcoI* and *SalI* and ligated into the *NcoI* and *SalI* sites of vector pET23d (Novagen), forming plasmid pGBE, encoding the native *E. coli* branching enzyme. The construction of plasmid pTRC1 encoding an enzyme with a 112 residue deletion at the amino terminal of *E. coli* BE was described earlier (16).

Expression of wild type and truncated BE in *E. coli* strain AC71 (glgB⁻). Overnight cultures of *E. coli* B containing vector pET23d or strain AC71 (*glgB*⁻, 3) transformed with plasmids pET23d, pGBE and pTRC1 were diluted 1:20 into fresh Kornberg Broth pH 7.4 containing 100 μg/ml ampicillin and 2 % glucose. The cells were grown at 37°C to OD600 = 0.5 before induction with isopropyl β-D-thiogalactoside to 0.5 mM. Incubation was continued at 25°C for 12 hrs before harvest. The α-glucan was isolated from about 25 g of cell paste according to the method of Preiss *et al.* (18). The yield (crude extract and purified product) was determined by the complete hydrolysis of α-glucan by glucoamylase and α-amylase (19) and subsequent quantification by NADPH formation through action of hexokinase and glucose-6-phosphate dehydrogenase (20).

Purification of branching enzymes: The native *E. coli* branching (BE-WT), *E. coli* branching enzyme treated with proteinase K (PK-BE) and the *E. coli* branching enzyme with 112 residues deleted at the N-terminal by recombinant DNA techniques (Nd_{1-112}) were purified to homogeneity as described earlier (16).

Branching enzyme activity. The branching enzyme activity was measured by either the phosphorylase stimulation assay (assay A) or the branching linkage assay (assay B).

Assay A. The phosphorylase A stimulation assay is based on the stimulation by BE of the synthesis of α-D-glucan from α-D-Glc-1-P catalyzed by rabbit phosphorylase a (21). Reaction mixtures contained in a final volume of 100 μl, 100 mM citrate (pH 7.0), 10 mM adenosine monophosphate, 0.2 mg phosphorylase a (Sigma) and 50 mM D-[^{14}C]-Glc-1-P (50 DPM · nmol^{-1}) and the assay was initiated by an appropriate amount of BE. One unit is defined as 1 μmol of Glc incorporated into α-D-glucan per min at 30°C.

Assay B. The branching linkage assay determines the number of branching points introduced by BE into the substrate, reduced amylose (11). Substrates were prepared by the reduction of enzymatically synthesized amylose (AS-320, d.p. 1815) as described by Takeda *et al.* (11). Reaction volumes contained in a final volume of 100 μl, 25 mM MOPS (pH 7.5) and an appropriate amount of substrate. The reaction was initiated by adding an appropriate amount of BE. One unit is defined as 1 μmol of branching linkages formed per min at 30°C.

Glycogen synthase assay. The glycogen synthase activity was measured by the primed glycogen synthesis reaction (22). The reaction mixture (200 μl) contained 300 nmol ADP-[^{14}C]glucose (350 DPM · nmol^{-1}), 0.5 mg rabbit liver glycogen, 2 μmol GSH, 100 μg BSA, 0.1 μmol magnesium acetate and 5 μmol potassium acetate in 0.1 M biscine pH 8.0. The reaction was initiated by adding an appropriate amount of glycogen synthase. One unit is defined as the incorporation of 1 μmol glucose into glycogen per min at 37°C.

Protein assay. Protein concentration was measured with the BCA protein assay reagent (23), using BSA as the standard.

Analysis of branched chain length. Reduced amylose (10 mg, AS-320, d.p. 1815) was incubated in 25 mM MOPS, pH 7.5 (1 ml) at 30°C with branching enzyme (10 mU of *E. coli* BE WT, PK-BE and Nd_{1-112} by assay B). After 2, 4 and 16 hrs, aliquots of the reaction was heated in boiling water bath for 2 min. The synthesized α-glucan was then debranched by adding isoamylase (100 U/ml) and Na-acetate pH 3.5 to a final concentration of 100 mM. After 90 min at 45°C, the solution was heated in a boiling water bath for 5 min and immediately analyzed by HPAEC and gel filtration.

HPAEC analysis. The debranched α-glucan solution was filtered through 0.22 μm membrane and 25 μl samples injected in the BioLC HPAEC (Dionex), using a CarboPac PA-1 column (250 × 4 mm). Eluent A was 150 mM sodium hydroxide; eluent B was 150 mM sodium hydroxide containing 500 mM sodium acetate. The gradient program was: 25 % eluent B at time 0, 45 % at 15 min, 60 % at 45 min, 70 % at 80 min, and 80 % at 100 min with a flow rate of 0.3 $ml \cdot min^{-1}$. The standard was 25 μl of 5 $mg \cdot ml^{-1}$ maltodextrin (d.p. 1-20, Aldrich).

Analysis of chain length by gel filtration. The debranched α-glucan solution was briefly centrifuged before loading 900 μl (containing 8 mg debranched sample or 3 mg substrate AS-320) on a TSK HW 50 gel filtration column (dextrin separation range MW 500-20000, Ø 1.6 cm × 55 cm) equilibrated in H_2O. Eluent was H_2O at flow rate 20 $ml \cdot hr^{-1}$. 2 ml fractions were analyzed for λ_{max} and maximal absorption of the iodine-polysaccharide complex and total carbohydrate content by the phenol-H_2SO_4 method using glucose as standard (24).

Glucan-iodine complex. λ_{max} of the glucan-iodine complex was performed as described by Krisman (25) in presence or absence of $CaCl_2$.

Average α-glucan chain length determination. First, the amount of α-(1,6) linkages were determined by isoamylase debranching followed by a Park-Johnson analysis as described above. Then, α-glucan samples (200 μl) were hydrolyzed to glucose by the concerted action of glucoamylase and α-amylase as described by Huijing (19) and total glucose measured by the Park-Johnson method. Average chain length was calculated as the ratio of total glucose to α-(1,6) linkages.

Results

Chain transfer pattern by PK-BE, Nd_{1-112}, and BE-WT. Modification of the structure of reduced amylose AS-320 by the branching enzymes was monitored by gel filtration and HPAEC. We analyzed the transferred chains by gel filtration after 2 and 4 hours branching for BE-WT, PK-BE, and Nd_{1-112} (Figure 1). The control, substrate amylose AS-320, eluted as a sharp peak with calculated average chain length of d.p. 1500-2000. After 2 hours branching, PK-BE and Nd_{1-112} showed a much broader range of transferred chains relative to BE-WT (Figure 1B-D). As the same number of units of activity (by assay B) was added for all three enzymes, this observation can not be attributed to differences in activity. Furthermore, the deduced average chain size for the collected fractions indicate the substrate has been modified by branching. In case of PK-BE and Nd_{1-112}, the maximal optical density of the iodine-polysaccharide complex (Figure 1C-D, solid line) shows a bimodal peak after 2 hours of branching, probably due to the strong absorption of long chains. After 4 hours branching, BE-WT (Figure 1F) shows a narrow peak compared to PK-BE and Nd_{1-112}, which furthermore is shifted to the right, indicating transfer of smaller oligosaccharide chains. The maximal optical density of BE-WT is much reduced compared to the truncated branching enzymes, further suggesting absence of long chains.

The data from gel filtration is summarized in Figure 2. Both truncated branching enzymes have very similar chain transfer patterns and are markedly different than BE-WT. For both 2 and 4 hours of branching the BE-WT has a higher population of small chains (d.p. <20) and lower amounts of intermediate chains (d.p. 20-30 and d.p. 30-90) compared to the truncated branching enzymes. All enzymes show a similar population of

Figure 1. Analysis of transferred chain length by gel filtration after 2 hrs (**A-D**) and 4 hrs (**E-H**) of branching using reduced amylose AS-320 as substrate. The conditions for sample preparation, column- and debranching conditions is detailed in materials and methods. The x-axis shows the elution volume scale (ml). Total carbohydrate (O) of each 2 ml fractions was measured by the phenol sulfuric acid method. The total carbohydrate scale (μg/ml) is shown at left on the Y-axis. λmax values are shown as the broken line. The Y-axis on the right represents the λmax wavelength (nanometers). The optical density (O.D.) of the iodine-polysaccharide complex (solid line) was measured at λmax for each fraction. The optical density scale is shown at far right on the Y-axis. The degree of polymerization (d.p., ■) was determined by using λmax values of the debranched glucans according to Banks *et al.* (26). Note the logarithmic scale of the deduced d.p.

A, E: Substrate reduced amylose AS-320.

B, F: BE-WT after 2 and 4 hrs of branching, respectively.

C, G: PK-BE after 2 and 4 hrs branching, respectively.

D, H: Nd1-112 after 2 and 4 hrs branching, respectively.

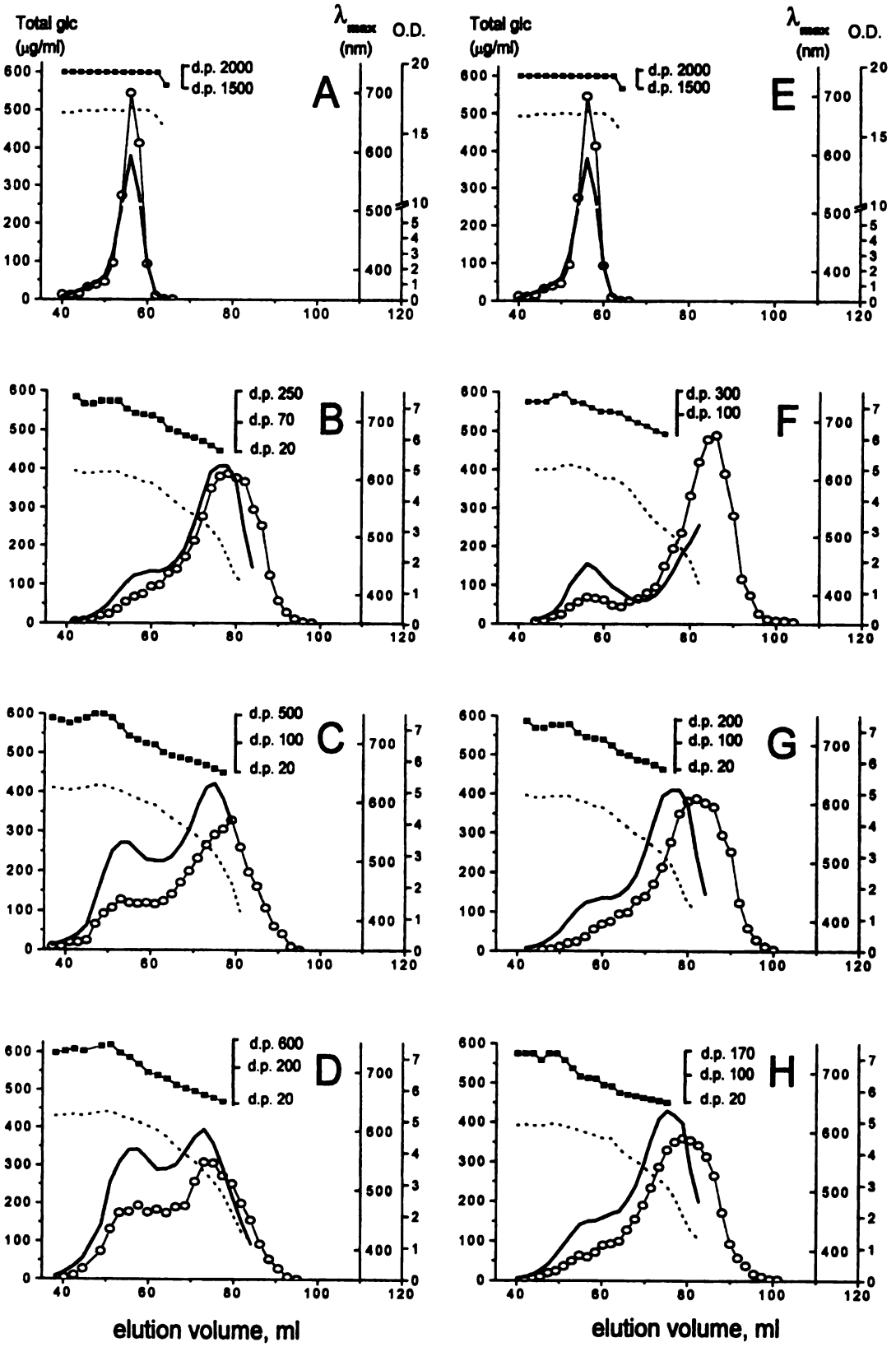
Total glc
(μg/ml)
λmax
(nm)
O.D.
d.p. 2000
d.p. 1500
A
d.p. 250
d.p. 70
d.p. 20
B
d.p. 500
d.p. 100
d.p. 20
C
d.p. 600
d.p. 200
d.p. 20
D
E
d.p. 300
d.p. 100
F
d.p. 200
d.p. 100
d.p. 20
G
d.p. 170
d.p. 100
d.p. 20
H
elution volume, ml
elution volume, ml

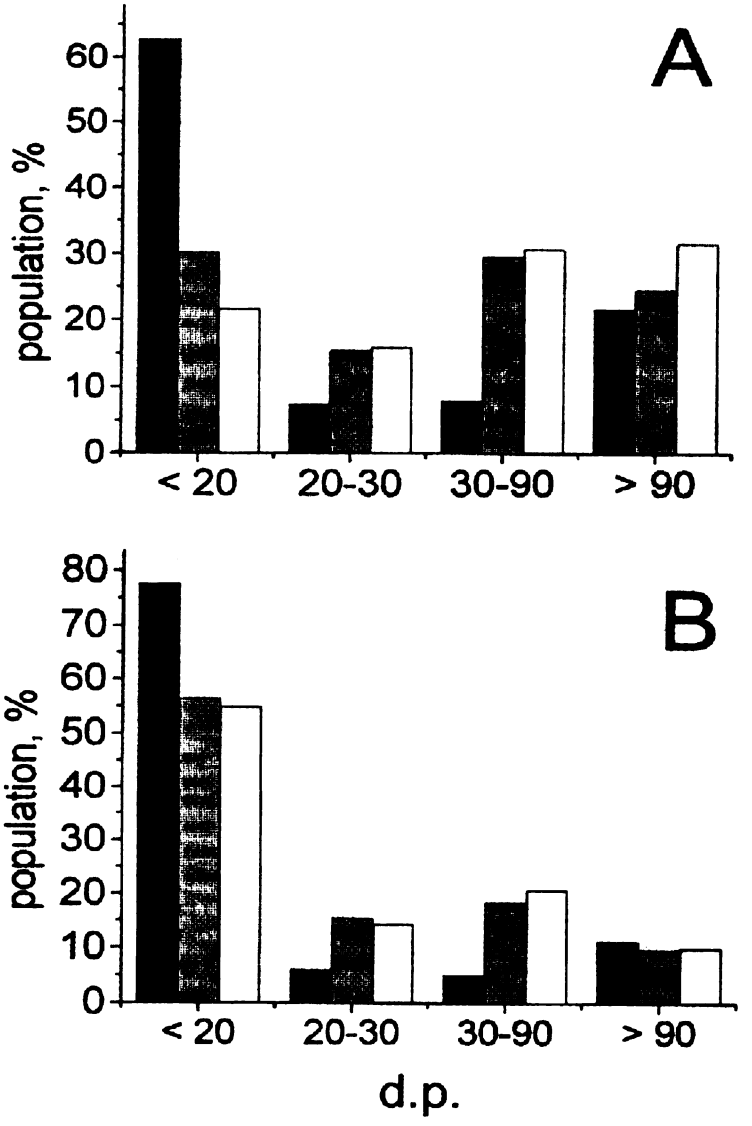

Figure 2. Relative distribution of transferred oligosaccharide chain sizes after 2 hrs (A) and4 hrs (B) branching based on data from gel filtration. BE-WT (black). PK-BE (gray). Nd1-112 (white). For explanation of deduced d.p., refer to legend of Fig. 1. The relative population was determined by measuring total carbohydrate of fractions of a given chain size. Sum of carbohydrate in all fractions was set to 100 %.

long chains (d.p. >90), most likely reflecting equal amounts of partly reacted substrate AS-320.

Further investigation of transferred short chains was performed by HPAEC. Figure 3 shows the HPAEC pulsed amperiometric detector (PAD) response chromatogram of BE-WT and Nd_{1-112} after 2 and 16 hrs of branching. There is a clear difference in chain transfer pattern between BE-WT and Nd_{1-112} after 2 hrs of branching (Figure 3A,B). The chromatogram of BE-WT (Figure 3A) shows a glucan distribution with d.p. 11 being most transferred, and few chains are detected above d.p. 25. In contrast, Nd_{1-112} shows a bimodal distribution centered at d.p. 11 and d.p. 16 with transferred chains up to d.p. 40 easily detected. These chromatograms are in agreement with the results obtained from gel filtration after 2 hrs of branching (Figure 2A). The glucan product after 16 hrs of branching is shown in Figure 3C,D. These chromatograms illustrate the branching limited products of amylose AS-320 by BE-WT and Nd_{1-112} as branching enzyme activity was still present after 16 hrs incubation and addition of 10-fold the branching activity yielded identical glucan structures (data not shown). λ_{max} of the synthesized glycogen was 460 nm and 474 nm for BE-WT and Nd_{1-112}, respectively. The peak areas from the HPAEC chromatograms after 16 hrs were calculated and the relative peak area difference between Nd_{1-112} and BE-WT is shown in Figure 4 for easy comparison. Nd_{1-112} transfers a relatively greater proportion of chains longer than d.p. 12 and fewer chains d.p. 4 to d.p. 11 compared to the native *E. coli* branching enzyme.

In order to investigate an *in vivo* comparison of BE-WT and truncated BE, the genes coding these were expressed individually in the *glgB* deficient *E. coli* strain AC71. Figure 5 shows iodine staining of *E. coli B* containing pET23d, AC71 transformed with

Figure 3. High Performance Anion Exchange Chromatography of debranched α-glucan formed by the action of BE-WT and Nd1-112 on reduced amylose AS-320 after 2 hrs (**A**,**B**) and 16 hrs (**C**,**D**) of branching. Numbers above peaks indicate particular chain sizes.

A, **C**: BE-WT after 2 and 16 hrs of branching, respectively.

B, **D**: Nd1-112 after 2 and 16 hrs branching, respectively.

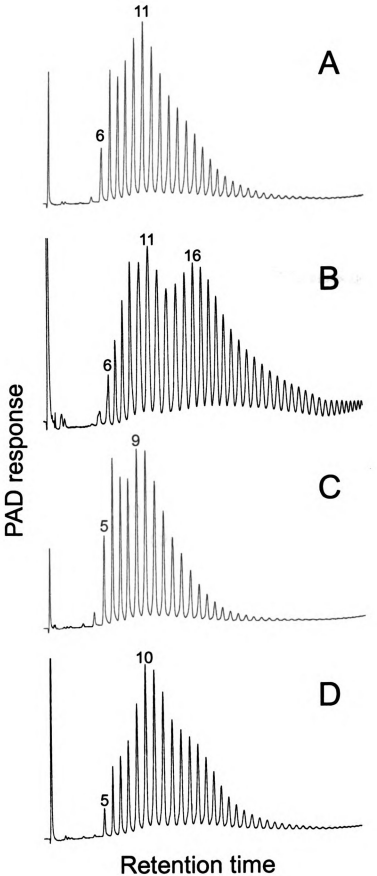
11
A
6
11
16
B
6
9
C
5
10
D
5
PAD response
Retention time

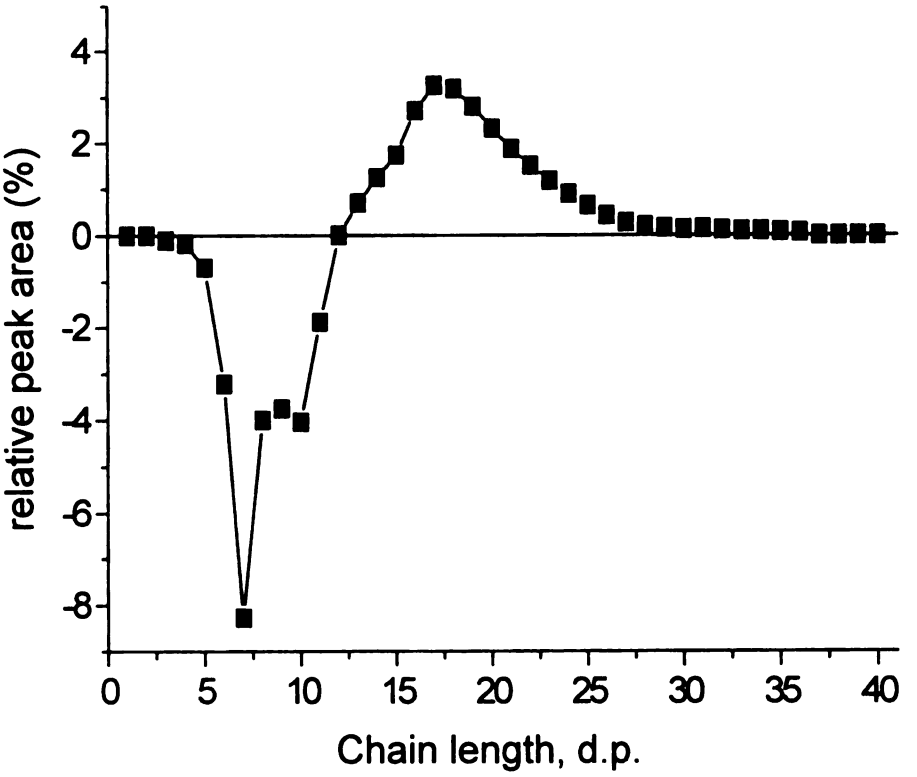

Figure 4. Difference in chain distribution between $Nd_{1\text{-}112}$ and BE-WT resulting from branching amylose AS-320 for 16 hrs. The difference was the relative peak areas from $Nd_{1\text{-}112}$ minus the relative peak area from BE-WT for a given chain length. The sum of chains with d.p. 1-40 was set as 100 %.

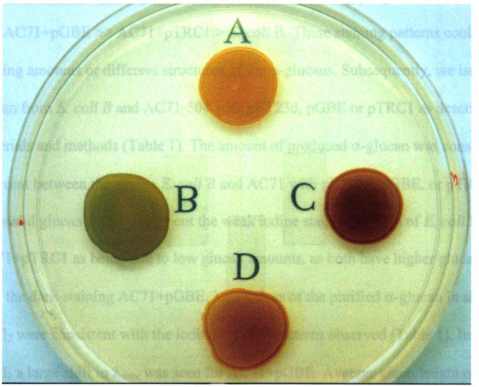

Figure 5. Staining of cell colonies with iodine vapor. (A) *E. coli* B transformed with pET23d. *E. coli* strain AC71 (glgB-) was transformed individually with control pET23d (B), pGBE encoding BE-WT (C) and pTRC1 encoding truncated BE (D). Overnight cultures were dispensed on Kornberg plates (pH 7.4) containing 100 mg/ml ampicillin, 1 mM isopropyl b-D-thiogalactoside and 2 % glucose. After 15 hrs at 37°C the plates were inverted over a lawn of iodine crystals for cell staining.

control pET23d, pGBE encoding BE WT and pTRC1 encoding truncated BE. AC71+pET23d results in a green-blue staining of the iodine-glucan complex characteristic of amylose (25). The order of brown iodine-glycogen color development was AC71+pGBE >> AC71+pTRC1 > *E. coli* B. These staining patterns could be due to varying amounts or different structures of the α-glucans. Subsequently, we isolated α-glucan from *E. coli B* and AC71-504 with pET23d, pGBE or pTRC1 as described in materials and methods (Table 1). The amount of produced α-glucan was consistently different between the strains *E. coli B* and AC71 with pET23d, pGBE, or pTRC1. The measured glucan amount rules out the weak iodine staining pattern of *E. coli* B and AC71+pTRC1 as being due to low glucan amounts, as both have higher glucan content than the dark-staining AC71+pGBE. λ_{max} values of the purified α-glucan in absence of $CaCl_2$ were consistent with the iodine staining patterns observed (Table 1). In presence of $CaCl_2$ a large shift in λ_{max} was seen for AC71+pGBE. Average chain length of AC71+pET23d was 38, indicating a largely linear α-glucan polymer. In contrast, average chain length of AC71+pTRC1 was slightly higher than *E. coli* B and AC71+pGBE. To further analyze the synthesized α-glucan, we performed HPAEC of the debranched polysaccharides as described in materials and methods (Figure 6). This analysis demonstrates effective complementation of AC71 with pGBE and pTRC1 and allows for comparison with the control strain *E. coli* B. As in *E. coli* B, the most transferred chain size of AC71 complemented with pGBE and pTRC1 was d.p. 8. However, AC71+pTRC1 shows a higher proportion of longer chains. Detection of short chains in the control strain AC71 was profoundly difficult, even at 50-100 times the usual HPAEC sensitivity (Figure 6D). The relative peak areas between AC71+pTRC1 and AC71+pGBE shows

Table 1. Expression of BE WT and truncated branching enzyme in *E. coli* AC71 (*glgB*$^-$) and properties of the synthesized α-glucans.

Strain	α-glucan	BE activity	GS activity	chain length	λ_{max} – $CaCl_2$	λ_{max} + $CaCl_2$
	mg	*U/mg*	*U/mg*	*d.p.*	*nm*	*nm*
E. coli B	104	0.510	0.083	11.8	450	428
AC71 + pET23d	13	<0.002	0.061	38	550	557
AC71 + pGBE	19	0.024	0.075	12.2	513	470
AC71 + pTRC1	24	0.780	0.082	13.1	475	463

Experiments were repeated twice. Enzymatic activity and α-glucan content was measured in crude extract.

Figure 6. High Performance Anion Exchange Chromatography of debranched α-glucan purified from *E. coli* B+pET23d (**A**), AC71+pGBE (**B**), AC71+pTRC (**C**) and AC71+pET23d (**D**). Isolation of the α-glucan was performed as described in materials and methods. Numbers above peaks indicate particular chain sizes. Sensitivity of detector in (**D**) was 50-100 times that of (**A-C**) in order to detect product and large peak on left (**D**) is due to buffer.

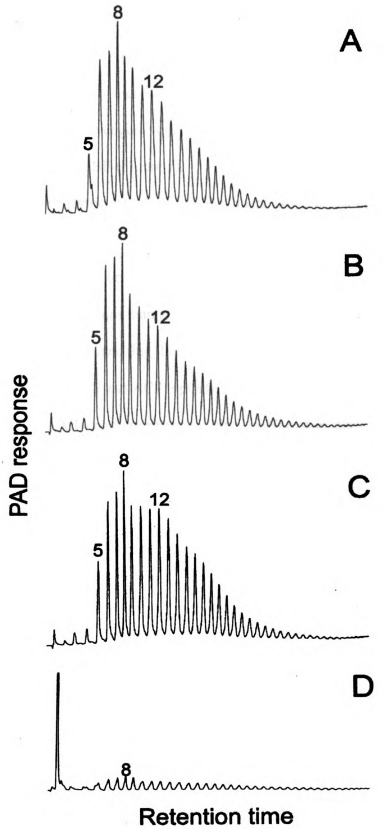
A
B
C
D
8
12
5
PAD response
Retention time

that the truncated branching enzyme in host strain AC71 transfers a smaller proportion of d.p. 5 to d.p. 11 and a greater proportion of chains longer than d.p. 12 compared to the native branching enzyme (Figure 7). We found the glycogen structure of AC71 complemented with pGBE was overall very similar to that isolated from a wild type *E. coli* B strain, although glycogen from *E. coli* strain B was slightly more branched than the product from AC71+pGBE (Figure 7).

Branching enzyme activity in crude extracts varied considerably as determined by the phosphorylase a stimulation assay but was consistent between isolations (Table 1). AC71+pTRC1 had higher branching activity than either *E. coli B* or AC71+pGBE but still transferred longer chains than either, ruling out attributing the different glycogen structure to incomplete branching. Interestingly, the 20-fold difference in branching activity between *E. coli B* and AC71+pGBE resulted in only a minor difference in glycogen structure. Glycogen synthase activity, unaffected in strain AC71, was measured as a control and found to be at similar levels in all strains.

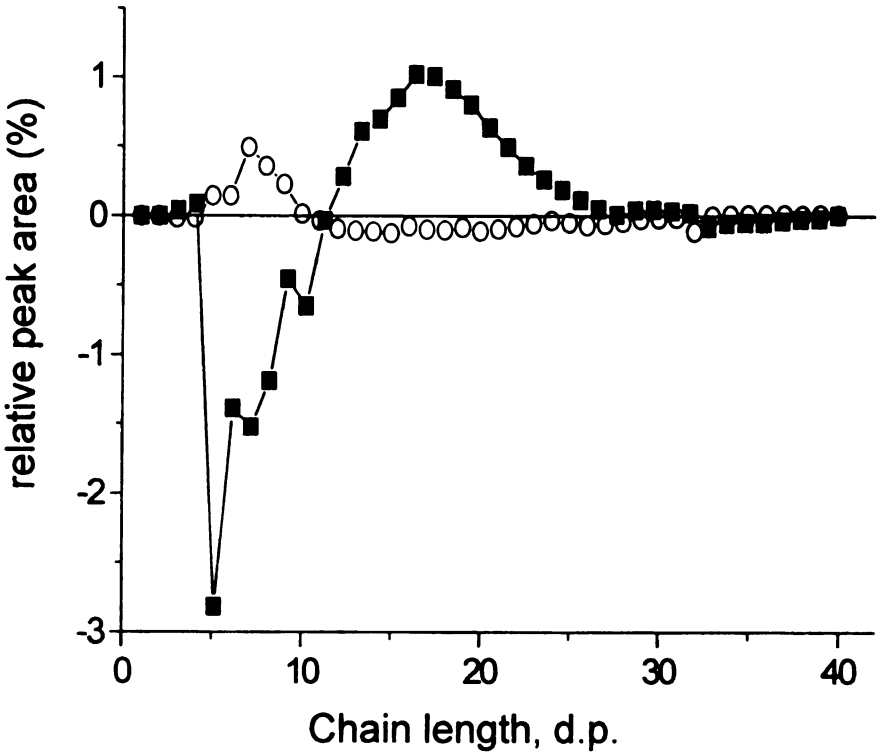

Figure 7. Difference in chain distribution between α-glucan purified from *E. coli* B, AC71+pGBE and AC71+pTRC. (■) Difference plotted as the relative peak areas from Nd_{1-112} minus the relative peak area from BE-WT for a given chain length. (O) Difference plotted as the relative peak areas from *E. coli* B minus the relative peak area from BE-WT for a given chain length. The graphs are average of two separate isolations of α-glucan. The sum of chains with d.p. 1-40 was set as 100 %.

Discussion.

By deleting 111 to 113 amino acids at the N-terminal of *E. coli* branching enzyme by either proteolysis or recombinant techniques, we have previously shown that the activity of the enzyme is reduced. In the present study, HPAEC and gel filtration experiments indicate that the transfer pattern of the truncated branching enzyme differ significantly from that of native *E. coli* branching enzyme in transfer of short and intermediate chain sizes. We base these conclusions on the glycogen structures resulting from branching amylose *in vitro* with purified branching enzyme in addition to isolation of α-glucan from *glgB* deficient strain AC71 complemented with either native or truncated BE. The *in vitro* branched amylose and the glycogen isolated from BE complemented AC71 have similar, although not identical structures, possibly due to the interplay of additional enzymes *in vivo*. However, in both cases we find that truncated branching enzyme transfers fewer chains shorter than d.p. 11 and more chains of d.p. 12 and longer relative to the native BE (compare Figure 4 and Figure 7).

For both enzymes we observe some relative long chains (d.p.>15), even after 16 hrs of branching of the amylose substrate. Also, there are long chains in the glucan product purified from the AC71 mutant complemented with WT or truncated BE. Rather than indicating incomplete branching, this probably reflects steric hindrance within the dense glucan polymer for further BE action. We believe the structures of these branching limited products indicate that the observed differences in chain transfer patterns between BE-WT and the N-terminally truncated branching enzyme are due to intrinsic properties of the enzymes.

We can not fully explain the iodine staining patterns (Figure 5) and the λ_{max}

values of the purified glucan polymers (Table 1). Based on average chain length and HPAEC, *E. coli* B and AC71+pGBE should have similar staining with iodine and λ_{max} values, both slightly below λ_{max} of AC71+pTRC1. In fact, when branching amylose with BE-WT or $Nd_{1\text{-}112}$, we find λ_{max} values consistent with the glycogen structures of 460 nm and 474 nm, respectively. Our observations could be explained by the presence of small amounts of linear chains or longer branches in AC71+pGBE, as the specific absorbance of such chains is high compared to that of glycogen (27). The effect of $CaCl_2$ in the absorbance of the glucan-iodine complex is a 10-fold increase for glycogen, whereas the absorbance of amylose is diminished (25). When measuring λ_{max} of AC71+pGBE in presence of $CaCl_2$ we observe a much shorter wavelength. This shift indicates the presence of both glycogen and linear chains in case of AC71+pGBE. The ratio of BE activity to GS activity in crude extract is 6:1 and 9:1 in *E. coli* B and AC71+pTRC1, respectively, whereas the ratio in AC71+pGBE is 1:3 (Table 1). This allows for speculation if the relatively large amount of glycogen synthase activity could have produced a small fraction of linear chains in the latter strain, explaining the staining patterns with iodine.

Our findings are consistent with chimeric enzyme constructions between the maize isoforms, where the amino terminal of branching enzyme was concluded to play a role in the size of oligosaccharide chains transferred (15). The low sequence conservation between branching enzymes complicates the construction of hybrid branching enzymes, especially in absence of a three-dimension structure. The study presented here establishes an alternative method for deducing valuable structure-function relationships of branching enzymes. Giving the large size variability of the amino and carboxy terminal regions of

branching enzymes (14, 16), it would be of interest to construct additional deletions by recombinant DNA technology. We believe this would allow for further investigation of the determinants of substrate specificity and transfer patterns, and these experiments are currently in progress in our laboratory. This approach may enable rational design of chain transfer patterns by branching enzymes, leading to desirable polysaccharides for specific industrial uses.

References

1. Preiss J. (1991) *Oxford Surv. Plant Mol. Cell Biol.* **7**, 59-114.

2. Preiss, J. (1984) *Annu. Rev. Microbiol.* **38**, 419-458.

3. Guan, H. P., Kuriki, T., Sivak, M. N. and Preiss, J. (1995) *Proc. Natl. Acad. Sci.* **92**, 964-967.

4. Ball, S., Guan, H. P., James, M., Myers, A., Keeling, P., Mouille, G., Buleon, A., Colonna, P. and Preiss, J. (1996) *Cell* **86**, 349-352.

5. Colleoni, C., Dauvillee, D., Mouille, G., Buleon, A., Gallant, D., Bouchet, B., Morell, M., Samuel, M., Delrue, B., d'Huelst, C., Bliard, C., Nuzillard, J-M. and Ball, S, (1999) *Plant Physiol.* **120**, 993-1003.

6. Borovsky, D., Smith, E. C. and Whelan, W. J. (1976) *Eur. J. Biochem.* **62**, 307-312.

7. Boyer, C. and Preiss, J. (1977) *Biochemistry* **16**, 3693-3699.

8. Guan, H. P. and Preiss, J. (1993) *Plant Physiol.* **102**, 1269-1273.

9. Nakamura, Y., Takeichi, T., Kawaguchi, K. and Yamanouchi, H. (1992) *Plant Physiol.* **84**, 329-335.

10. Smith, A. M. (1988) *Planta* **175**, 270-279.

11. Takeda, Y., Guan, H. P. and Preiss, J. (1993) *Carbohyd. Res.* **240**, 253-263.

12. Baba, T., Kimura, K., Etoh, H., Ishida, Y., Shida, O. and Arau, Y. (1991) *Biochem. Biophys. Res. Commun.* **181**, 87-94.

13. Jespersen, H. M., MacGregor, A. E., Henrissat, B., Sierks, M. R. and Svensson, B. (1993) *J. Prot. Chem.* **12**, 791-805.

14. Jespersen, H. M., MacGregor, A. E., Henrissat, B., Sierks, M. R. and Svensson, B. (1991) *Biochem. J.* **280**, 51-55.

15. Kuriki, T. Stewart, D. C. and Preiss, J. (1997) *J. Biol. Chem.* **272**, 28999-29004.

16. Binderup, K., Mikkelsen, R. and Preiss, J. (2000) *Arch. Biochem. Biophys.* In Press.

17. Guan, H. P., Li, P., Imparl-Radosevich, J., Preiss, J. and Keeling, P. (1997) *Arch. Biochem. Biophys.* **342**, 92-98.

18. Preiss, J., Greenberg, E. and Sabraw, A. (1975) *J. Biol. Chem.* **250**, 7631-7638.

19. Huijing, F. (1970) *Clin. Chim. Acta* **30**, 567-572.

20. DiPietro D. L. and Weinhouse S. (1960) *J. Biol. Chem.* **235**, 2542-2445.

21. Hawker, J. S., Ozbun, J. L., Ozaki, H., Greenberg, E. and Preiss, J (1974) *Arch. Biochem. Biophys.* **160**, 530-551.

22. Holmes, E. and Preiss, J. (1979) *Arch. Biochem. Biophys.* **196**, 436-448.

23. Smith, P. K., Krohn, R. I., Hermanson, G. T., Mallia, A. K., Gartner, F. H., Provenzano, M. D., Fujimoto, E. K., Goeke, N. M., Olson, B. J. and Klenk, D. C. (1985) *Anal. Biochem.* **150**, 76-85.

24. Dubois, M., Gilles, K. A., Hamilton, J. K., Rebers, P. A. and Smith, F. (1956) *Anal. Chem.* **28**, 350.

25. Krisman, C. R. (1962) *Anal. Biochem.* **4**, 17-23.

26. Banks, W., Greenwood, C. T. and Khan, K. M. (1971) *Carbohyd. Res.* **17**, 25-33.

27. Murdoch, K. A. (1992) *Carbohydr. Res.* **233**, 161-174.

CHAPTER 6

AN *IN VITRO* RECONSTITUTION SYSTEM FOR GLYCOGEN BIOSYNTHESIS

Abstract.

We have constructed a reconstitution system for biosynthesis of bacterial glycogen *in vitro*. The *E. coli* glycogen synthase and two different branching enzymes were purified to homogeneity and used in glucan synthesis from ADP-glucose. We also used branching enzymes and phosphorylase in synthesis of glucan with glucose-1-phosphate as substrate for comparison. The *in vitro* synthesized polysaccharides were purified before debranching and subsequent analysis of chain lengths by high performance anion exchange chromatography. From the resulting elution profiles we are able to evaluate several parameters suspected to affect the polyglucan yield and structure.

Introduction.

Glycogen is a polymer of glucose with 90 % α-(1,4) glucosidic linkages and 10 % α-(1,6) glucosidic linkages at branch points. Many bacteria are able to accumulate glycogen as an energy storage polymer (1), and biosynthesis of bacterial glycogen involves at least three enzymes. ADP-glucose pyrophosphorylase catalyzes the formation of ADP-glucose from glucose-1-phosphate and ATP, releasing PPi as a by-product (2). The rate of glycogen biosynthesis is allosterically regulated at the step of ADP-glucose pyrophosphorylase, and in most bacteria the enzyme is activated by fructose-1,6-bisphosphate and inhibited by adenosine monophosphate (3). Glycogen synthase (GS) forms the α-(1,4) glucosidic linkages of glycogen using ADP-glucose as a substrate (4). Finally branching enzyme (BE) catalyzes the cleavage and subsequent transfer of α-(1,4) glucan chains to α-(1,6) branch points (5). It is believed the properties of glycogen synthase and branching enzyme mainly define the α-glucan structure *in vivo*. Previously, it has been suggested that a glycoprotein might be involved in the priming of the α-(1,4) glucan synthesis in *E. coli* (6), as in the case with glycogenin in yeast (7,8). However, evidence has since accumulated that the three enzymes described above are sufficient for *E. coli* glycogen biosynthesis, and that an additional primer is not required, apart from the endogenous α-(1,4)-glucan primer associated with glycogen synthase (9).

Carl and Gerti Cori first described *in vitro* synthesis of a polyglucan by use of phosphorylase and glucose-1-phosphate as substrate (10), which led researchers to believe phosphorylase was a biosynthetic enzyme. Phosphorylase has now long been known as involved in glycogen degradation, and the three enzymes described above as constituting the biosynthetic pathway. However, no studies have reported *in vitro*

glycogen synthesis based on the biosynthetic enzymes. This report describes a glycogen biosynthetic reconstitution system based on purified preparations of glycogen synthase and branching enzyme with ADP-glucose as the substrate (Figure 1A). This allows us to study several parameters suspected to influence the final polyglucan structure. First, we use the native *E. coli* branching enzyme (BE WT) as well as purified truncated *E. coli* branching enzyme (Nd_{1-112}; Chapter 4), which has been shown to have an altered chain transfer pattern (Chapter 5). This enables us to measure if branching enzymes with different properties result in distinct polysaccharide structures from *de novo* synthesis. Furthermore, we use branching enzyme and phosphorylase a (PA) with glucose-1-phosphate as substrate, in order to compare α-(1,4)-glucan synthesis by GS vs. PA and the corresponding effects on the polysaccharide structures (Figure 1B). We also vary the incubation time to measure its impact on α-glucan yields and structures. Finally, we analyze how using different enzymatic ratios of branching enzyme and GS or PA may affect the structure and yields of the polysaccharides. Our results indicate several parameters influence the polysaccharide product and that we may be able to design specific α-glucan structures by the *de novo* synthesis method described here.

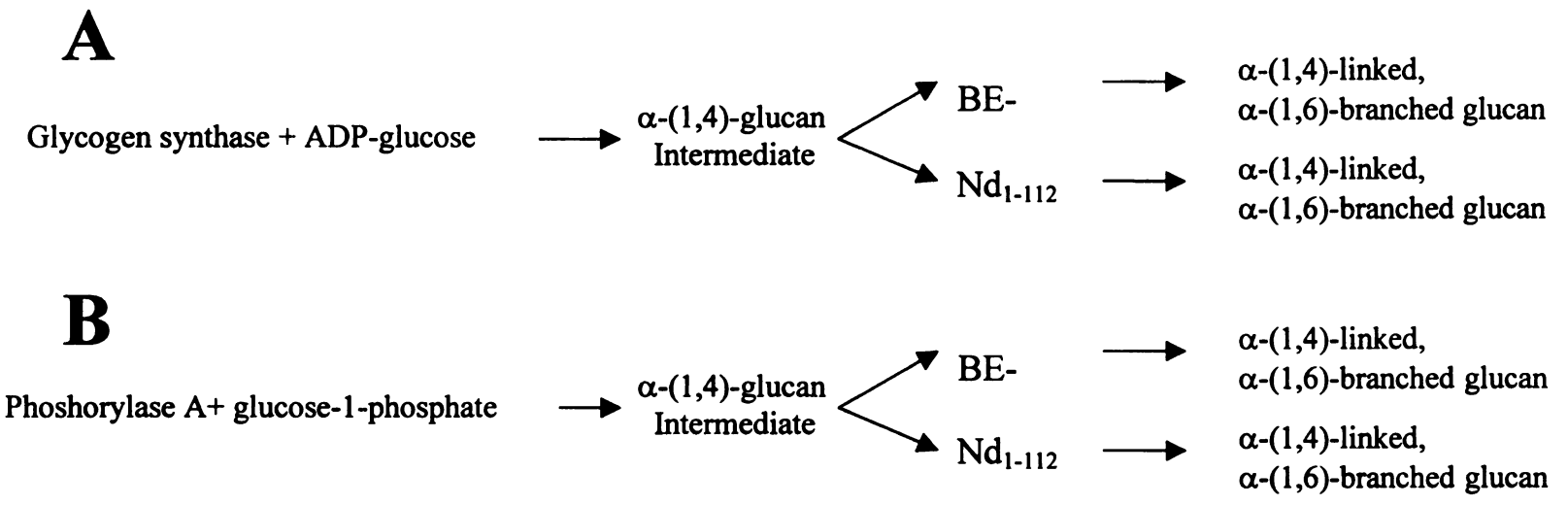

Figure 1. Reaction scheme of *de novo* glucan synthesis. The α-(1,4) glucosidic linkages were synthesized from the substrate ADP-glucose by glycogen synthase (**A**) or from glucose-1-phosphate by glycogen phosphorylase (**B**). Formation of the α-1,6 branch points was catalyzed by *E. coli* wild-type branching enzyme (BE WT) or the *E. coli* truncated branching enzyme (Nd_{1-112}). The structure of the resulting α-(1,4)-linked, α-(1,6)-branched glucan product was analyzed by high performance anion exchange chromatography as described in materials and methods.

Materials and methods

Purification of enzyme material. *E. coli* BE-WT and Nd_{1-112} were purified as described by Binderup *et al* (11). The purification of *E. coli* glycogen synthase was performed as described by Furukawa *et al* (12).

Branching enzyme activity. The branching enzyme activity was measured by the phosphorylase stimulation assay (assay A).

Assay A. The phosphorylase A stimulation assay is based on the stimulation by BE of the synthesis of α-D-glucan from α-D-Glc-1-P catalyzed by rabbit phosphorylase a (13). Reaction mixtures contained in a final volume of 100 µl, 100 mM citrate (pH 7.0), 10 mM adenosine monophosphate, 0.2 mg phosphorylase a (Sigma) and 50 mM D-[^{14}C]-Glc-1-P (50 DPM · $nmol^{-1}$) and the assay was initiated by an appropriate amount of BE. One unit is defined as 1 µmol of Glc incorporated into α-D-glucan per min at 30°C.

Glycogen synthase assay. The glycogen synthase activity was measured by the primed glycogen synthesis reaction (14). The reaction mixture (200 µl) contained 300 nmol ADP-[^{14}C]glucose (350 DPM · $nmol^{-1}$), 0.5 mg rabbit liver glycogen, 2 µmol GSH, 100 µg BSA, in 0.1 M citrate pH 7.0. The reaction was initiated by adding an appropriate amount of glycogen synthase. One unit is defined as the incorporation of 1 µmol glucose into glycogen per min at 37°C.

Phosphorylase activity assay. The phosphorylase activity was measured by synthesis of α-D-glucan from α-D-glucose-1-phosphate into a glycogen primer. The reaction mixture (200 µl) contained 100 mM D-[^{14}C]-Glc-1-P (50 DPM · $nmol^{-1}$), 10 mM adenosine monophosphate and 200 µg glycogen in 0.1 M citrate pH 7.0. The assay was

initiated by adding phosphorylase a (Sigma). One unit is defined as 1 μmol of Glc incorporated into α-D-glucan per min at 30°C.

Protein assay. Protein concentration was measured with the BCA protein assay reagent (15), using BSA as the standard.

SDS-PAGE analysis. SDS-PAGE was performed by 4-15 % polyacrylamide gels according to the method of Laemmli (16).

Synthesis of α-D-glucan by branching enzyme and glycogen synthase. Synthesis of α-D-glucan through the concerted action of glycogen synthase and branching enzyme was performed using ADP-glucose as substrate. The reaction mixture (200 μl) contained 67 mM ADP-[^{14}C]-glucose (3.1 DPM · nmol^{-1}), 2 μmol GSH, and 100 μg BSA, in 0.1 M citrate pH 7.0. The incubation time at 30°C and amount of branching enzyme and glycogen synthase was varied as indicated in each experiment. At each time point, the reaction was terminated by boiling and the α-D-glucan product washed with methanol and ethanol, before drying overnight in a vacuum desiccator.

Synthesis of α-D-glucan by branching enzyme and phosphorylase a. Synthesis of α-D-glucan through the concerted action of phosphorylase a and branching enzyme was performed using glucose-1-phosphate as substrate. The reaction mixture (200 μl) contained 125 mM D-[^{14}C]-glucose-1-phosphate (2.0 DPM · nmol^{-1}) and 10 mM adenosine monophosphate in 0.1 M citrate pH 7.0. The incubation time at 30°C and amount of branching enzyme and phosphorylase a was varied as indicated in each experiment. At each time point, the reaction was terminated by boiling and the α-D-glucan product washed with methanol and ethanol, before drying overnight in a vacuum desiccator.

Analysis of branched chain length. The synthesized α-glucan was solubilized in H_2O and debranched by adding isoamylase (500 U/ml) and Na-acetate pH 3.5 to a final concentration of 100 mM. After 4 hrs at 45°C, the solution was heated in a boiling water bath for 5 min and immediately analyzed by HPAEC.

HPAEC Analysis. The debranched α-glucan solution was filtered through 0.22 μm membrane and 25 μl samples injected in the BioLC HPAEC (Dionex), using a CarboPac PA-1 column (250 × 4 mm). Eluent A was 150 mM sodium hydroxide; eluent B was 150 mM sodium hydroxide containing 500 mM sodium acetate. The gradient program was: 25 % eluent B at time 0, 45 % at 15 min, 60 % at 45 min, 70 % at 80 min, and 80 % at 100 min with a flow rate of 0.3 $ml \cdot min^{-1}$. The standard was 25 μl of 5 $mg \cdot ml^{-1}$ maltodextrin (d.p. 1-20, Aldrich).

Results.

Enzymatic activities. All enzymes used in this study were purified to near-homogeneity to prevent any interfering reactions from enzymes involved in carbohydrate modification or catabolism (Figure 2). The specific activities of the enzyme preparations were determined in the conditions used during the α-glucan synthesis in presence of a glycogen primer, in order to perform direct comparisons of enzymatic activities. The specific activities of *E. coli* BE WT and Nd_{1-112} branching enzymes were 1100 U/mg and 650 U/mg, respectively. The activity of *E. coli* glycogen synthase was measured under standard conditions (37°C, 0.1 M biscine pH 8.0) and the conditions used for α-glucan synthesis (30°C, 0.1 M citrate pH 7.0), and corresponding specific activities were 540 U/mg and 450 U/mg, respectively. Phosphorylase a was measured in the enzyme's non-physiological synthesis direction and the specific activity determined as 12.5 mU/mg. Although the substrates of glycocen synthase (ADP-glucose) and phosphorylase (Glc-1-P) are different, their specific activities under substrate-saturated conditions may be directly compared, as both assays measure the incorporation of glucose into an existing glycogen primer. With decreasing substrate concentrations the comparison of glycogen synthase and phosphorylase a enzymatic activities becomes meaningless due to the reversibility of the phosphorylase a reaction (equilibrium at 70 % towards synthesis at pH 7.0 (17)), whereas the reaction of glycogen synthase at pH 7.0 is essentially irreversible (18). Furthermore, the K_m value of glycogen synthase for ADP-glucose (18) is much lower than the K_m value of phosphorylase a for Glc-1-P (17).

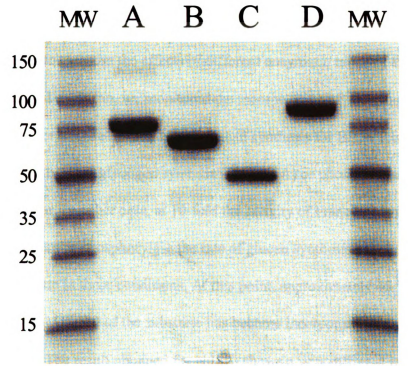

Figure 2. SDS-PAGE of purified enzymes for glycogen reconstitution system. **(A)**, *E. coli* wild-type branching enzyme; **(B)**, *E. coli* truncated branching enzyme; **(C)**, *E. coli* glycogen synthase; **(D)**, rabbbit liver glycogen phosphorylase. Loading was 2-4 μg total protein per lane.

Synthesis of α-D-glucan. Previous results indicated the *in vivo* ratio of activity between *E. coli* branching enzyme and *E. coli* glycogen synthase to range from 4:1 to 10:1. We measured a specific activity of 0.51 U/mg and 0.083 U/mg *in vivo* for branching enzyme and glycogen synthase, respectively, corresponding to an enzymatic activity ratio of 6:1. In order to measure the effects of different enzymatic ratios of the amount of *in vitro* synthesized α-glucan, we monitored the incorporation of ^{14}C-glucose into the glycogen product (Figure 3). The rate of glucan synthesis for BE WT when in combination with either glycogen synthase (Figure 3A) or phosphorylase a (Figure 3B) were very similar. In either case, at 10-fold the activity of branching enzyme compared to glycogen synthase or phosphorylase the rate of glucan synthesis becomes independent of branching enzyme in these conditions. At this point, approximately 45 % (1 unit GS/Pa) or 30 % (0.5 unit GS/Pa) of the substrate has become incorporated into the growing polysaccharide. The result obtained for $Nd_{1\text{-}112}$ shows a very different rate of α-glucan synthesis when in combination with glycogen synthase (Figure 3C) than phosphorylase a (Figure 3D). The concerted action of glycogen synthase and $Nd_{1\text{-}112}$ yields much less polysaccharide synthesis for a specific amount of branching enzyme used, than in the case of BE WT. It is evident from the "lag" phase that there is no significant α-glucan synthesis with low branching enzyme amounts, which can be partly compensated by addition of more glycogen synthase. The kinetics from Figure 3C suggests that $Nd_{1\text{-}112}$ may require a longer primer before transfer of chains can be initiated. After glycogen synthase synthesizes a primer of sufficient length for $Nd_{1\text{-}112}$, the simultaneous action of branching enzyme and glycogen synthase will then lead to rapid glucan accumulation.

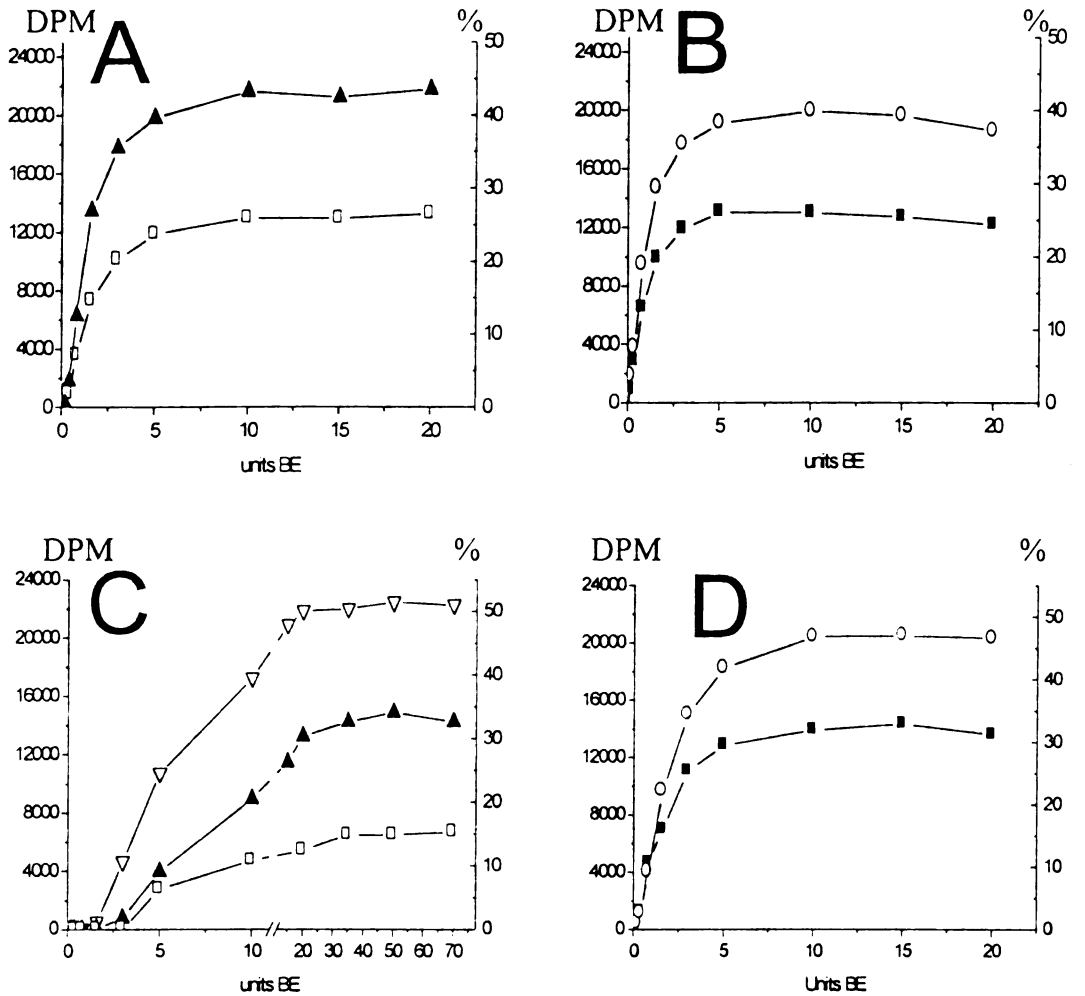

Figure 3. Effect of different ratios of enzymatic activity on α-glucan yields. Various amounts of branching enzyme were incubated with glycogen synthase (GS) or phosphorylase A (PA) and the appropriate substrate for 30 min. 0.5 units GS (□); 1.0 unit GS (▲); 2.0 units GS (▽); 0.5 units PA (■); 1.0 unit PA (○). The incorporation of ^{14}C labeled substrate is indicated in DPM (left Y-axis) and as percentage of total substrate (right Y-axis).

A: BE WT and GS using ADP-glucose as substrate.

B: BE WT and PA using glucose-1-phosphate as substrate.

C: Nd_{1-112} and GS using ADP-glucose as substrate.

D: Nd_{1-112} and PA using glucose-1-phosphate as substrate.

This theory may be verified by adding small amounts of malto-oligosaccharides as a primer for the reaction. Figure 3D shows that in combination with phosphorylase, Nd_{1-112} leads to rapid glucan synthesis. The absence of a "lag" phase here due to the requirement of Nd_{1-112} for a long primer, is most likely due to the presence of glucan primers which is invariantly found in the commercial preparations of purified phosphorylase a.

The synthesis of α-glucan at various incubation times using 10 units of branching enzyme activity and 1 unit of GS or Pa activity is shown in Figure 4. Using BE WT or Nd_{1-112} in concert with glycogen synthase led to 80 % conversion of the substrate ADP-glucose into the polysaccharide in 3 hrs (Figure 4A). There was a late on-set of α-glucan synthesis for Nd_{1-112} compared to BE WT, consistent with the requirement of a longer oligosaccharide primer for the truncated branching enzyme. α-glucan synthesis from BE WT or Nd_{1-112} in combination with phosphorylase a reached the maximum conversion of Glc-1-P to the polysaccharide product in 2 hrs under these conditions (Figure 4B). The observed equilibrium point of 60 % towards synthesis direction of phophorylase a is close to the theoretical value (70%) at this particular pH (17, 19).

Structures of synthesized α-glucans. We investigated the effects of incubation time on the structure of the synthesized α-glucan structures, while keeping the amounts of branching enzyme (10 units) and GS/PA (1 unit) constant (Figure 5). Under these conditions, the synthesis of α-glucan proceeded for 1, 3, or 16 hrs and the resulting polysaccharide was debranched and analyzed by HPAEC as described in materials and methods. The PAD chromatogram for each polysaccharide structure was integrated and

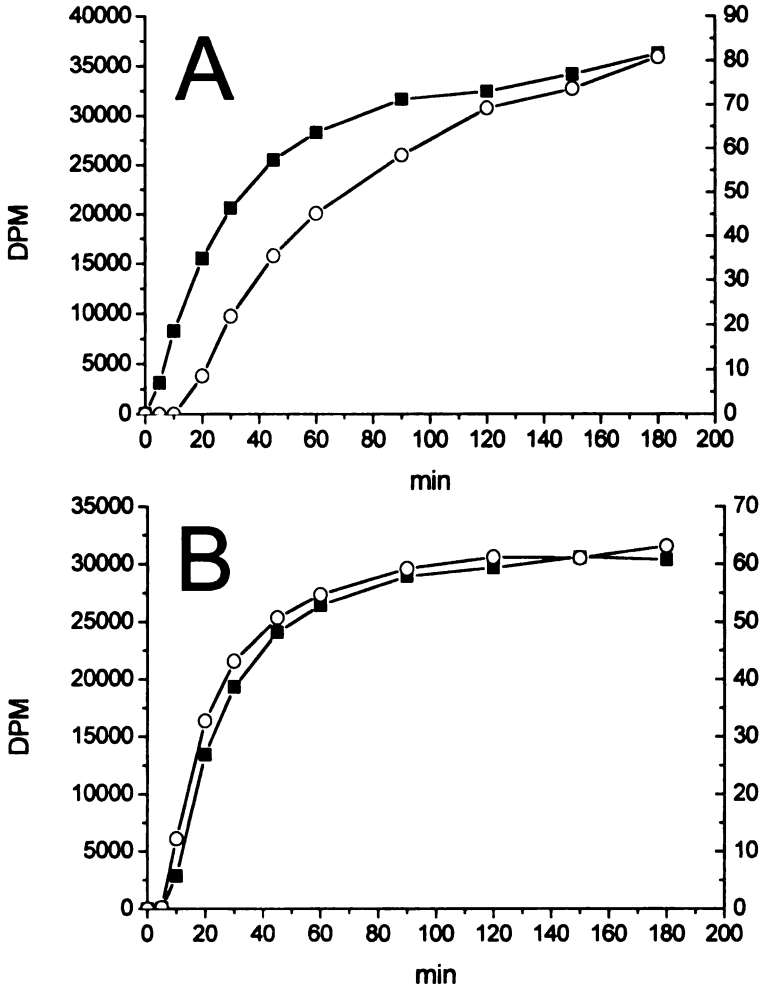

Figure 4. Effect of reaction time on glucan yields. 1.0 unit of glycogen synthase (**A**)or phosphorylase A (**B**) was incubated with 10 units BE-WT (■) or $Nd_{1\text{-}112}$ (O) and the appropriated substrate. The incorporation of ^{14}C labeled substrate is indicated in DPM (left Y-axis) or as percentage of total substrate (right Y-axis).

Figure 5. Analysis of transferred chains after 1 hr (Black), 3 hrs (White) and 16 hrs (Grey) of branching, using 10 units of BE activity and 1 unit of GS/PA activity. The synthesized glucans were debranched and analyzed by HPAEC. The relative peak areas were calculated using the sum of d.p. 1-40 as 100 %.

A - C: BE-WT and GS using ADP-glucose as substrate

D – F: $Nd_{1\text{-}112}$ and GS using ADP-glucose as substrate.

G – I: BE-WT and PA glucose-1-phosphate as substrate.

J – L: $Nd_{1\text{-}112}$ and PA glucose-1-phosphate as substrate.

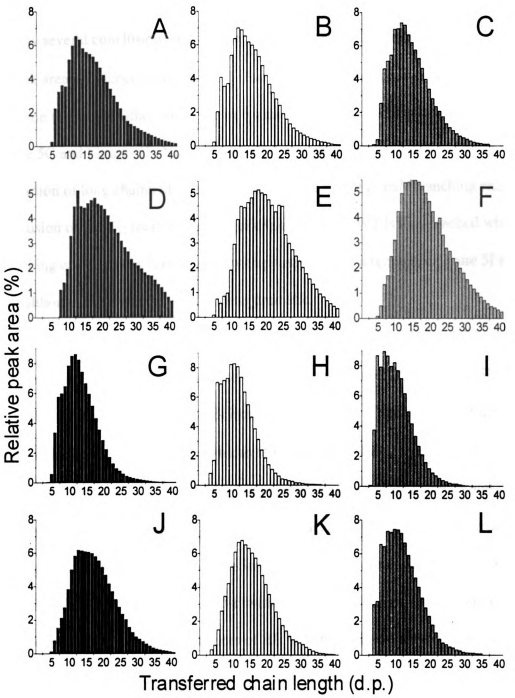
A
B
C
D
E
F
G
H
I
J
K
L
Relative peak area (%)
Transferred chain length (d.p.)

the relative peak area of a particular chain length calculated, to allow for direct comparison of the chain transfer patterns between various conditions. Figure 5 allows us to draw several conclusions of variables affecting the α-glucan structures by construction of peak area difference plots. Figure 6 illustrates the difference in α-glucan structures based on the use of either wild-type or truncated *E. coli* branching enzyme, derived from Figure 5C and Figure 5F. Nd_{1-112} transfers fewer short chains (d.p. 4 - 16) and a higher proportion of long chains (d.p. > 16) relative to the native *E. coli* branching enzyme. This conclusion of Nd_{1-112} transferring longer chains than BE WT is also reached when branching enzyme is in combination with phosphorylase a (compare Figure 5I and Figure 5L), although the observed effect is less dramatic.

The effect of reaction time on the structure of the synthesized α-glucan is illustrated in Figure 7. This difference plot, based on Figure 5B and Figure 5C, shows that a longer time of incubation will increase the number of short chains of the polysaccharide. It suggests the α-glucan structure, while being synthesized, is continuously processed by branching enzyme, leading to a more compact and dense molecule. The most dramatic effect on the polysaccharide structure is in the use of glycogen synthase or phosphorylase a in glucan synthesis (compare Figure 5A-C with Figure 5G-I (BE WT), or Figure 5D-F with Figure 5J-L (Nd_{1-112})). A difference plot between the polysaccharide structures of BE WT in combination with either glycogen synthase or phosphorylase a clearly shows how using phosphorylase a causes a high degree of branching (Figure 8). In fact, more than 85 % of all the chains are of d.p. ≤ 15 after 16 hrs of glucan synthesis with BE WT and phosphorylase a (Figure 5I).

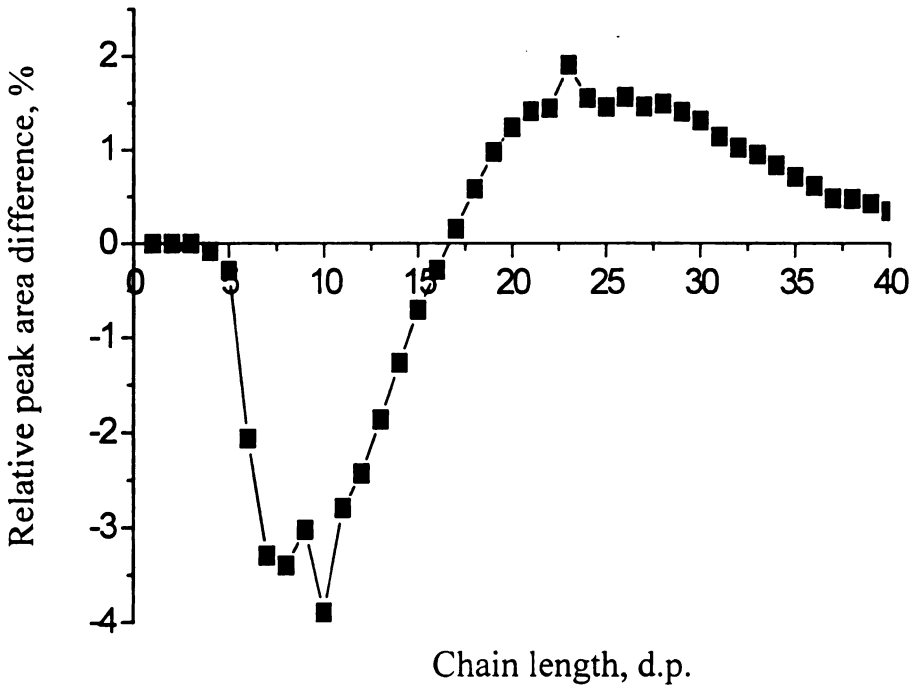

Figure 6. Difference plot showing the effect of BE-WT vs. Nd_{1-112} on the glucan structure. Difference in chain distribution between BE-WT and Nd_{1-112} after 16 hrs in combination with glycogen synthase (GS) using a BE:GS ratio of 10:1. The difference was the relative peak area from Nd_{1-112} minus the relative peak area from BE-WT for a given chain length. The sum of chains with d.p. 1-40 was set as 100 %.

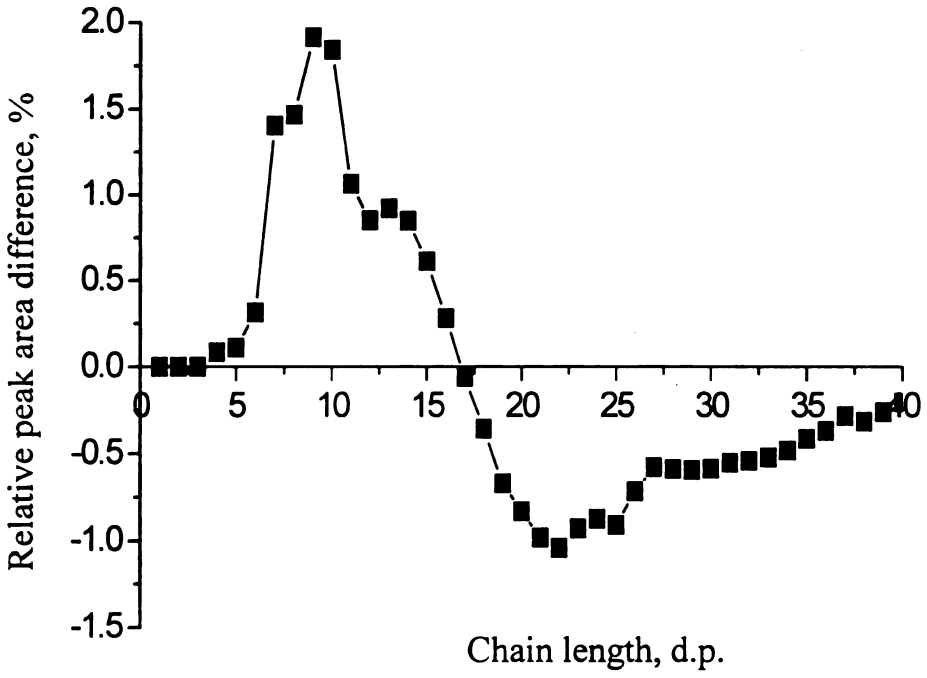

Figure 7. Difference plot showing the effect of reaction time on the synthesized glucan structures. The difference was the relative peak area using BE-WT after 16 hrs minus the relative peak area using BE-WT after 3 hrs for a given chain length. The ratio of BE:GS was 10:1. The sum of chains with d.p. 1-40 was set as 100 %.

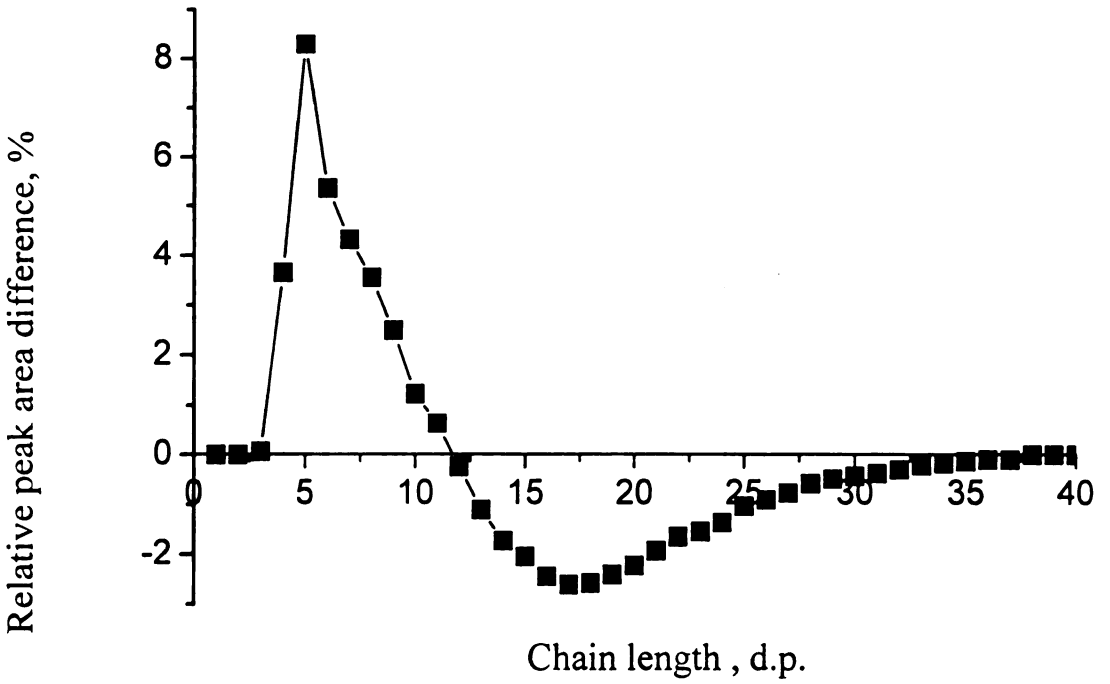

Figure 8. Difference plot showing the effect of phosphorylase A (PA) vs. glycogen synthase (GS). The difference was the relative peak area using BE-WT in combination with PA minus the relative peak area from BE-WT in combination with GS for a given chain length. The ratio of BE:PA or BE:GS was 10:1 and the incubation time was 16 hrs. The sum of chains with d.p. 1-40 was set as 100 %.

We also investigated the effects of different enzymatic ratios of activity on the structure of the synthesized α-glucan structures (Figure 9). This was performed by use of 3, 6, or 20 units of branching enzyme (BE WT or Nd_{1-112}) with a constant amount of GS/Pa (1 unit). Different ratios of branching enzyme and GS/Pa activity resulted in a large effect of the polysaccharide structures. The difference plot of transferred chains when using 3-fold or 20-fold excess of branching enzyme is shown in Figure 10. A greater proportion of short chains (d.p. 4 –15) is observed with 20 units of branching enzyme, meaning higher branching activity leads to a more branched structure. From Figure 9 we can verify that Nd_{1-112} transfers longer chains than BE WT (compare Figure 9A-C with Figure 9D-F). Also, we again observe that phosphorylase a causes a more branched glucan structure compared to when glycogen synthase is utilized (compare Figure 9A-C with Figure 9A-I), consistent with our observations earlier.

Figure 9. Analysis of transferred chains using BE:GS and BE:PA enzyme activity ratios of 3:1 (Black), 6:1 (White) and 20:1 (Grey). Branching enzyme was incubated with glycogen synthase or phosphorylase A and the appropriate substrate for 16 hrs. at 30°C prior to debranching and analysis by HPAEC. The relative peak areas were calculated using the sum of d.p. 1-40 as 100 %.

A - C: BE-WT and GS using ADP-glucose as substrate

D – F: $Nd_{1\text{-}112}$ and GS using ADP-glucose as substrate.

G – I: BE-WT and PA using glucose-1-phosphate as substrate.

J – L: $Nd_{1\text{-}112}$ and PA using glucose-1-phosphate as substrate.

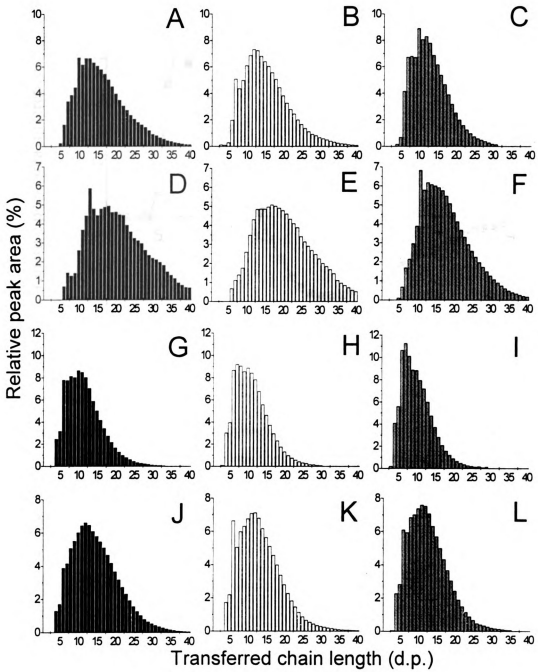
A
B
C
D
E
F
G
H
I
J
K
L
Relative peak area (%)
Transferred chain length (d.p.)

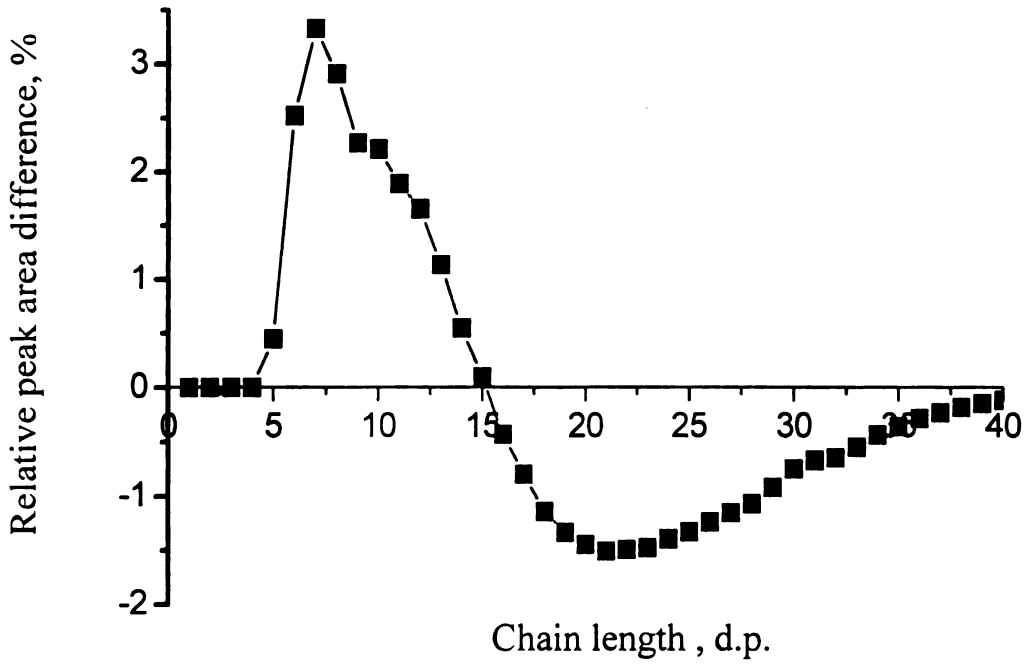

Figure 10. Difference plot showing the effect of enzyme ratio on the synthesized glucan structures. The difference was the relative peak area using a BE-WT:GS ratio of 20:1 minus the relative peak area using BE-WT:GS ratio of 3:1 for a given chain length. The incubation time was 16 hrs. The sum of chains with d.p. 1-40 was set as 100 %.

Discussion.

The work presented here is the first attempt to create a reconstitution system for *in vitro* bacterial glycogen biosynthesis. In order to limit the number of variables and simplify the data analysis we have not included the *E. coli* ADP-glucose pyrophosphorylase in this study. Still, we are able to make several interesting conclusions related to the parameters that affect the structure of the synthesized α-glucans. All our experiments indicate that the truncated branching enzyme transfers longer chains than BE WT, consistent with our conclusions from *in vivo* purified α-glucan structures and *in vitro* branching of amylose (Chapter 5). The fact that the *de novo* α-glucan synthesis described in this study leads to distinct structures depending on BE WT or Nd_{1-112} was used, is additional proof of a difference in chain transfer pattern between these enzymes. An unexpected observation was the late onset of glycogen synthesis when the truncated branching enzyme was combined with glycogen synthase. This brings up new questions about the substrate required for Nd_{1-112} branching. It would be of interest to investigate further if the minimum chain length for Nd_{1-112} branching differs from BE WT, and if this is the origin of the distinct polysaccharide structures produced by the two enzymes.

Increasing incubation time not only affected the yield of the α-glucan, but also resulted in a more branched structure, as branching enzyme continuously processed the polysaccharide. However, the effect of incubation time on the α-glucan structure did not appear as large as the other parameters investigated (e.g. source of branching enzyme, GS vs. PA and enzymatic activity ratios). The use of phosphorylase a instead of glycogen synthase caused a much higher degree of branching. This is possibly due to the reversibility of the phosphorylase a reaction, which may trim the overall α-glucan

structure. This argument is also supported by the fact that the difference between the BE WT or Nd_{1-112} polysaccharide structures was not as great when using phosphorylase a compared to *E. coli* glycogen synthase.

It has been proposed that the chain transfer and substrate specificities of branching enzyme are the primary determinants of the glycogen structure (20). However, we observed that changing the ratio of enzymatic activity between branching enzyme and GS/PA highly affected the α-glucan product. This suggests the interplay of branching enzyme and glycogen synthase is an important factor affecting the final polysaccharide structure. We suggest the branching enzymes and glycogen synthase to be co-expressed in *E. coli* and their expression levels regulated through using different promotor systems. The activity levels could then be measured and the resulting α-glucan analyzed to see if novel polysaccharide structures could be produced *in vivo*.

Recent advancements in the study of enzymes modifying α-glucan have spiked a renewed interest in the starch industry for biochemical processing of the raw materials. We believe our result demonstrate that polysaccharides with quite distinct physical properties can be manufactured by controlling a small set of parameters.

References.

1. Preiss, J. (1984). *Annu Rev. Microbiol.* **38**, pp. 419-458.
2. Espada, J. (1962). *J. Biol. Chem.* **237**, 3577-3581.
3. Preiss, J. (1996). Regulation of Glycogen Synthesis. In *Escherichia coli* and *Salmonella typhimurium*: Cellular and Molecular Biology, second edition, Amer. Soc. Microbiol., Washington, D.C. Vol. 1, pp. 1015-1024.
4. Greenberg, E. and Preiss, J. (1964). *J. Biol. Chem.* **239**, 4314.
5. Boyer, C., Preiss, J. (1977). Biochem. **16**, 3693-3699.
6. Barengo, R., Flawia, M., and Krisman, C. R. (1975). *FEBS lett.* **53**, 274-278.
7. Chrisman, C. R. and Barengo, R. (1975). *Eur. J. Biochem.* **52**, 117.
8. Lomako, J., Lomako, W. M., and Whelan, W. J. (1988). *FASEB J.* **2**, 3097.
9. Kawaguchi, K., Fox, J., Holmes, E., Boyer, C., and Preiss, J. (1978). *Arch. Biochem. Biophys.* **190**, 385-397.
10. Cori, J. F. and Cori, G. R. (1939). *J. Biol. Chem.* **131**, 397.
11. Binderup, K, Mikkelsen, R., and Preiss, J. (2000). *Arch. Biochem. Biophys.* **377**, 366-371.
12. Furukawa, K., Tagaya, M., Inouye, M., Preiss, J., and Fukui, T. (1990). *J. Biol. Chem.* **265**, 2086-2090.
13. Takeda, Y., Guan, H.P., Preiss, J. (1993) *Carbohydr. Res.* **240**, 253-263.
14. Holmes, E. and Preiss, J. (1979). *Arch. Biochem. Biophys.* **196**, 436-448.
15. Smith, P.K., Krohn, R.I., Hermanson, G.T., Mallia, A.K., Gartner, F.H., Provenzano, M.D., Fujimoto E.K., Goeke, N.M., Olson, B.J., Klenk, D.C. (1985) *Anal. Biochem.* **150**, 76-85.

16. Laemmli, U. K. (1970) *Nature* **227**, 680-685.

17. Madsen, N. B. (1991). *in* A study of Enzymes, (Kuby, S. A., Ed.), CRC Press, New York, Vol II, pp. 139-158.

18. Fox, J., Kawaguchi, K., Greenberg, E., and Preiss, J. (1976). *Biochemistry* **15**, 849.

19. Cori, C.F., Cori, G.T., and Green, A.A (1943). *J. Biol. Chem.* **151**, 39.

20. Guan, H. P., Li, P., Imparl-Radosevich, J., Preiss, J. and Keeling, P. (1997). *Arch. Biochem. Biophys.* **342**, 92-98.

CHAPTER 7

CRYSTALLIZATION OF ADP-GLUCOSE PYROPHOSPHORYLASE

Part of this data is published:

Binderup, K., Watanabe, L., Polikarpov, I., Preiss, J. and Arni, R. K. (2000) "Crystallization and Preliminary X-ray Analysis of the Catalytic Subunit of Potato Tuber ADP-Glucose Pyrophosphorylase" *Acta Cryst.* D **56**, 192-194.

Abstract

ADP-glucose pyrophosphorylase is the key regulatory enzyme in the biosynthesis of starch in plants and glycogen in bacteria. There is no three-dimensional structure of this important enzyme to help explain its catalysis or complex allosteric behavior. Here we describe the expression, purification, and crystallization of the enzyme from *Escherichia coli* and the 50 kDa catalytic subunit from potato tuber. Two multiple anomalous dispersion data sets were collected to 2.9 Å and 3.5 Å of *E. coli* ADP-glucose pyrophosphorylase from crystal forms belonging to the space group $P2_12_12$ and P622, respectively. Furthermore, native data sets from two different potato small subunit crystal forms have been obtained.

Introduction

ADP-glucose pyrophosphorylase (ADPGlc PPase, EC 2.7.7.27) catalyzes the synthesis of ADP-glucose from ATP and glucose-1-phosphate, releasing pyrophosphate as a product (1). This enzyme plays the key regulatory role in the biosynthesis of starch in plants (2) and of glycogen in bacteria (3). ADPGlc PPase from all sources is found to be allosterically controlled, but the specificity toward the effector depends upon the source of enzyme. Enzyme from enteric bacteria is activated by fructose 1,6-bisphosphate (FBP) and inhibited by adenosine monophosphate (4), whereas the enzyme from almost all higher plant sources is activated by 3-phosphoglyceric acid and inhibited by orthophosphate (5).

ADPGlc PPase from all sources is found to exist as a tetramer in solution. The enzyme from enteric bacteria is homotetrameric (6), whereas the enzyme from higher plants is comprised of two subunits, forming a $\alpha_2\beta_2$ structure (7). The enzyme from *Escherichia coli* has been cloned and expressed using the M13mp18RF bacteriophage (8,9). A combination of chemical modification and site-directed mutagenesis studies has identified several amino acids important for catalysis or allosteric regulation of the *E. coli* ADP-Glc PPase (10). The cDNAs of two potato (*Solanum tuberosum* L.) tuber ADPGlc PPase subunits have been cloned from separate genes (11). The subunits have dissimilar sizes of 50 kDa and 51 kDa and display an overall protein sequence identity of 59 %. The amino acid sequence identity of ADPGlc PPases from different plant sources ranges between 85-90 % for the small subunit and 50-60 % for the large subunit. The enzyme from potato tuber exists physiologically as a heterotetramer ($\alpha_2\beta_2$). However, the recombinant smaller subunit (50 kDa) forms an enzymatically active homotetramer when

expressed in the absence of the large subunit (12). The small subunit expressed alone has higher enzymic activity with lower affinity for the activator 3-phosphoglyceric acid and higher sensitivity toward orthophosphate inhibition. In contrast, the large subunit is not by itself active. Furthermore the small subunit has proved more stable upon storage and easier to purify in large quantities. The above observations have led to the suggestion that the plant ADPGlc PPase small subunit functions as the catalytic subunit whereas the large subunit is involved in allosteric regulation.

Despite being extensively studied for decades, there is not a three-dimensional structure available for ADP-Glc PPase from any organism. Earlier attempts to determine the structure of ADPGlc PPase from *E. coli* were unsuccessful due to the extremely rapid decay and the fact that crystals diffracted to low resolution (13). Here we present initial crystallization and X-ray diffraction analysis of the *E. coli* and potato tuber small subunit ADPGlc PPases.

Materials and methods.

Reagents. ^{32}PPi was obtained from DuPont-New England Nuclear. ^{14}C-Glc-1-P was from ICN. Chemicals for protein crystallization were obtained from Hampton Research including Crystal Screen I and II. All other reagents were of the highest quality available.

Plamids and bacteriophages.

pML10. pML10 is an expression vector containing the mature potato tuber small subunit ADP-Glc PPase gene under control of the *lac* promotor (12). It has kanamycin resistance and ori-pACYC from pACYC177 (Novagen).

pMON17336. pMON17336 is an expression vector derived from pBR327 that contains an insert encoding the large subunit of potato tuber ADP-Glc PPase (14). It has the spectinomycin/ streptomycin (*Spc/Str*) resistance gene from Tn7, ori-327 and the *PrecA* and G1OL expression cassette (15).

pGLGC. The WT *E. coli* ADP-Glc PPase gene (*glgc*) was subcloned from the plasmid pOP12 (16) and inserted in the NcoI/SacI sites of pET28. This was achieved by PCR using the primers 5'-GGAGTTAGCCATGGTTAGTTTAGAGAAGAACG-3' (JP403) and 5'-GAACATACATGGTCGACCTGCATTATCGCTCC-3' (JP404) and pOP12 as DNA template.

M13mp18RF. Previous work provided the mutant *E. coli* ADP-Glc G336D gene inserted in M13mp18RF bacteriophage (17). The bacteriophage contains the coding region of the respective genes as well as the promoter regions necessary for expression.

Expression of *E. coli* ADP-Glc PPase. *E. coli* strain BL21(DE3) was transformed with pGLGC for expression of WT *E. coli* ADP Glc PPase. 300 ml of

overnight cultures was added to a Biostat E10 fermentor containing 12 l fresh LB with 50 $\mu g \cdot ml^{-1}$ kanamycin. Cells were grown at 37°C at 200 rpm to A_{600} = 0.5 before induction with 0.5 mM isopropyl-D-thiogalactoside (IPTG). The incubation was continued at 25°C for 16 hrs before harvesting by centrifugation.

For production of seleno-methionine substituted *E. coli* WT ADP-Glc PPase, The pGLGC plasmid was transformed into *E. coli* strain CT-13, kindly provided by Dr. Honggao Yan, Michigan State University. *E. coli* strain CT-13 is a methionine-auxotroph BL21(DE3) derivative and tetracyclin resistant. The culture medium (minimal medium) consisted of 1X Eagle Basal medium (GibcoBRL), 0.2 % glucose, 0.5 mM $MgSO_4$, 100 μM $CaCl_2$, 10 μM $ZnCl_2$, 10 μM $FeCl_3$, 0.4 mg/l thiamine, 4 mg/l d-biotin, 50 μg/ml kanamycin, and 10 μg/ml tetracyclin. Cells from 500 ml minimal medium overnight culture containing 100 μg/ml L-methionine were washed and added to a Biostat E10 fermentor containing 12 l fresh minimal medium with 50 μg/ml selenium-methionine (Se-met, Sigma). The cells were grown at maximum aeration with 200 rpm stirring at 37°C to A_{600} = 0.5 before addition of 1 mM IPTG and selenium-methionine to 100 μg/ml. After 15 hrs induction at 25°C, cells were harvested and stored at -80°C.

The expression of the ADP-Glc PPase mutant G336D in the *E. coli* strain G6MD3 was achieved as described earlier by Meyer *et al* (17).

Purification of *E. coli* ADP-Glc PPases. Purification of the WT and mutant G336D enzyme was performed as described earlier (17). Cells were resuspended in buffer (50 mM glycylglycine pH 7.5, 1 mM EDTA and 5 mM DTT) before disruption by sonication. After centrifugation, the supernatant was subjected to a heat treatment at 60°C (WT) or 55°C (G336D) for 5 min and re-centrifuged. The resulting supernatant was taken

to 60 % saturation of ammonium sulfate and centrifuged. The pellets were dissolved in dialysis buffer (50 mM glycylglycine pH 7.5, 1 mM EDTA, 2.5 mM DTT, 5% glycerol) and dialyzed against 2 x 2 l of the same buffer. The protein was applied on a DEAE fractogel column (EM Science) and washed with buffer (30 mM K-phosphate pH 7.5, 5 % glycerol, 1 mM DTT) followed by a wash with 60 mM K-phosphate pH 7.3, 100 mM KCl, 5 % glycerol and 1 mM DTT (Buffer A). The enzyme was eluted with a 1 l linear gradient of buffer A to 200 mM K-phosphate pH 7.0, 300 mM KCl, 5 % glycerol and 1 mM DTT. Fractions containing pyrophosphorolysis activity were pooled and taken to 60 % ammonium sulfate. After centrifugation, the pellet was resuspended in buffer B (50 mM Tris-Cl pH 7.5, 1 mM EDTA and 1 mM DTT) and applied on a MonoQ 16/10 column. The protein was eluted with a linear gradient (400 ml) of buffer C to 40 % buffer C (as buffer B + 1 M KCl). The purified protein was concentrated by ultrafiltration and stored at –80°C.

Expression and purification of potato tuber α_4 and $\alpha_2\beta_2$. *E. coli* strain AC70R1-504 deficient in the endogenous *E. coli* ADP-Glc PPase (*glgC*$^-$) was used for expression of both the small subunit and heterotetramer of the potato tuber enzyme as described earlier (14). For expression of the small subunit, kanamycin (25 μg/ml final) and 0.5 mM final concentration IPTG was used for selection and induction of the pML10 plasmid, respectively. In case of expression of the heterotetramer, both kanamycin (25 μg/ml final) and spectinomycin (70 μg/ml) was used for selection of pML10 and pMON17336, respectively. The two plasmids were coordinately induced by addition of IPTG (0.5 mM final) and nalidixic acid (5 μg/ml final), but apart from these differences, the expression and purification methods were identical (12).

Overnight cultures of 5 ml selective LB media was diluted 1:1000 v/v into flasks of 1 l fresh LB and grown at 37°C until OD_{600} reached 1.0-1.2. At this time expression of the ADP-Glc PPases was induced as described above, and the cultures allowed continuos shaking for an additional 40 hrs at 25°C. The cells were harvested by centrifugation, resuspended in buffer A (50 mM HEPES pH 7.5, 5 mM $MgCl_2$, 1 mM EDTA, 20 % sucrose) and disrupted by sonication. The crude extract was subjected to heat treatment at 65°C for 5 min and centrifuged. The supernatant was applied on a DEAE fractogel column and eluted with a linear gradient from buffer A to 40 % buffer B (as buffer A + 1 M KCl). Active fractions were pooled and taken to 60 % saturation of ammonium sulfate. The resulting pellet was dissolved in buffer C (20 mM Bis-Tris-propane pH 7.0, 5 mM K-phosphate, 5 mM $MgCl_2$, 1 mM EDTA, 10 % sucrose) and dialyzed against buffer C. The sample was applied on a MonoQ 10/10 column and eluted with a linear gradient of 0-0.5 M KCl in buffer C. Active fractions were concentrated by ultrafiltration, diluted 1:2 with 2 M K-phosphate pH 7.0 and applied on an aminopropyl-agarose column (C-3 column, 1x12 cm). The enzyme was eluted with a gradient of 1–0.05 M K-phosphate buffer (pH 7.0). The purified enzyme was concentrated by ultrafiltration and stored at -80°C.

ADP-Glc PPase assay. Pyrophosphorolysis of ADP-Glc was determined by the formation of [^{32}P]ATP from ^{32}PPi. The reaction was done in presence of 3-PGA or FBP according to the source of enzyme (Table 1).

Table 1: Pyrophosphorolysis assay of ADP-Glc PPase.

	Potato tuber α_4, $\alpha_2\beta_2$	*E. coli* WT, G336D
Buffer	80 mM glycylglycine pH 8.0	40 mM HEPES pH 7.0
Bovine serum albumin	0.2 mg/ml	0.4 mg/ml
NaF	10 mM	5 mM
$MgCl_2$	8 mM	8 mM
ADP-Glc	2 mM	0.8 mM
^{32}PPi (1-2 x10^3 cpm/nmol)	1.5 mM	2 mM
Dithiothreitol (DTT)	3 mM	- not added -
3-PGA	1 mM	- not added -
FBP	- not added -	1.2 mM

All concentrations are in 250 µl final volume.

The reactions were initiated by addition of an appropriate amount of enzyme and after 10 min incubation at 37°C, the reaction was terminated by addition of 3 ml cold 5% trichloroacetic acid. The [^{32}P]ATP formed was measured as described by Morell and coworkers (7). One unit of ADP-Glc pyrophosphorolysis activity is defined as the amount of enzyme forming 1 µmol of ATP/ min under the conditions described.

Protein assay. Protein concentration was determined using bicinchoninic acid reagent (18, Pierce) with bovine serum albumin as the standard.

Protein crystallization. Initial crystallization experiments were set up at 25°C and 4°C by the sparse-matrix approach using the hanging drop vapor-diffusion method described by Janick and Kim (19).

X-ray diffraction analysis.

Rotating anode X-ray source: Crystals were harvested using the reservoir solution and mounted in thin-walled glass capillary tubes or mounted in nylon cryo-loops. X-rays

were generated by a Rigaku RU-200 rotating anode generator operating at 100 mA and 50 kV and monochromatic CuKα radiation was obtained using the MSC/ Yale mirrors. Crystals were cooled to 4°C during data collection. Diffraction intensities were measured by utilizing an R-AXIS II imaging plate detector. Data was indexed with DENZO scaled and reduced using SCALEPACK (20).

Syncrotron X-ray source. Crystals were mounted in nylon cryo-loops (Hampton, CA) and stored in liquid N_2. High resolution data were collected at the Advanced Photon Source at Argonne on the Structural Biology Center ID-19 beamline. Intensity data was collected in a 3x3 (3072x3072 pixel) CCD area detector. The crystal to detector distance was set to 220 mm and 160° of data was collected with an oscillation range of 0.5°. Diffraction data was indexed and integrated using DENZO and scaled by the software SCALEPACK (20).

Results.

Expression and purification of ADP-Glc PPases. A subcloning of *E. coli* ADP-Glc PPase into the pET28 expression vector system was performed in order to improve the yield and purity of the protein, as well as to facilitate the production of selenium-substituted protein. Initially, the *E. coli* ADP-Glc PPase gene was subcloned into pET23, but the BL21(DE3) cells hosting this construct were unable to grow, due to expression of the plasmid even in absence of IPTG (data not shown). Expression of ADP-Glc PPase is known to greatly affect the growth rates of *E. coli*, as is seen by the lack of colonies when *E. coli* cells hosting an ADP-Glc PPase gene are plated on solid medium containing inducer, e.g. IPTG (M. Ballicora, personal communication). The selection of the double-repressed pET28 expression vector system circumvented the problems of culture growth, and the optimized expression conditions in LB media produced 44 mg/l of purified *E. coli* ADP-Glc PPase, representing an 8-fold improvement compared to earlier expression techniques based on M13mp18RF (17).

In order to crystallize ADP-Glc PPase, enzyme from both *E. coli* (wild-type and mutant G336D) and potato tuber (α_4 and $\alpha_2\beta_2$) were purified as described in materials and methods. Table 2 summarizes the yields of single purification batches, many of which were conducted several times in order to provide sufficient material of the desired purity. The purity of the enzymes was typically 80-90 % as judged by SDS-PAGE protein gels stained by Coomassie blue (Figure 1). Table 2 reflects the level of difficulty associated with the particular protein purification, as the level of expression and required effort varies significantly. The expression of potato tuber ADP-Glc PPase is relatively low with 0.4 % and 4 % of the total protein for the α_4 and $\alpha_2\beta_2$, respectively.

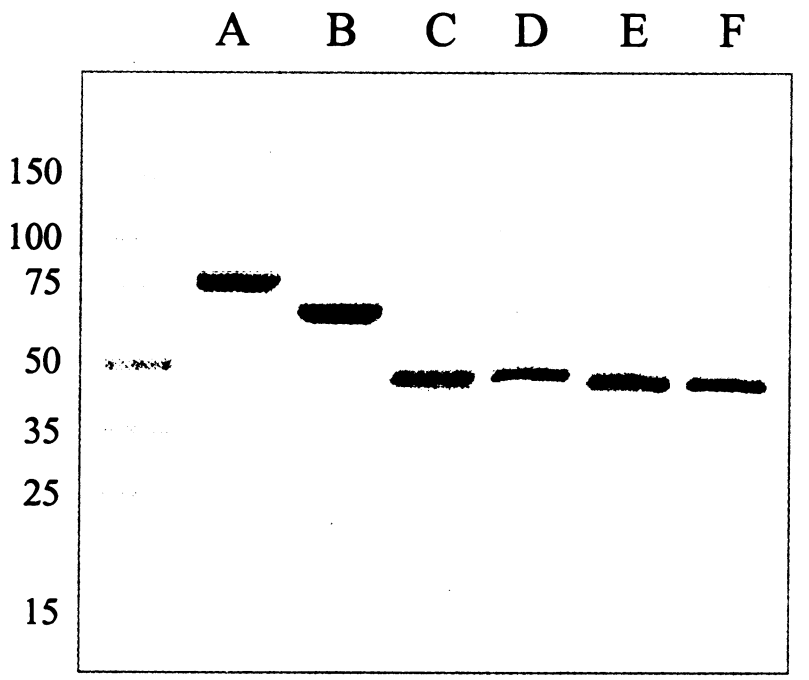

Figure 1. SDS-PAGE of purified enzymes for protein crystallization. Loading was 1-3 μg protein per lane. **A**: *E. coli* BE WT; **B**: *E. coli* truncated BE; **C**: *E. coli* ADP-Glc PPase; **D**: *E. coli* ADP-Glc PPase G336D mutant. **E**: potato α_4 ADP-Glc PPase; **F**: potato $\alpha_2\beta_2$ ADP-Glc PPase.

Table 2. Summary of single protein purifications.

Protein	Volume	Purification fold[a]	Recovery[b]	Yield[c]
E. coli ADP-Glc PPase, WT	4 liters	3	60 %	175 mg
E. coli ADP-Glc PPase, G336D	12 liters	38	39 %	40 mg
Potato tuber α_4	30 liters	250	20 %	8 mg
Potato tuber $\alpha_2\beta_2$	30 liters	25	10 %	10 mg

[a]Purification fold indicates the ratio of specific activity of purified protein to that of the crude extract. [b]Recovery is number of units of purified protein relative to that of crude extract. [c]Yield is the final mass of purified protein.

Selenium-substituted *E. coli* ADP-Glc PPase was produced by the methionine auxotroph *E. coli* strain CT-13 hosting the pGLGC plamid. After purification, a total of 51 mg of Se-Met substituted protein was obtained from 4 liters. Mass spectrometry of native and Se-met protein suggested the protein was fully substituted (Table 3). Furthermore, HPLC analysis indicated the complete absence of methionine in the selenium-substituted enzyme (data not shown).

Table 3. Mass spectrometry analysis of *E. coli* ADP-Glc PPase.

	Theoretical MW[a]	Measured MW[a]	Deviation, %
Native enzyme	48740.76 Da	48779.16 Da	0.08
Se-Met enzyme	49397.22 Da	49434.76 Da	0.08

[a] MW per monomer.

Crystallization of *E. coli* ADP-Glc PPase WT. Initial screening of the protein either uncomplexed or in presence of 1.5 mM FBP was performed and several conditions

produced small crystals directly from Hampton Crystal Screen I and II. Optimization of initial crystallization conditions including temperature, protein concentration and crystallization reagents, led to the crystals depicted in Figure 2.

a. Crystal form ECWT#1 was derived from the conditions reported previously (13) and was found to diffract to a maximal resolution of 3.0 Å. The cell parameters and space group ($P2_12_12_1$) were identical to those reported by Mulichak and coworkers (Figure 3). The crystals appeared after 2-4 weeks and were very sensitive to small changes in conditions of the experimental set-up. Furthermore, the crystals frequently appeared cracked or hollow and were very easy to disrupt during mounting. The crystals decayed rapidly in the X-ray beam (1-2 frames), and cryo-cooling conditions were sought in order to stabilize the crystal. By including 30 % v/v glycerol in the well solution, it was possible to collect a native data set by cryo-cooling (-150°C) from a crystal of dimensions 0.2x0.2x0.7 mm (Figure 3). The quality of the processed data set is very poor with low redundancy and high R-factors even in the lower resolution shells. Given the problems of obtaining good crystals and the quality of the data set, this crystal form was not analyzed further.

b. Crystal form ECWT#2 grew very large (up to 1.0x0.5x0.5 mm) by macroseeding of smaller crystals. The crystal belongs to the hexagonal system (P622), and diffracted to a maximum resolution of 3.0 Å. However, this particular crystal form diffracts weakly and requires a powerful X-ray source for measuring data. Initially, crystals decayed rapidly in the X-ray beam, but using 30 % glycerol as cryo-protectant stabilized the crystals sufficiently during data collection. Crystals grown from selenium-substituted protein were analyzed at the Argonne synchrotron source. The X-ray

Crystal form ECWT#1

Crystallization conditions:
5 mg/ml protein, 278 K
15% PEG 8000
0.1 M HEPES pH 7.1
0.2 M ammonium sulfate
size (mm): 0.2X0.2X0.7

Crystal form ECWT#2

Crystallization conditions:
5 mg/ml protein, 278 K
1.6 M ammonium sulfate
0.1 M HEPES pH 7.5
0.2 M sodium acetate
size (mm) 0.5X0.5X1.0

Crystal form ECWT#3

Crystallization conditions:
9 mg/ml protein, 298 K
20 % PEG 4000
5 % iso-propanol
0.1 M sodium citrate pH 6.2
size (mm) 0.3X0.3X0.3

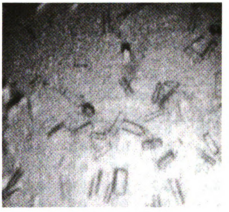

Crystal form ECWT#4

Crystallization conditions:
9 mg/ml protein, 278 K,
1.5 mM FBP
30 % PEG 1500
size (mm) 0.1X0.05X0.05

Figure 2. Crystallization conditions of *E. coli* ADP-Glc PPase WT.

Space group: $P2_12_12_1$

Unit Cell, Å: a = 149.05, b = 149.33, c = 172.69

Summary of reflection intensities and R-factors by resolution shells.

Lower shell Å	Upper shell Å	Average I	Error	Chi^2	Linear R-factor	Square R-factor
15.0	7.27	2079.9	134.2	1.042	0.044	0.044
7.27	5.89	630.7	84.8	1.052	0.124	0.104
5.89	5.18	522.2	99.4	0.973	0.124	0.123
5.18	4.72	584.5	121.0	1.036	0.153	0.128
4.72	4.39	550.5	139.6	1.155	0.197	0.161
4.39	4.14	429.7	157.4	1.085	0.267	0.208
4.14	3.93	278.3	184.0	1.160	0.469	0.358
3.93	3.77	245.3	225.0	1.114	0.642	0.502
3.77	3.62	205.1	265.2	0.978	0.798	0.622
3.62	3.50	192.2	287.7	1.042	0.000	0.812
All reflections		629.9	161.5	1.053	0.126	0.097

R linear = $\Sigma(ABS(I-\langle I\rangle))/\Sigma(I)$
R square = $\Sigma((I-\langle I\rangle)^2)/\Sigma(I^2)$
$Chi^2 = \Sigma((I-\langle I\rangle)^2)/(error^2*N/(N-1)))$

Redundancy of measured data

Shell		% of reflections with given number of observations									
lower	upper	0	1	2	3	4	5-6	7-8	9-12	>12	Total
15.0	7.27	13.5	15.2	32.3	15.0	23.7	0.0	0.0	0.0	0.0	86.3
7.27	5.89	15.3	13.0	34.8	19.2	17.7	0.0	0.0	0.0	0.0	84.7
5.89	5.18	19.3	18.2	34.6	17.7	10.3	0.0	0.0	0.0	0.0	80.7
5.18	4.72	21.4	27.3	33.5	13.3	4.8	0.0	0.0	0.0	0.0	78.6
4.72	4.39	25.5	33.4	30.1	8.3	2.8	0.0	0.0	0.0	0.0	74.5
4.39	4.14	30.0	35.1	25.7	7.4	1.8	0.0	0.0	0.0	0.0	70.0
4.14	3.93	33.9	35.7	22.5	6.8	1.1	0.0	0.0	0.0	0.0	66.1
3.93	3.77	36.5	36.8	20.1	5.9	0.7	0.0	0.0	0.0	0.0	63.5
3.77	3.62	39.1	37.5	17.8	5.2	0.4	0.0	0.0	0.0	0.0	60.9
3.62	3.50	40.5	36.8	17.4	4.9	0.4	0.0	0.0	0.0	0.0	59.5
All hkl		27.4	28.8	26.9	10.4	6.5	0.0	0.0	0.0	0.0	72.6

Figure 3. X-ray data set of *E. coli* ADP-Glc PPase crystal form ECWT#1.

absorption spectrum confirmed the enzyme contained selenium and had a sharp absorption edge. The cell parameters and processing statistics of the multiple anomalous dispersion (MAD) data set is shown in Figure 4. The diffraction does not extend beyond 3.5 Å, as seen by the sharp drop in percentage of measured reflections in the 3.57-3.41 Å resolution shell. The poor quality of this particular data has hindered finding the expected 64 selenium sites in the asymmetric unit, although this is sufficiently low for modern software. However, as we observe a large variation in crystal diffraction limits and data quality, more crystals should be analyzed at a synchrotron radiation source.

c. With crystal form ECWT#3, initial experiments using small crystals (0.1x0.1x0.2 mm) revealed X-ray diffraction to about 3.3 Å and a cryo-cooling condition was found by including 10 % glycerol in the solution. Selenium-substituted protein crystals (0.3x0.3x0.3 mm) were brought to the Argonne Advanced photon source and two MAD data sets were collected to 3.0 and 3.3 Å completion. Some decay occurred during data collection, as the crystals initially showed a maximal diffraction of 2.6 Å. The two data sets were merged to enhance the completion and redundancy of the measured data (Figure 5). This data set is very complete to 3.0 Å with reasonable R-factors, but diffracts poorly beyond the 3.00-2.90 Å resolution shell. The crystal form has very large unit cell dimensions and at least 250 selenium sites are expected in the asymmetric unit, posing problems for calculating an electron density map.

d. ECWT#4 was too small to test for X-ray diffraction. Here, the ADP-Glc PPase is bound to the activator FBP included in the protein sample (1.5 mM final concentration). Optimizing this condition as well as crystal seeding techniques in order to

Space group: P622

Unit Cell, Å: a =b = 180.9, c = 225.4

expected selenium sites = 64

Summary of reflection intensities and R-factors by resolution shells.

Lower shell Å	Upper shell Å	Average I	Error	Chi^2	Linear R-factor	Square R-factor
99.0	6.82	917.5	38.1	3.658	0.093	0.135
6.82	5.41	233.8	16.4	1.699	0.140	0.146
5.41	4.73	249.0	19.6	1.656	0.159	0.336
4.73	4.30	259.0	22.7	1.634	0.175	0.189
4.30	3.99	151.5	23.9	1.334	0.284	0.702
3.99	3.75	109.4	27.5	1.294	0.437	0.449
3.75	3.57	100.4	30.7	1.254	0.538	0.000
3.57	3.41	55.3	32.4	1.088	0.882	0.777
All reflections		285.4	25.9	1.758	0.180	0.189

R linear = $\Sigma(ABS(I-<I>))/\Sigma(I)$
R square = $\Sigma((I-<I>)^2)/\Sigma(I^2)$
$Chi^2 = \Sigma((I-<I>)^2)/(error^2*N/(N-1)))$

Redundancy of measured data

Shell		% of reflections with given number of observations									
lower	upper	0	1	2	3	4	5-6	7-8	9-12	>12	Total
99.0	6.82	2.7	1.9	11.8	12.0	22.4	44.8	4.3	0.0	0.0	97.3
6.82	5.41	0.9	1.2	7.0	9.5	21.3	55.4	4.7	0.0	0.0	99.1
5.41	4.73	0.7	1.6	6.2	8.1	20.1	60.2	3.2	0.0	0.0	99.3
4.73	4.30	0.6	1.3	6.4	6.4	19.9	63.1	2.2	0.0	0.0	99.4
4.30	3.99	0.4	1.3	5.9	6.5	21.2	62.9	1.7	0.1	0.0	99.6
3.99	3.75	0.5	1.1	6.1	7.6	21.5	61.2	1.8	0.2	0.0	99.5
3.75	3.57	0.4	1.5	5.4	7.8	22.1	60.3	2.2	0.2	0.0	99.6
3.57	3.41	70.7	1.2	2.2	2.9	6.4	15.9	0.6	0.0	0.0	29.3
3.41	3.28	100	0.0	0.0	0.0	0.0	0.0	0.0	0.0	0.0	0.0
3.28	3.17	100	0.0	0.0	0.0	0.0	0.0	0.0	0.0	0.0	0.0
All hkl		27.2	1.1	5.2	6.2	15.6	46.2	2.1	0.0	0.0	72.8

Figure 4. X-ray data set of *E. coli* ADP-Glc PPase crystal form ECWT#2.

Space group: $P2_12_12$, Z = 16-20

Unit Cell, Å: a = 154.4, b = 273.5, c = 209.1

Mosaicity = 0.339

selenium sites = 250+

Summary of reflection intensities and R-factors by resolution shells.

Lower shell, Å	Upper shell, Å	Average, I	σ	I/σ	Norm. R-factor
30.00	6.23	3033.1	104.2	29.0	0.031
6.23	4.95	1640.1	65.9	25.0	0.052
4.95	4.33	2614.4	95.1	27.0	0.049
4.33	3.93	1838.8	86.9	21.0	0.066
3.93	3.65	1341.7	86.7	15.0	0.095
3.65	3.44	920.1	86.7	10.0	0.128
3.44	3.27	580.9	86.2	6.7	0.192
3.27	3.12	394.2	86.1	4.5	0.279
3.12	3.00	292.8	86.2	3.3	0.354
3.00	2.90	220.5	87.1	2.5	0.461
All reflections		1266.5	87.0	14.5	0.085

R linear = $\Sigma(ABS(I-<I>))/\Sigma(I)$
R square = $\Sigma((I-<I>)^2)/\Sigma(I^2)$
$Chi^2 = \Sigma((I-<I>)^2)/(error^2*N/(N-1)))$

Redundancy of measured data

Shell		% of reflections with given number of observations										
lower	upper	0	1	2	3	4	5-6	7-8	9-12	13-19	>19	Total
40.0	6.24	2.8	5.4	23.5	3.5	7.6	6.0	7.6	10.5	33.1	0.0	97.2
6.24	4.96	0.4	3.7	24.3	3.8	8.0	6.4	7.1	12.8	33.5	0.0	99.6
4.96	4.33	0.2	3.1	23.4	3.9	8.4	6.7	7.2	13.7	33.4	0.0	99.8
4.33	3.94	0.1	3.0	22.4	4.3	8.5	6.8	7.3	14.2	33.5	0.0	99.9
3.94	3.65	0.1	2.8	21.7	4.3	8.6	6.9	7.8	15.1	32.8	0.0	99.9
3.65	3.44	0.1	2.6	21.1	3.9	9.2	6.9	8.0	15.5	32.6	0.0	99.9
3.44	3.27	0.1	2.9	20.0	3.9	9.5	7.2	8.3	17.3	30.8	0.0	99.9
3.27	3.12	0.4	3.0	19.1	4.0	9.8	7.2	8.4	21.5	26.6	0.0	99.6
3.12	3.00	1.4	6.3	14.6	4.6	9.2	7.9	10.1	26.5	19.6	0.0	98.6
3.00	2.90	18.3	4.9	8.8	3.4	5.4	14.4	12.8	24.6	7.5	0.0	81.7
All hkl		2.4	3.8	19.9	4.0	8.4	7.6	8.4	17.1	28.4	0.0	97.6

Figure 5. X-ray data set of *E. coli* ADP-Glc PPase crystal form ECWT#3.

produce larger crystals were unsuccesful, and thus the crystal form was not pursued further.

Crystallization of potato tuber ADP-Glc PPase. The α_4 form was screened for crystallization conditions in the uncomplexed form or with Cr^{3+}-ATP (0.3 mM final) or ADP-Glc (3 mM final) included in the protein sample. Figure 6 depicts crystals from four separate conditions.

a. Crystal form α_4#1 was obtained after 1-2 months and grew as very large rods (>1 mm in length) or as plates. This crystal form diffracted X-rays well (2.2 Å maximum) and found to be reasonably stable during data collection. A native data set was collected to 3.4 Å without cryo-cooling and the data is summarized in Table 4. Attempts to refine conditions so crystals could be reproduced in a shorter time have been unsuccessful, complicating further analysis.

b. The α_4#2 crystal form is a reasonable candidate for solving the structure of a potato ADP-Glc PPase small subunit. α_4#2 diffracted X-rays well (2.8 Å), grew large (0.5x0.2x0.2 mm) in 1-2 weeks and was found to be stable during data collection. Furthermore, a cryo-cooling condition has been obtained by including 20 % glycerol in the well solution, which may prevent crystal decay altogether. A native data set has been collected to 3.0 Å (94 % complete) and is summarized in Table 4.

c. Crystal form α_4#3 were obtained with ADP-Glc included in the protein sample. These were obtained with relative ease in 1-2 days, but unfortunately diffracted X-rays poorly (4.5 Å) and were concluded to be unsuitable for X-ray diffraction analysis.

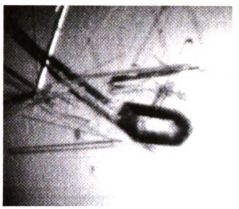

Crystal form α_4# 1

Crystallization conditions:
5 mg/ml protein, 278 K,
0.3 mM Cr-ATP
30 % PEG 4000
0.2 M ammonium acetate
0.1 M sodium citrate pH 5.6
size (mm) 0.1X0.1X0.1

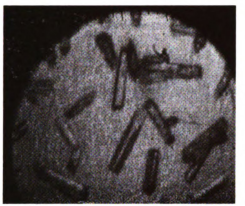

Crystal form α_4# 2

Crystallization conditions:
5 mg/ml protein, 278 K
20 % PEG MME 2000
0.15 M ammonium sulfate
0.1 M sodium acetate pH 4.6
size (mm) 0.2X0.2X0.5

Crystal form α_4# 3

Crystallization conditions:
5 mg/ml protein, 298 K,
3 mM ADP-Glucose
11 % PEG 8000
0.1 M magnesium chloride
0.1 M sodium cacodylate pH 6.5
size (mm) 0.1X0.2X0.4

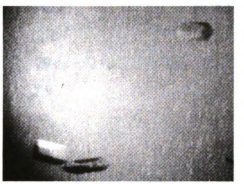

Crystal form α_4# 4

Crystallization conditions:
5 mg/ml protein, 298 K
18 % PEG 8000
0.1 M magnesium chloride
0.1 M sodium cacodylate
pH 6.5
size (mm) 0.1X0.1X0.2

Figure 6. Crystallization conditions of potato tuber α_4 ADP-Glc PPase.

Table 4. Data collection and processing statistics for potato tuber small subunit crystal forms α_4#1 and α_4#2

Crystal form	α_4#1	α_4#2
Space group	$P4_1$	P2
Cell constants (Å)	a=b=110.57 c=190.14	a=80.06 b=138.84 c=92.20 β=112.40°
Maximum resolution (Å)	2.2	2.8
Resolution of dataset (Å)	3.4	3.0
Number of unique reflections	24429	30342
[a] R_{merge} (%)	12.1	9.5
Completeness (%)	79	82
V_M	2.9	2.4
Number of molecules per asymmetric unit	4	4

[a] $R_{merge}=\Sigma\Sigma|I(h)i - \langle I(h)\rangle|/\Sigma\langle I(h)\rangle$; $I(h)$ is the observed intensity of the *i*th measurement of reflection *h*, and $\langle I(h)\rangle$ the mean intensity of reflection *h* calculated after scale.

d. Crystal form α_4#4 diffracted X-rays reasonably well (3.5 Å), but we could not produce crystals of a sufficient size by refining conditions or even seeding techniques. Also, these crystals were very sensitive to handling and decayed rapidly during data collection.

In addition, the potato tuber $\alpha_2\beta_2$ protein has been screened for crystallization conditions. Although small crystals have been produced, these are yet too small for X-ray diffraction analysis.

Crystallization of *E. coli* ADP-Glc PPase mutant G336D. G336D was screened uncomplexed or with 0.5 mM FBP included in the sample for crystallization conditions. Figure 7 shows an example of a crystal produced in absence of FBP. Despite a decent appearance and reasonable size (0.2x0.2x0.2 mm) these crystal diffracted X-rays very poorly (>7Å) and hence were concluded to be unsuitable for diffraction analysis. In other conditions, small crystals of G336D have been produced and these are currently being optimized.

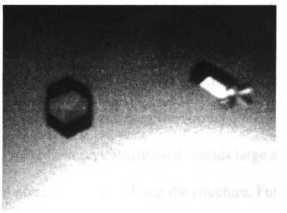

***E. coli* ADP-Glc PPase G336D**

Crystallization conditions:
4 mg/ml protein, 298 K.
20 % PEG MME 550
0.1 M MES pH 6.5
10 mM zinc sulfate
size (mm): 0.2x 0.15x 0.15

Figure 7. Crystallization conditions of *E. coli* ADP-Glc PPase G336D.

Discussion.

It is evident from the results described above that obtaining a three-dimensional structure of ADP-Glc PPase poses a challenging task. Despite numerous crystal forms of both ADP-Glc PPase from *E. coli* and the potato small subunit, and a large effort in data collection and processing, we have not yet been able to produce an electron density map of the enzyme. However, we have obtained several results that could make a solution of the structure eventually possible. This includes increasing the protein yield and purity of the *E. coli* ADP-Glc PPase by subcloning the corresponding gene into a pET28 expression vector. As protein crystallization demands large amounts of purified material, this is an important prerequisite for solving the structure. Furthermore, the pET28 expression system has enabled us to produce protein substituted with selenium methionine with good yields, necessary for our strategy in obtaining phasing information.

The low level of potato α_4 expression complicates its crystallization but experiments to produce larger amounts of soluble protein have been unsuccessful (Ballicora and Preiss, unpublished results). As there are no atomic coordinates available for an ADP-Glc PPase, we are seeking phasing information by measurements of MAD data obtained from selenium-methionine substituted crystals. However, frequently a 10-fold reduction in protein expression is observed as a result of using the minimal media required in producing selenium substituted proteins. This would render the production of selenium-substituted potato α_4 enzyme exceedingly difficult. In fact, the limitation on potato α_4 protein yields leaves the *E. coli* ADP-Glc PPase currently the only candidate for producing the first three-dimensional structure of the enzyme.

The two crystal forms P622 (ECWT#2) and $P2_12_12$ (ECWT#3) of *E. coli* ADP-Glc PPase have successfully been produced with selenium-substituted protein. For crystal form $P2_12_12$, this has resulted in a very complete 3.0 Å MAD data set with a sharp absorption edge for selenium. In most circumstances this information would be adequate for constructing an electron density map. However, the high number of expected selenium sites in the assymmetric unit (250+) has hindered the calculation of a map, due to limitations in software capability. By obtaining an additional source of phasing information (i.e. isomorphous replacement) it is plausible the selenium sites in crystal form $P2_12_12$ can be found, enabling the calculation of an electron density map.

Alternatively, the structure could be solved based on the hexagonal crystal form of *E. c*oli ADP-Glc PPase, as the lower number of expected selenium sites (64 sites) makes locating their positions in the assymmetric unit possible. The weak diffraction of this particular crystal form requires the most powerful beamline (SBC) at the Argonne Advanced Photon Source in order to collect X-ray data of sufficient quality, which in this case has hindered rapid progress. The ADP-Glc PPase is a crystallographic challenge but the results presented in this report encourage us to continue working on solving its three-dimensional structure.

References.

1. Espada, J. (1962). *J. Biol. Chem.* **237**, 3577-3581.
2. Preiss, J. (1991). *Oxford Surveys of Plant Molecular and Cell Biology, Vol. 7* edited by B. Mifflin, pp. 59-114. Oxford.
3. Preiss, J. (1984). *Annu. Rev. Microbiol.* **38**, 419-458.
4. Preiss, J., Shen, L., Greenberg, E. and Gentner, N. (1966). *Biochemistry* **5**, 1833-1845.
5. Ghosh H. P. and Preiss, J. (1966). *J. Biol. Chem.* **241**, 4491-4504.
6. Haugen, T. H., Ishaque, A. and Preiss, J. (1976). *J. Biol. Chem.* **251**, 7880-7885.
7. Morell M. K., Bloom, M., Knowles, V. and Preiss, J. (1987). *Plant Physiol.* **85**, 182-187.
8. Baeker, P.A., Furlong, C.E., and Preiss, J. (1983) *J. Biol. Chem.* **258**, 5084-5088.
9. Hill, M.A., Kaufmann, K., Otero, J., and Preiss, J. (1991) *J. Biol. Chem.* **266**, 12455-12460.
10. Preiss, J. and Sivak, M. (1998) *in* Comprehensive Natural Products Chemistry (B. M. Pinto, Ed.) Vol. 3, pp. 441-495, Pergamon Press, Oxford.
11. Nakata P. A., Greene, T.W., Anderson, J. M., Smith-White, B. J., Okita, T. W. and Preiss, J. (1991). *Plant Mol. Biol.* **17**, 1089-1093.
12. Ballicora, M. A., Laughlin, M. J., Fu, Y., Okita, T. W., Barry, G. F. and Preiss, J. (1995). *Plant Physiol.* **109**, 245-251.
13. Mulichak, A.M., Skrzypzak-Jankun, E., Rydel, T.J., Tulinsky, T., and Preiss, J. (1988). *J. Biol. Chem.* **263**,17237-17238.

14. Iglesias, A.A, Barry, G.F., Meyer, C., Bloksberg, L., Nakata, P.A., Greene, T., Laughlin, M.J., Okita, T.W., Kishore, G.M., and Preiss, J. (1993) *J. Biol. Chem.* **268**, 1081-1086.

15. Olins, P.O. and Rangwala, S.H. (1989) *J. Biol. Chem.* **264**, 16973-16976.

16. Okita, T.W., Rodriguez, R.L., and Preiss, J. (1981) *J. Biol. Chem.* **256**, 6944-6952.

17. Meyer, C.R., Bork, J.A., Nadler, S., Yirsa, J. and Preiss, J. (1998) *Arch. Biochem. Biophys.* **353**, 152-159.

18. Smith, P.K., Krohn, R.I., Hermanson, G.T., Mallia, A.K., Gartner, F.H., Provenzano, M.D., Fujimoto E.K., Goeke, N.M., Olson, B.J., and Klenk, D.C. (1985) *Anal. Biochem.* **150**, 76-85.

19. Jancarik, J. and Kim S-H (1991). Sparce matrix sampling; a screening method for crystallization of proteins. *J. Appl. Cryst.* **24**, 409-411.

20. Otwinowski, Z. andMinor, W. (1997) *Methods Enzymol.* **276**, 307-326.

CHAPTER 8

CONCLUDING REMARKS AND RESEARCH PERSPECTIVES

The work described above has aimed at increasing our understanding of the structure-function relationships of branching enzyme and ADP-glucose pyrophosphorylase. This objective has been pursued *via* X-ray crystallography to solve the three-dimensional structures of both enzymes, as well as conventional biochemical approaches for branching enzyme. Solving the crystal structures of branching enzyme and ADP-glucose pyrophosphorylase currently represents the most important research challenges in our laboratory. For branching enzyme, we believe the crystal form of the truncated enzyme will enable us to achieve this goal. The quality of the native data set, the availability of selenium-methionine substituted protein, and the sufficiently low number of selenium sites in the asymmetric unit, all indicate we can solve the structure, although much work clearly remains.

Based on sequence homology with the α-amylase family I would like to conclude my thesis by discussion of a possible catalytic mechanism for branching enzyme which is a variation of the proposed catalytic mechanism for CGTase (1; Figure 1). This hypothetical branching enzyme mechanism utilizes Asp335 of region 2 (β4-H4 loop) and Glu458 of region 3 (β5-H5 loop) conserved in the $(\alpha/\beta)_8$-barrel. The mechanism proceeds via two half-chair oxo-carbenium transition states (TS1 and TS2) and a covalent intermediate with Asp335. A covalent intermediate involving this Asp has been observed in the crystal structure of CGTase by soaking crystals in 4-deoxy-maltotriosyl-α-flouride (1). The reaction of all enzymes in the α-amylase family may have this first part of the reaction in common. However, the last part of the reaction differs between the amylolytic enzymes. In branching enzyme, for example, the nucleophile attacking the TS2 half-chair

Figure 1. Proposed catalytic mechanism for branching enzyme. The two conserved amino acids Asp335 and Glu458 of regions 2 and 3, respectively, act as catalytic residues. Initially, the α-1,4 glucosidic linkage is cleaved by transfer of a proton from Glu458. The transition state TS1 involves an oxo-carbenium in a half-chair conformation. Asp335 forms a covalent linkage with the C-1 as an intermediate. The next transition state (TS2) involves a second half-chair oxo-carbenium. Glu458 acts here as a base and the new α-1,6 linkage is formed by nucleophilic attack of the 6-OH oxygen.

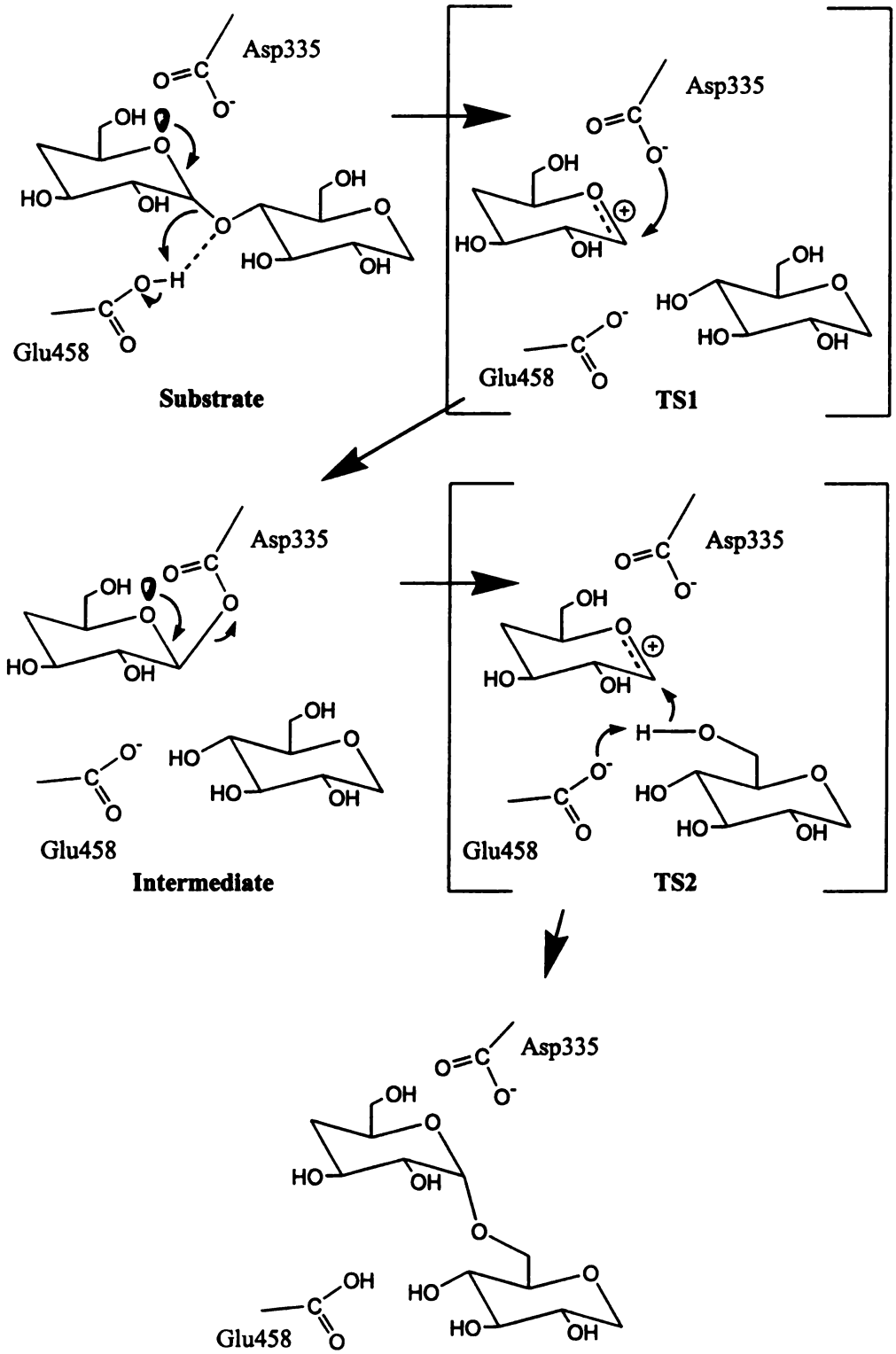
Asp335
Glu458
Substrate
TS1
Intermediate
TS2
Product

is oxygen of the 6-OH group, whereas it is the oxygen of 4-OH in CGTase and H_2O in α-amylase. The challenge is to explain how such a specificity is maintained in these related enzymes.

For branching enzyme in particular, dual-labeling studies have shown that transfer between two glucan molecules is possible (2). In other words, the donor and acceptor α-glucans are not necessarily from the same molecule. It is therefore possible branching enzyme has an additional α-glucan binding site. Obviously, it would be desirable to obtain a crystal structure of branching enzyme with bound substrate, or substrate analogue to answer some of these questions. The BAYe4609 inhibitor described in this thesis may be utilized in such crystallization trials. As BAYe4609 contains a mixture of varying size glucan-like chains, purification or even chemical synthesis of BAYe4609 may be required.

Another approach involves creating the double mutant D335N-E458Q of the *E. coli* branching enzyme and soak crystals with commercially available amyloses of high purity. The approach involving a double Asp-Glu mutant has previously been successful in obtaining an enzyme-substrate complex of CGTase, although the enzyme had a very low turn-over (3).

A considerable work effort has concentrated on crystallization of ADP-glucose pyrophosphorylase. Despite that many different crystal forms have been obtained of both the *E. coli* enzyme and the potato tuber small subunit, the majority of these crystals have proved unsuitable for X-ray diffraction analysis. Low protein yields have also posed problems, in particular for the potato tuber α_4 enzyme. The expression of the *E. coli*

ADP-glucose pyrophosphorylase in a pET expression vector system has not only improved the yield, but also facilitated the production of selenium-methionine protein. This has led to MAD data sets of two *E. coli* ADP-glucose pyrophosphorylase crystal forms.

Although diffracting X-rays reasonably well, the many selenium sites of *E. coli* ADP-glucose pyrophosphorylase crystal form $P2_12_12$ hinders the construction of an electron density map. There are at least two different strategies for obtaining an *E. coli* ADP-glucose pyrophosphorylase structure: A) Isomorphous replacement by heavy atom soaks of $P2_12_12$ crystals can provide additional information, thereby assisting in finding the selenium sites. B) The structure can be solved initially with crystal form P622, before working with the higher-resolution data of the $P2_12_12$ crystal form.

The three-dimensional structure of *E. coli* N-acetylglucosamine 1-phosphate uridylyltransferase (GlmU) does provide us with some structural information about the pyrophosphorylase domain. Although the atomic coordinates are not available, many experiments based on the GlmU structure combined with sequence alignments, can be designed. One example is site-directed mutagenesis of Asp142 in *E. coli* ADP-Glc PPase, already described in Chapter 1. However, for understanding the complex allosteric regulation and subunit interactions of ADP-glucose pyrophosphorylase, obtaining a structural model remains an absolute requirement, and therefore an important research challenge.

References.

1. Uitdehaag, J.C.M., Mosi, R., Kalk, K.H., Van der Veen, B.A., Dijkhuizen, L., Withers, S.G. and Dijkstra, B.W. (1999) *Nat. Struc. Biol.* **6**, 432-436.

2. Knegtel, R.M.A, Strokopytov, B., Penninga, D., Farber, O.G., Rozeboom, H.J., Kalk, K.H., Djikhuizen, L., and Dijkstra, B.W. (1995). *J. Biol. Chem.* **270**, 29256-29264.

3. Nielsen, A.N., Blennow, A., Nielsen, T.H., and Moeller, B.L. (1998).

117, 869-875.